2020

The integration of pumped hydro storage systems into PV microgrids in rural areas

Navid Mousavi
Edith Cowan University

Edith Cowan University

Copyright Warning

The integration of pumped hydro storage systems into PV microgrids in rural areas

This thesis is presented for the degree of

Doctor of Philosophy

Navid Mousavi

Edith Cowan University

School of Engineering

2020

Graphical abstract

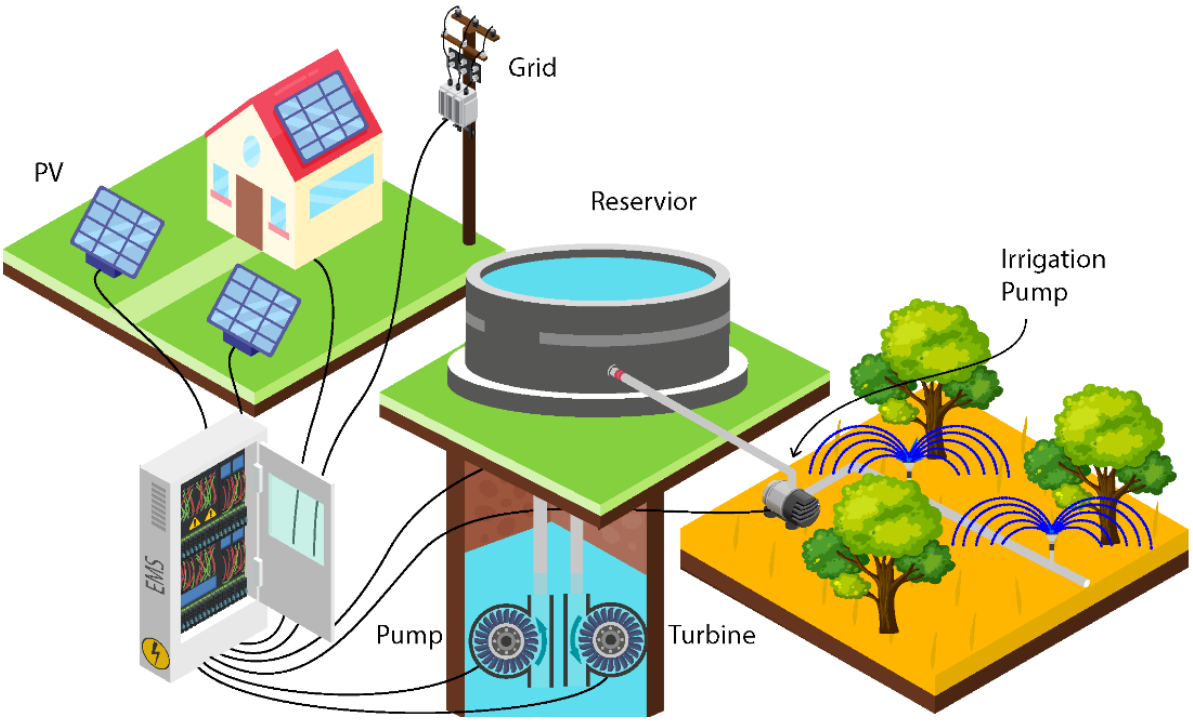

Abstract

Photovoltaic (PV) systems are popular in rural areas because they provide low cost and clean electricity for homes and irrigation systems. The primary challenge of PV systems is their intermittent nature. The typical solution is storing energy in batteries; however, they are expensive and possess a short lifespan. This research proposes a new type of pumped hydro storage (PHS) which can be implemented as an alternative to batteries. The components of the system are modelled to consider losses of the system accurately. The mathematic model developed in this project assists the management system to make more efficient decisions. The proposed storage is integrated into a farmhouse that has a PV pumping system where economic aspects of implementing the proposed storage is investigated. The integration of the proposed PHS into a microgrid needs a management system to make this system efficient and

cost-effective. This research proposes a multi-stage management system to schedule and control the microgrid components for optimal integration of the PHS. The designed management system is able to manage the pump, turbine, and irrigation time on real-time taking into account both present and future conditions of the microgrid. This study investigates the technical aspects of the proposed system. The PHS and the management system are tested experimentally in a setup installed at smart energy laboratory at Edith Cowan university. Data used in this project are real data collected in the laboratory in order to have a realistic analysis. Economic analysis is done in different sizes with different conditions. Results indicate that the proposed system has a short payback period and a large lifetime benefit, featuring as a cost-effective and sustainable energy storage system for use in rural areas.

Video abstract

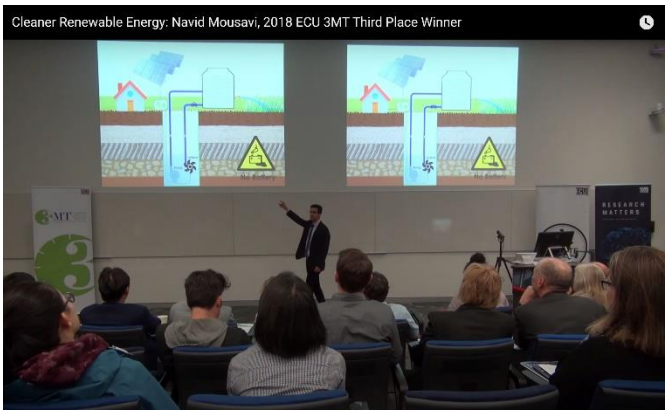

https://youtu.be/VuyEvHRY7W8

Keyword: Pumped hydro storage system; Energy management system; Pumped hydro storage system modelling; Energy storage system; Renewable energy; Solar photovoltaic system; PV-PHS Microgrid;

Declaration

I certify that this thesis does not, to the best of my knowledge and belief:

(i) incorporate without acknowledgement any material previously submitted for a degree or diploma in any institution of higher education;

(ii) contain any material previously published or written by another person except where due reference is made in the text; or

(iii) contain any defamatory material.

I also grant permission for the Library at Edith Cowan University to make duplicate copies of my thesis as required.

Signed: Navid Mousavi

Date: 1/05/2020

Acknowledgment

Firstly, I would like to gratefully acknowledge my principal supervisor, Associate Professor Ganesh Kothapalli, for his constructive criticisms, valuable advice, and continuous support in every aspect of my research. I would also like to express my sincere gratitude to my co-supervisor, Professor Daryoush Habibi, for his assistance, encouragement, and excellent recommendations which has added great value to my research. The valuable suggestions, recommendations, and scholarly comments of anonymous reviewers and editors from the various international journals are gratefully acknowledged. These individuals and organisations have helped me to improve the quality of this project.

I would like to thank Dr Mehdi Khiadani, Choton Kanti Das, Ali Baniasadi, and Farhad Farivar, who helped me with their advice, guidance and generous personal support to overcome the difficulties of this research project.

I would like to express my profound gratitude to my parents, Abbas and Zohreh, for being such wonderful sources of support and pride. I thank them for inspiring me to follow my dreams and giving me the confidence to be my best. They taught me there is no right or wrong, and we are all special.

I would like to acknowledge Edith Cowan University (ECU) for awarding me an Australian Government Research Training Program Scholarship (RTP) to enable me to pursue my PhD study program. The generous support from the technical and administration staff of the School of Engineering at ECU is highly appreciated.

List of publications arising from this thesis

[1] N. Mousavi, G. Kothapalli, D. Habibi, M. Khiadani, and C. K. Das, "An improved mathematical model for a pumped hydro storage system considering electrical, mechanical, and hydraulic losses," Applied energy, vol. 247, pp. 228-236, 2019.

https://doi.org/10.1016/j.apenergy.2019.03.015

[2] N. Mousavi, G. Kothapalli, D. Habibi, and C. K. Das, "Operational Cost reduction of PV-PHS systems in farmhouses: Modelling, Design, and Experimental validation," in IOP Conference Series: Earth and Environmental Science, 2019, vol. 322, no. 1: IOP Publishing, p. 012011.

https://doi.org/10.1088/1755-1315/322/1/012011

[3] N. Mousavi, G. Kothapalli, D. Habibi, C. K. Das, and A. Baniasadi, "Modelling, design, and experimental validation of a grid-connected farmhouse comprising a photovoltaic and a pumped hydro storage system," Energy Conversion and Management, vol. 210, p. 112675, 2020.

https://doi.org/10.1016/j.enconman.2020.112675

[4] N. Mousavi, G. Kothapalli, D. Habibi, C. K. Das, and A. Baniasadi, "A novel photovoltaic-pumped hydro storage microgrid applicable to rural areas," Applied Energy, vol. 262, p. 114284, 2020.

https://doi.org/10.1016/j.apenergy.2019.114284

[5] N. Mousavi, G. Kothapalli, D. Habibi, S. W. Lachowicz, V. Moghaddam " A real-time energy management strategy for pumped hydro storage systems in farmhouses," Journal of Energy Storage, (Under Review).

Contents

List of Figures

List of Tables

List of Abbreviations and Symbols

P_p	Pump power [W]
P_m	Motor power in the pump unit [W]
η_m	Motor efficiency in the pump unit
Q_p	Pump flow rate [m^3/s]
η_p	Pump efficiency
ρ	Density of water (ρ=997 at 25°C) [Kg/m^3]
g	Acceleration due to gravity ($g = 9.8$) [m/s^2]
H_p	Pump head [m]
H_s	Static head [m]
H_{pl}	Head loss of pump mode [m]
H_{tl}	Head loss of turbine mode [m]
H_r	Vertical distance between the lower reservoir and the upper reservoir [m]
H_{uwl}	Water level in the upper reservoir [m]
H_{lwl}	Water level in the lower reservoir [m]
H_{lr}	Height of the lower reservoir (inside) [m]
H_{ur}	Height of the upper reservoir (inside) [m]
H_t	Turbine head [m]
K	Resistance coefficient
K_{pipe}	Pipe resistance coefficient
$K_{fittings}$	Fittings resistance coefficient
v	Water velocity [m/s]
D_p	Pipe diameter between the pump and the reservoir [m]
f	Friction factor
L_p	Pipe length of pump [m]
L_t	Pipe length of turbine [m]
ε/D	Pipe relative roughness
ε	Absolute roughness [mm]
Re	Reynolds number
μ	Dynamic viscosity of water ($\mu = 8.9 \times 10^{-4}$) [Pa. s]
$ET_\circ$	Reference evapotranspiration [$mm/hour$]
R_n	Net radiation [$MJ/m^2/hour$]
G	Soil heat flux density [$MJ/m^2/hour$]

T_{hr}	Mean hourly air temperature [°C],
RH	Relative humidity
Δ	Saturation slope vapour pressure curve at T_{hr} [kPa/°C]
γ	Psychrometric constant [kPa/°C]
$e^{\circ}(T_{hr})$	Saturation vapour pressure at air temperature T_{hr} [kPa]
e_a	Average hourly actual vapour pressure [kPa]
u_2	Average hourly wind speed [m/s]
Δt	Time interval $[s]$
$\forall_{eva}(\Delta t)$	Volume of evaporated water during one time interval $[m^3]$
A	Reservoir surface area $[m^2]$
$\forall$	Volume of water in the upper reservoir $[m^3]$
$\forall_{res}$	Upper reservoir volume $[m^3]$
Q_t	Turbine flow rate $[m^3/s]$
$\forall_{pre}(\Delta t)$	Volume of precipitation during one time interval $[m^3]$
I	Precipitation [mm/h]
P_t	Turbine power [W]
η_t	Turbine efficiency
P	Pressure [KPa]
h	Head [m]
D_t	Diameter of the turbine pipe $[m]$
a	Area of the turbine pipe $[m^2]$
T_v	The percent openness of the turbine valve
Q_w	Flow rate between well and aquifer (m3/s)
K_h	Hydraulic conductivity of aquifer (m/s)
h_1	Aquifer head (m)
h_w	Well head (m)
r_1	Radius of influence (m)
r_w	Well radius (m)
s_w	Drawdown at the well (m)
ω_{kj}	Synaptic weight of input j at neuron k
x_j	Input signal j of neuron k
y_k	Activation value of neuron k
φ	Activation function of neuron k
b_k	Bias of neuron k
Q_p	Pump flow rate $[m^3/s]$

$\forall$	Volume of water in the reservoir $[m^3]$
P_t	Turbine power [W]
T_v	The percent openness of the turbine valve [%]
E_{PVt}	Energy generation of PV at interval t [Wh]
E_{Tt}	Energy generation of Turbine at interval t [Wh]
$E_{Grid\ t}$	Energy imported from the grid at interval t [Wh]
E_{Dt}	Energy consumption of demand at interval t [Wh]
E_{Pt}	Energy consumption of pump at interval t [Wh]
E_Cost	Electricity cost [AUD]
λ_t	Energy tariff (AUD/Wh]
PP	Payback period [Year]
CC	Capital costs [AUD]
EBS	Annual saving on the electricity bill [AUD]
$O\&M$	Annual operation and maintenance costs [AUD]
WT	Annual water treatment costs [AUD]
ω_{kj}	Synaptic weight of input j at neuron k
x_j	Input signal j of neuron k
y_k	Activation value of neuron k
φ	Activation function of neuron k
b_k	Bias of neuron k
P_{IP}	Irrigation pump power [W]
Q_{IP}	Irrigation pump flow rate $[m^3/s]$
ρ	Density of water $[Kg/m^3]$
g	Acceleration due to gravity $(g = 9.8)$ $[m/s^2]$
H_{Ip}	Total head of the irrigation pump [m]
η_{Ip}	Efficiency of the irrigation pump
E_{IPt}	Energy consumption of the irrigation pump at interval t [Wh]
$\forall$	Volume of water in the reservoir $[m^3]$
ID	Irrigation day [day]
$FPID$	First possible irrigation day [day]
$LPID$	Last possible irrigation day [day]
D	Current day [day]
LI	Last irrigation [day]
IH	Irrigation hour [hour]
II	Irrigation interval [hour]

IL	Length of each irrigation [hour]
$\forall_{24}$	Minimum water volume at the end of the day [m^3]

Chapter 1: **Introduction**

1.1 Motivation

Renewable electricity generation as a practical solution for global warming is growing very fast, but it increases the complexity of the power system. Renewable electricity not only reduces greenhouse gas emissions on the earth, but it is also a suitable solution for the energy crisis. If the current situation continues, in the near future conventional energy reserves will run out [1]. However, using clean energy sources instead of conventional power plants has three major problems.

The first problem is the intermittent nature of RESs. Unlike conventional power plants, which use fossil fuel, the output power of RESs depends on environmental factors [2]. For example, the power of photovoltaic (PV) systems depends on solar radiation. Therefore, alternative energy sources should meet energy demands while the PV systems are not able to generate enough energy. One solution is integrating energy storage systems (ESSs) into the PV systems. In this case, when power generation is higher than demand, ESSs are charged, and when energy generation is lower than demand, the ESSs supply the energy deficit. Batteries are the conventional ESSs, but have a small capacity, a short lifespan, a limited number of cycles, and a high carbon footprint [3]. In recent decades, numerous papers have developed different kinds of chemical, thermal, mechanical, and electrochemical ESSs [4], but still more research is required to address storage problems.

The second problem with the use of RESs is the cost. The capital cost and operating cost of RESs with ESSs are high, so developing new methods of storage and power generation to reduce the cost is vital [5]. Typically, half of the capital costs for a PV-battery microgrid is for the battery. Therefore, developing other cost-effective energy storage systems is vital in order to encourage more people to use clean energy sources.

The third problem is energy management. RESs are being used to reduce carbon dioxide emissions, but because of their intermittent nature, they cannot meet energy demand all the time. Hence, a microgrid

needs a management system to schedule and control energy sources and ESSs in order to use the RESs efficiently [6]. A hybrid microgrid needs a multi-stage management system because of the complexity of the system. Both energy generation and consumption have uncertainty, and the management system should stabilise the microgrid in any situation.

Many researchers around the world are working hard to solve these problems since any improvement in RES technology will encourage more people to use clean energy. In this regard, this project proposes a new type of PHS to solve RES problems in rural areas.

1.2 Significance

Generally, the conventional type of storage in small microgrids is a battery, but it has several disadvantages. The battery is the most expensive part of a microgrid. Its costs can be categorised as initial, operational, maintenance, and repair costs. In addition, it has a short lifespan, so replacement costs are significant. Another drawback is the greenhouse-gas emissions of battery manufacturing [7]. Many studies are currently underway to introduce new ESSs. An economical and eco-friendly ESS will encourage the market to increase their use of RESs. Therefore, this research will develop an environmentally friendly storage system in order to reduce the cost of the microgrid.

This research will propose a PHS that can be implemented in an irrigation system. It will use the structure of irrigation systems in rural areas to store energy by adding a hydro turbine. The proposed system will work as a storage system and irrigation system simultaneously. It will solve the RES problems with a low carbon footprint. It is cost-effective because it needs only a turbine instead of a large battery.

Furthermore, this project proposes a multilayer management system to reduce operating cost. The proposed management system has different layers that schedules and controls the microgrid components to ensure its optimum operation.

Chapter 2: **Literature review and methodology**

The aim of this chapter is giving a brief synopsis of relevant literature related to the various aspects of the proposed project. At first microgrids and management systems in microgrids are introduced. PHS is the main part of this research, so its advantages, disadvantages, and performance are explained. Many studies are conducted to improve PHS drawbacks. Specifically, this chapter focuses on studies using PHSs in rural areas. This literature review indicates the problems and the gaps of the PHS integration into microgrids in rural areas. Finally, research questions of this project are written according to these problems and gaps.

2.1 Microgrid

A microgrid is the combination of energy sources, storage systems and loads. Microgrids are important and necessary parts of a smart grid. The power flow in traditional power systems is from large conventional power plants through transmission lines to consumers. However, in a smart grid, electricity can be exchanged between microgrids and the main grid. A smart grid enables RESs to be integrated efficiently into the power system. A microgrid can work stand-alone or grid-connected. microgrids by generating energy close to the loads, increase the efficiency and facilitate the integration of RESs [8]. Fig 2.1 shows a microgrid including controllable generators, non-controllable generators, ESSs, and controllable loads. The energy sources can be RESs such as PV and wind turbine (WT) or conventional generators such as diesel generators [9]. In a microgrid, a management system controls all the units to ensure providing reliable, sustainable, price-competitive electricity for loads.

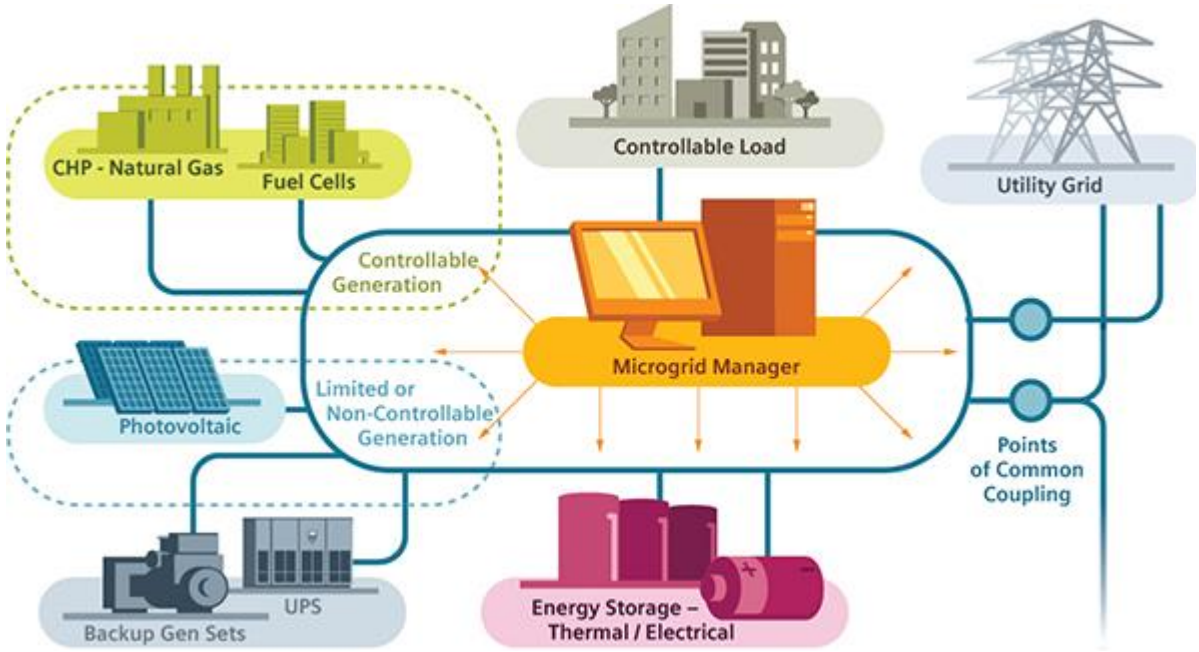

Fig 2.1: An example of a microgrid [9]

Normally, a microgrid has two operating modes: the island mode and the grid-connected mode. If a microgrid operates in an island mode, the microgrid does not exchange energy with the main grid. In the island mode, power sources and ESSs inside of the microgrid meet the energy demand. While the microgrid works in the grid-connected mode, it can exchange energy with the main grid. The operating mode of a microgrid depends on power generation, power demand, the ESS state, and electricity price. If a fault occurs in the main grid, single RESs should be disconnected avoiding any further damage. In that situation, a microgrid can work in island mode, and RESs in the microgrid can operate under normal conditions without any damage. From this point of view, it is easy to see a more flexible operation feature of microgrids than the RESs connected directly to the main grid [10].

2.2 Management systems

A management system manages components of a microgrid in order to produce required power with the least cost and the least environmental effect [11]. In a microgrid, there are some power generation units and some storage units to meet energy demand. A management system monitors the system operation and controls all the units to manage the microgrid optimally [10, 12]. Energy management strategies highly depend on the configuration of the microgrid and the policy of the power system.

Generally, the management system schedules the microgrid units for the next time interval based on the forecast data and the constraints of the system. The microgrid using an optimisation method provides references profiles for all the microgrid components [13]. The objectives of a management system are:

- to minimise fuel cost[11];
- to reduce gas emissions[11];
- to optimise usage pattern of the storage system to prevent fast degradation [14, 15];
- to reduce the correlated cost[13];
- to improve energy utilisation efficiency[13];
- to maximise the microgrid operation profits under different operational conditions [10].

Generally, a management system schedules the microgrid by solving an optimisation problem. It finds the optimum performance of the microgrid for the given forecast data. The forecast data is the prediction of power generation, power demand, and electricity price during the period of optimisation. The output of the optimiser is the schedules of the microgrid units that will be given to a controller to implement the scheduled program [13]. In Section 2.2, management systems suggested for PV-PHS systems are explicitly explained.

2.3 PHS systems

A PHS is a type of storage system that usually is used for load balancing. Several studies have been conducted on the utilization of the PHS in microgrids [16-20]. Fig 2.2 shows a schematic diagram of a PHS. It is comprised of two reservoirs, a pump, and a turbine. When power generation is higher than demand, the water is pumped to the upper reservoir, and when power generation is lower than demand, the stored water is released back into the lower reservoir through a turbine to generate energy. In fact, it stores electrical energy into the form of gravitational potential energy. Generally, the lower reservoir is a natural lake or a river, and the upper reservoir is an artificial lake. The capacity of a PHS depends on the volume of the reservoirs and the height difference between two reservoirs [21]. A typical PHS

switches between charging mode and discharging mode from once to more than 40 times per day operation [22, 23], and the changing mode can occur within minutes [23].

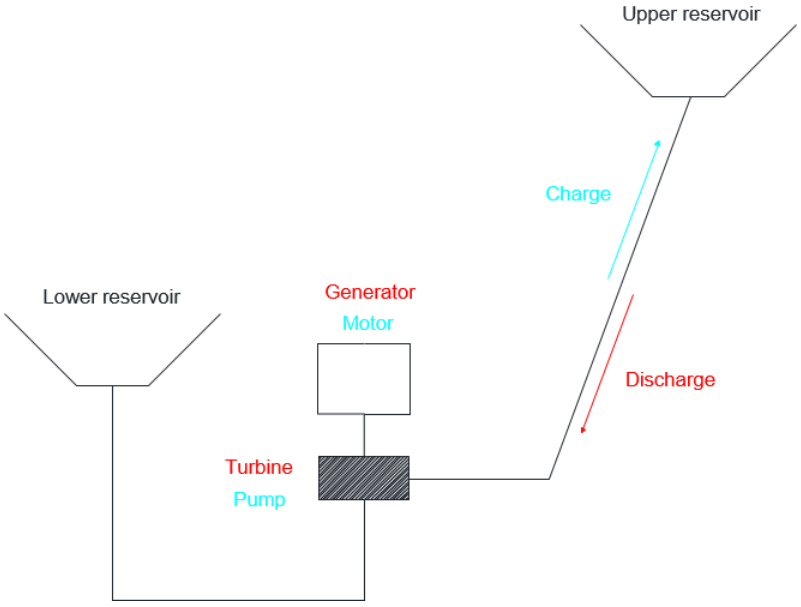

Fig 2.2: The schematic diagram of a PHS [24]

This method of storage has attracted much attention in recent years because of the fast growth of the RESs in power systems [25]. The PHS has a variety of applications such as capacity firming, load levelling, power quality improvement, spinning reserve, and peak shaving [26]. Fig 2.3 compares the rated power of different ESSs for each application. It shows the 99% of the ESSs used for electric energy time-shifting are PHSs. In electric bill management application and capacity firming almost half ESSs are PHSs.

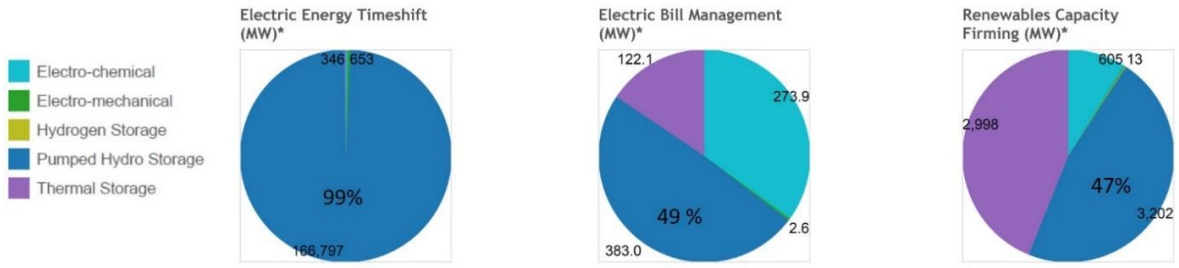

Fig 2.3: The percentage of PHS usage in three applications[27]

There are two kinds of PHS. The turbine and pump can operate in two separate unit or in a single unit named reversible pump-turbine (RPT). An RPT is a machine that can operate both as a pump and as a turbine [28]. It has lower efficiency, but it needs only one machine for both charging and discharging modes, which reduce costs. On the other hand, when the pump and the turbine are separate, the efficiency is higher than RPT, but it is more expensive because it needs a separate pump and a separate turbine and more piping [29].

In comparison to other kinds of ESSs, PHS has a long-lasting lifetime. The number of charge and discharge does not have any impact on the lifespan. In term of life-cycle cost, which includes various costs such as initial, operating, maintenance, repair, and replacement costs, PHS is ideal storage [30]. The costs of a PHS, including turbine, pumps, and upper reservoir, are about 47% of a microgrid total cost the same as a battery-based system [31]. Nonetheless, operating cost in a PHS based system is lower than a battery-based system, demonstrating its cost-effectiveness. In addition, it can provide a large discharge rate in a short time [32]. The efficiency of this system depends on evaporation losses and conversion losses. Because the upper reservoir is exposed to the sun, some of the stored water is evaporated. On the other hand, in the pump operation and turbine operation, there are losses because of energy transformation [33]. The technology of variable speed drives (VSD) allows PHS units to store power in a more effective manner. Before the VSD the PHS could store excess energy only if the surplus power was in the range of pump rated power, but now this technology able the PHS to store a wide range of power. A VSD can increase the efficiency of PHS by 5% to 10% and the capacity by 15% to 20% [34]. In conclusion, PHS has the following advantages:

- Cost-effective, particularly in the area where naturally there is an upper and lower reservoir (from $2000 to 4000/kW);
- High capacity[24];
- Long-lasting lifetime [32];
- Low capital cost per unit of energy [24, 35];

- Low operating costs [30];
- High efficiency (65–75%) [36];
- Fast respond to changes within seconds [24];
- Eco-Friendly storage system (low carbon footprint) [16];
- Able to supply all the energy needed for a stand-alone microgrid [37].

On the other hand, PHSs have a number of disadvantages: 1) The main problem is that a PHS needs two reservoirs in two different heights [38]. 2) Constructing large artificial reservoirs causes environmental issues. 3) PHS can only be implemented in places with special geographical conditions. They need a water source in the lower reservoir and a geographical height for the upper reservoir. 4) The construction of a large PHS lasts about 10 years and costs millions of dollars [39] [36, 40] [24, 41, 42]. 5) In areas with a warm climate, evaporation losses decrease the efficiency of this system[43]. Many different PHSs have been proposed recently to solve these problems.

A pump-back hydroelectric dam is a storage system that can be installed in conventional hydroelectric dams. The usage of existing reservoirs, turbine, and transmission system makes this method cost-effective [44]. One study investigated ten underground taconite mines to use as the lower reservoirs of PHS systems [45]. The underground space of the former mines can be used to reduce the construction cost of PHSs. [46] proposed the construction of a 200-MW PHS by means of a coal mine as a lower reservoir. [33] presents a PHS in the sea. A concrete hollow sphere is placed deep underwater on the seabed where a pump-turbine pumps water out of the hollow sphere during periods when there is excess energy. During periods of high electricity demand, water is allowed to flow back into the hollow sphere through a pump-turbine, which generates electricity. [47] suggests a new principle PHS that is based on the underground storage reservoir. The water reservoir is surrounded by soil. The soil weight gives the needed pressure to run the turbine. This type of PHS is implemented in Denmark with 1-metre head and 2500 m3, which can store 34 kWh.

2.4 PHS systems in rural areas

Many investigations have been conducted on the utilisation of PV systems as power sources for water-pumping systems in rural areas. The integration of PV systems with water pumping systems significantly reduces cost and pollution [48]. However, current technology uses batteries for storage, which are very expensive and need frequent maintenance.

A large and growing body of literature has focused on large-scale PHS for power balancing, and there are a few studies about small-scale PHSs. One study investigated the integration of a small PHS into a microgrid including a PV, a diesel generator, and a battery [49]. It demonstrates that a small PHS can reduce the fuel cost of the microgrid. Another study proposed a standalone system consisting of a PV, a diesel generator, a battery, and a small PHS to supply energy to irrigate the land and meet the domestic needs of 50 families in the village (Fig 2.4) [50]. Its objective is to minimise annual operating costs. The authors calculated the size of the reservoir, battery, diesel generator and the PV with the PSO method in different scenarios. The results show that the PHS decreased diesel fuel consumption by 4%.

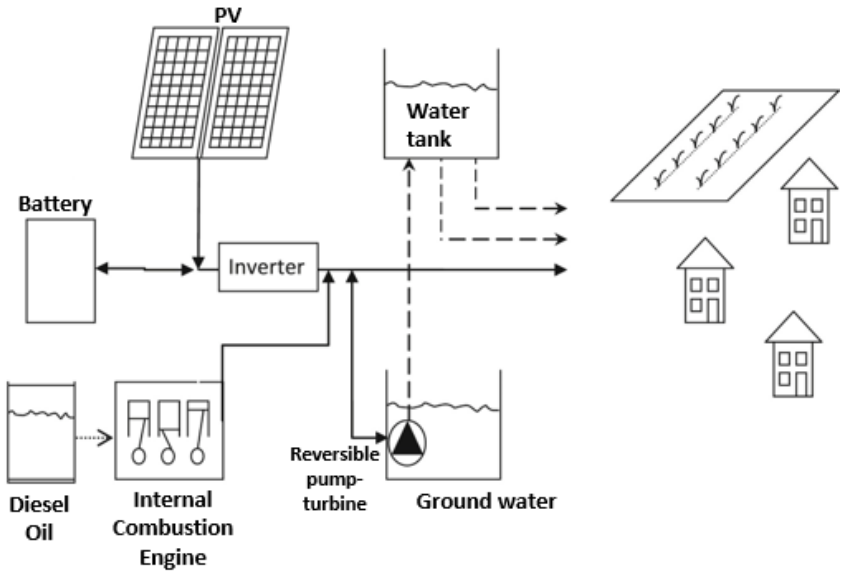

Fig 2.4**:** The microgrid schematic of ref [50]

The authors in [51] propose a PHS implemented in an open well to reduce the cost of residential electricity (Fig 2.5). When there is excess energy or the price of energy is low, it pumps water from well into a reservoir and stores energy in the form of gravitational potential energy, and when the energy price is high, the water is released back into the well through a turbine. The open well is utilised as the working head of the turbine. The research uses a PSO optimisation to schedule units in order to minimise the residential electricity cost and water flow rate (WFR). The authors use two turbines with different rated power to optimise the use of the water that is available for power generation in the reservoir. Thus, the optimisation objective function has two parts. One objective is to minimise electricity cost, and the other to minimise WFR.

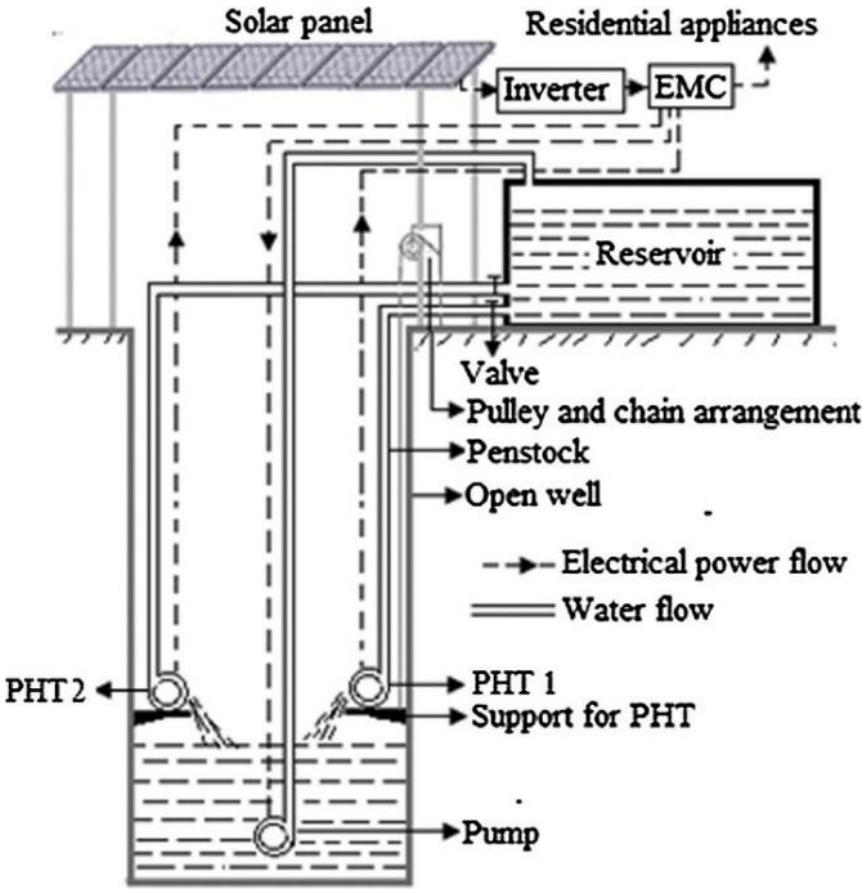

Fig 2.5**:** The microgrid schematic of ref [51]

A major criticism of [51] is that its assumption about the output power of the PV is not realistic. The authors present a 12% root-mean-square error (RMSE) to simulate the uncertainty of output PV power.

This means the PV power fluctuates around the predicted number with a small error (Fig 2.6), but on a cloudy or rainy day during the operation of the PV, the output power may fluctuate between the maximum power and zero (Fig 2.7). When the RMSE is low, it does not change the power balance in the system significantly, so the scheduled program is close to the optimum operation of the system. However, on a cloudy day when the RMSE is large, power generation is very different from the scheduled program, so the scheduled program is not necessarily close to the optimum operation of the system. In a system with a large error, the optimum operation may be completely different from the scheduled program. Therefore, the proposed management system in [51] does not work efficiently on cloudy days.

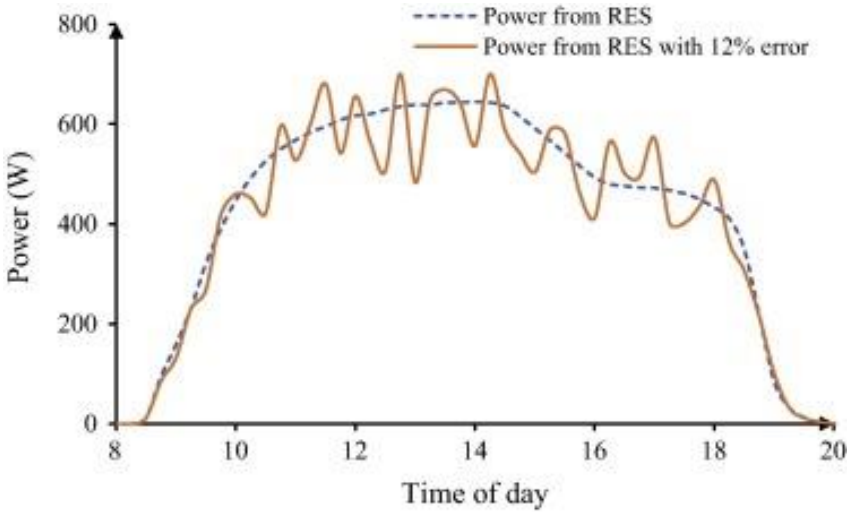

Fig 2.6**:** The profile of PV output power in ref [51]

The second problem of [51] is that the management system does not determine the required stored water (RSW) at the end of the day. The optimiser that schedules the PHS, needs to know the desired volume of water at the end of the day. The authors in this article omit to find the optimum RSW and arbitrary selected 40% of maximum storage. However, the RSW has an important impact on the performance of the system on the next days. Maybe the next day is cloudy and storing more water on the current day would, therefore, have been beneficial for the microgrid to minimise the total operating cost.

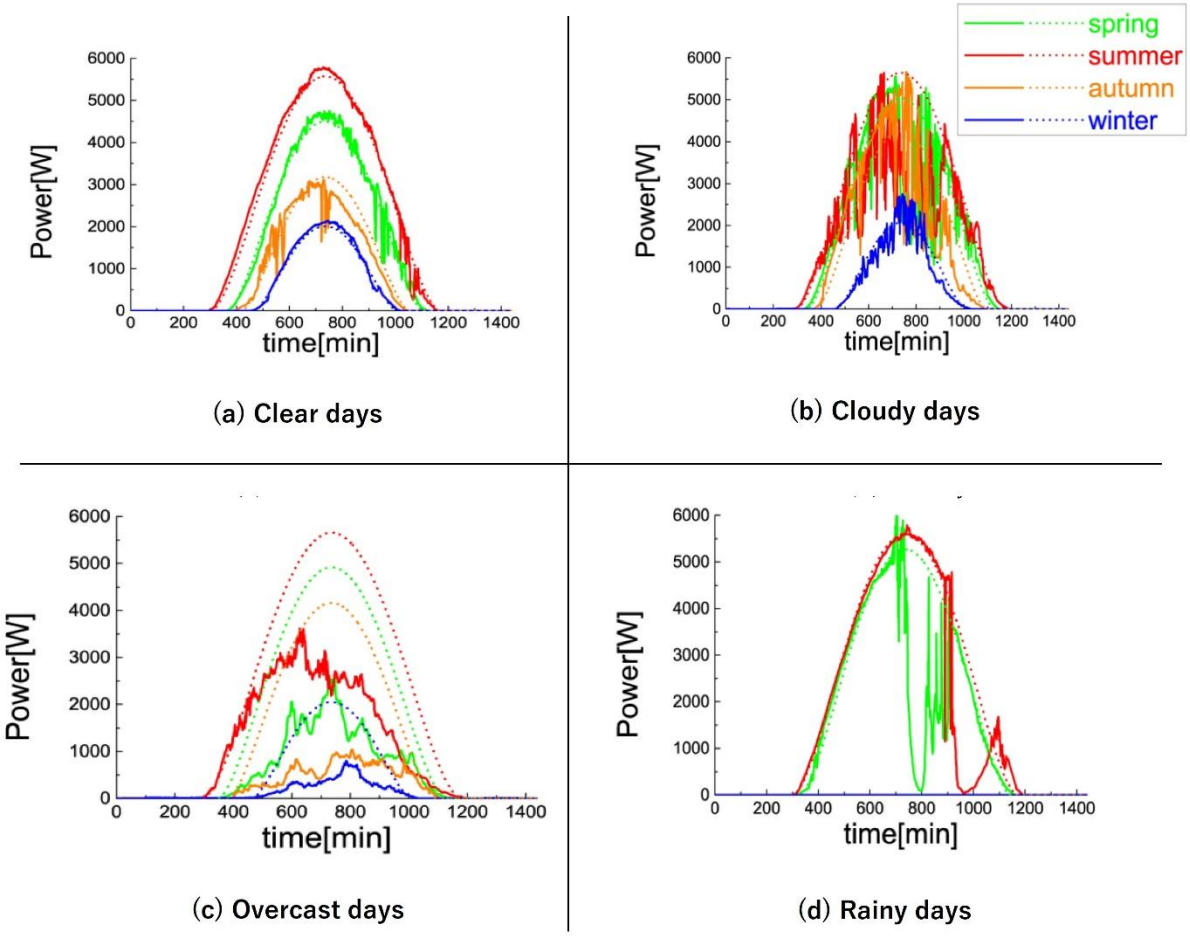

Fig 2.7**:** PV output power for different types of days in terms of their level of solar irradiance among known terms: (a) clear days, (b) cloudy days, (c) overcast days, (d) rainy days [52]

A small PHS for a stand-alone microgrid is developed by [53]. Fig 2.8 shows its microgrid configuration. In a stand-alone microgrid, the loss of load (LOL) is crucial, so this research determines RSW based on the predicted energy generation for the next day. Hence, if the ratio of energy generation to demand is predicted to be high for the next day, the microgrid consumes more energy on the current day. Likewise, if the predicted energy generation for the next day is low, the system stores more energy on the present day to reduce LOL. In the proposed algorithm, the RSW is a function of the ratio of the input energy from RESs to the energy demand.

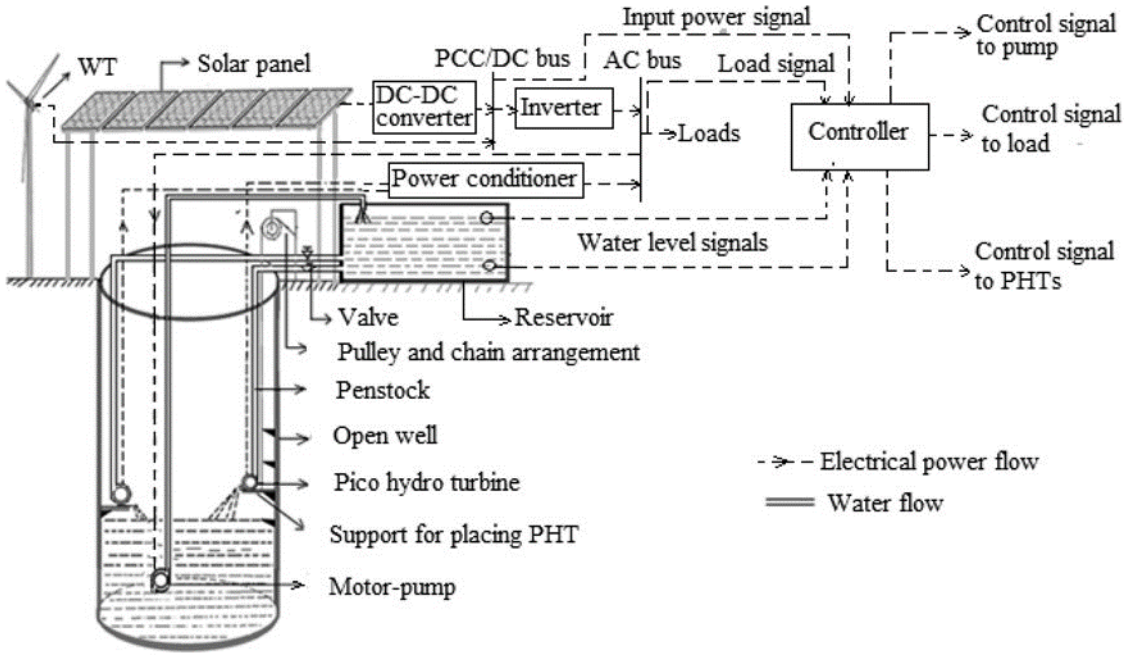

Fig 2.8**:** The microgrid schematic of ref [53]

Although [49, 51] demonstrate that a small PHS is cost-effective and can reduce the operating costs of the microgrid, there are many gaps in the literature about the management of a PHS in rural areas. The authors in [49-51, 53] ignore irrigation water demand and focus on the charging and discharging modes of the PHS. However, in these papers, PHS systems are a part of irrigation systems, so, the management system should consider the amount of water that is used for irrigation. For this purpose, the management system should manage the irrigation along with other units to improve the performance of the system.

All the proposed management systems are highly dependent on the accuracy of the forecast data, but forecast data presents an average of power generation, and electricity demand for each time interval. Most of the time, the output power of PV is very different from the average, so managing a microgrid based only on forecast data is not very efficient. Hence, more research should be carried out in regard to optimally managing in the presence of error in the forecast data.

The authors in [38, 49-51] propose that the volume of the water stored in the reservoir at the end of the day should be same every day, but the RSW has an impact on the performance of the system on the following days. Maybe the next day is cloudy and storing more water would be beneficial for the

microgrid to reduce operating costs more. One study determined the volume of the water according to the ratio of energy generation to demand [53]. However, the optimum volume of the water depends on the environmental effects, the performance of the microgrid, and energy demand on the present day and the following days. Thus, a management system needs to assess all the criteria and find the optimum range of the water volume in the reservoir.

This literature review has looked at the available literature relating to small scale PHS implemented in rural areas with irrigation systems. The literature reveals some significant gaps regarding the provision of the management system, where the following questions are the gaps that the present research will seek to fill.

2.5 Research questions

- **Question 1:** What are the hydraulic, mechanical and electrical losses of a PHS System?

  Answering this question will assist the management system to schedule the PHS more efficiently. Scheduling methods calculate costs of any possible solution with the system model. If the model does not calculate losses, the prediction of pump flow rate, stored water, and turbine power will be inaccurate which will cause wrong decisions. Chapter 3 will answer this question by developing a comprehensive PHS model calculating all the losses of the system.
- **Question 2:** How a PHS system can be integrated into an irrigation system?

  Answering this question requires a broad study on the available infrastructure, needed modifications, constraints, and limitations of the system. Chapter 4 investigated the feasibility of implementing a PHS in an irrigation system in a farmhouse including simulation, experimental tests and economic analysis to answer this question.
- **Question 3:** How a management system can schedule both the microgrid and the irrigation system to minimise electricity costs?

  In the proposed system If management system controls both the PHS and irrigation system, the microgrid can save more costs. Chapter 6 will answer this question by proposing a scheduling

method that not only manages pump power and turbine flow rate but also manages irrigation times and water volume.

- **Question 4:** How the proposed microgrid can be controlled efficiently when there is a mismatch between forecast data and actual values?

  Scheduling methods are useful when there is no fluctuation in power generation and demand. However, in cloudy days or when demand fluctuates significantly, scheduling methods are inefficient since they use forecast data. This problem is solved in chapter 7 by designing a real-time management system which is able to control the microgrid considering the current and future condition of the system.

2.6 Research Methodology

The purpose of this section is to describe the methodology of this project. The section begins by describing the proposed scheme, which is a new type of PHS suitable for rural areas. Section 2.6.1 discusses how an existing irrigation system will be used to store energy. Section 2.6.2 moves on to describe the proposed management system and explains a new type of management systems that is appropriate for the proposed PHS. The management system has two levels of scheduling and one controller to manage the microgrid. In Section 2.6.3 and 2.6.4 optimisation algorithms and control methods are described. Section 2.6.5 describes the software programs and the hardware components that will be used to test the proposed system.

2.6.1 Proposed scheme

One way of reducing costs is by using an existing structure and equipment in the design of the system. A typical PHS needs two reservoirs, a pump, and a turbine. On the other hand, a typical agricultural land has a water well, pump, and a reservoir for irrigation. If the irrigation well is used as the lower reservoir, adding a turbine to this system changes it to a PHS.

Fig 2.9 is a schematic of the proposed system. The PHS has a pump, a turbine, and a reservoir. The hydraulic part is comprised of the pump, the reservoir, the turbine, and the irrigation system. The proposed PHS uses the well, the reservoir, and the pump of an existing irrigation system in a rural area. When there is excess energy, the surplus power is used to pump water from the well to the reservoir. Then, the stored water in the reservoir can be used for irrigation, or it can be released into the well through the turbine in order to generate energy. Thus, the proposed system can work as a storage system without disturbing the primary function of the irrigation system.

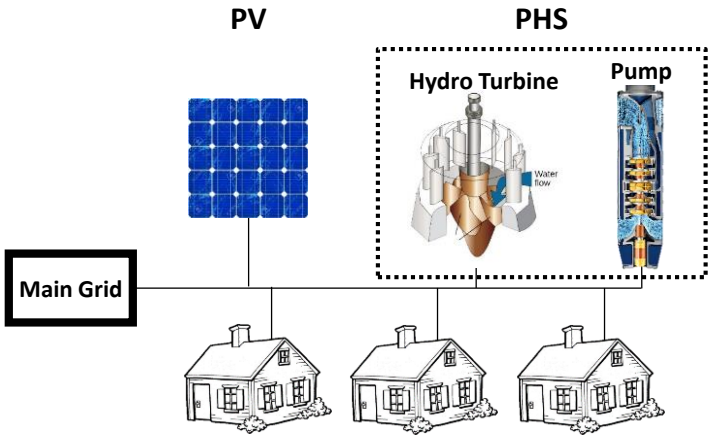

(a)

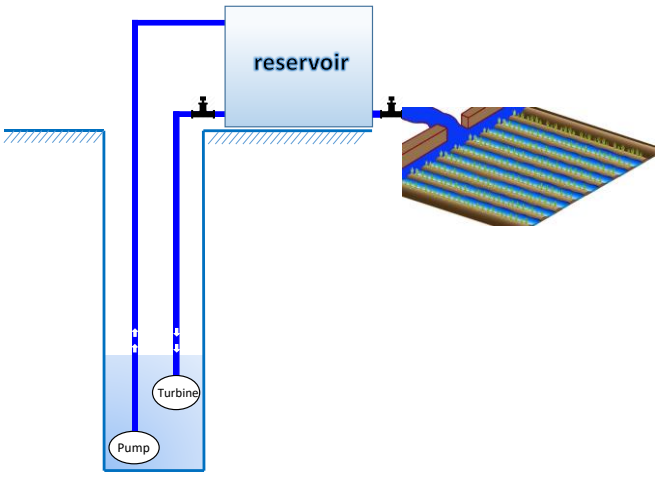

(b)

Fig 2.9**:** The proposed microgrid, (a) electrical components, (b) hydraulic components

Using a PV farm and a PHS will significantly reduce cumulative electricity cost in a rural area [51]. Fig 2.10 shows that 1 kW PV system and a PHS with an 80000 L reservoir can decrease electricity consumption by 47%.

Although using one structure for two functions makes the system more complex, it can also increase the efficiency of the two systems. The major advantage of this combination is that the amount of energy wasted is decreased. The output power of RESs fluctuates significantly day by day due to environmental effects. The weather can be sunny one day and may cloudy the next. On the other hand, a storage system has a certain amount of capacity, irrespective of its type. Thus, on a sunny and windy day, a microgrid needs a large storage system with the capacity to store all the excess energy. If the sunny and windy weather continues for several days, the microgrid needs a huge storage unit to store the excess energy without any waste. However, in practice, an ESS is designed based on the average power generation during the year. Therefore, on sunny or windy days, some of the energy is wasted due to the ESS capacity limitation. This project will solve this problem by combining an irrigation system and a PHS.

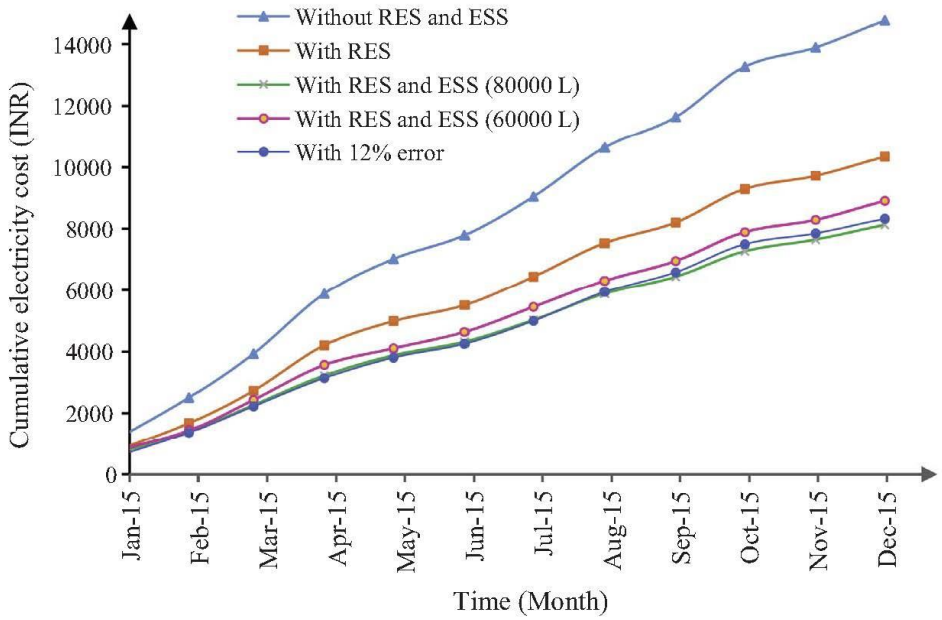

Fig 2.10**:** The cumulative electricity cost of a PV-PHS microgrid in different configurations [51]

The proposed PHS has a reservoir with a certain capacity, but this limited capacity can be managed efficiently. The proposed PHS has two options for using the stored water in the reservoir: it can be used to generate energy, or for irrigation. In the proposed scheme, if the management system sets the irrigation time just before the periods of high excess energy, the water level will be decreased, so the reservoir will have more space to store water, hence, the PHS can store more energy. For example, take a situation in which forecast data shows that energy generation will be high and the excess energy will be 90% of the PHS's capacity. If the management system uses the stored water in the reservoir for irrigation to decrease the stored water to 10% before or while the high generation period, the PHS can store all the excess energy. In fact, instead of wasting energy, the excess energy is used for another purpose.

Another advantage of using an irrigation system as the structure of the PHS is cost reduction. This system is more cost-effective than a typical PHS because the depth of the well is exploited as the working head, the irrigation pump is used for charging mode, and the existing reservoir is utilised as the upper reservoir. The only thing that this system needs to work as a PHS is a turbine.

The fluctuation of the water level in the well is the main concern in this type of PHS. This project will use a submersible pump, so if the water level in the well drops below the level of the pump during charging mode, the pump's impellers will melt because submersible pumps are cooled by the water flowing through them and cannot work without water. On the other hand, if the water level in the well rise, the turbine power generation will reduce. The water level, therefore, needs to be kept in a narrow range. Authors in [54] showed that the fluctuation of the water level depends on the aquifer type. The authors found that the water flows during pumping water to the reservoir and releasing water to the well should be proportional to the flow rate between the well and the aquifer.

2.6.2 Energy management

The proposed PV-PHS system needs a complex management system to control pump power, turbine flow rate, irrigation times, and stored water. This management system receives many forecast and actual

data to make efficient decisions. One input is the constraints of irrigation, which are the required frequency and duration of irrigation in each month. Required frequency and duration of irrigation can be determined by farmer experience or they can be calculated as a function of weather conditions and the kind of crops. The required frequency and duration of irrigation depend on the month. Sometimes land needs to be irrigated every day, and sometimes it can be irrigated once a month [55]. Another input is the current water level in the reservoir, which can show the amount of stored energy. Other inputs are weather and demand forecast, which are necessary for scheduling the microgrid.

Two prediction models are needed in this system to forecast PV power and demand. PV power prediction requires clear sky irradiance, cloud cover prediction, and temperature. Demand prediction requires an hour, day, and month. Both prediction models use artificial neural networks, which are trained by previous data.

The accuracy of the management system highly depends on the accuracy of the PHS model. Any scheduling methods require the model of the system to calculate costs for different schedules and determine the best answer. In this project, a comprehensive PHS model is developed to calculate the pump flow rate, stored water and turbine power considering electrical, mechanical, and hydraulic losses of the system,

The proposed management system has several layers of decision making. The first layer determines the irrigation times and required stored water for the next day. The second layer schedules the PHS for the next interval. The duration of the intervals depends on the resolution of the forecast data. In this project, each interval is one hour since the weather forecast data interval is one hour. The scheduling algorithm determines the best microgrid schedule for the rest of the day and updates the schedule hourly. The final layer is a controller to manage the PHS components based on the scheduled program and the current situation of the system. If the current power generation and demand are close to the forecasted data, the controller follows the reference profiles produced by the scheduling method; otherwise, the controller compensates the difference between the forecast data and the actual measurement by adjusting the pump power or turbine flow rate.

2.6.3 Optimisation methods

The scheduling part of the proposed management system needs an optimisation algorithm. The optimisation algorithm schedules the pump, turbine, irrigation and stored water. Many different classical optimisation methods are proposed for energy management like Lambda Iteration, Newton-Raphson, Gradient method, Base Point and Participation Factor method, etc., but they need incremental cost curves to be piecewise linear or monotonically increasing [56]. Classical optimisation methods cannot solve a nonlinear and non-convex problem. Numerous studies have proposed heuristic methods for solving problems that classic optimisations are not able to solve or are too slow for. Heuristic methods that are used in energy management systems are genetic algorithm (GA) [57], ant colony optimisation [58], differential evolution [59], particle swarm optimisation (PSO) [59], bacterial foraging [60], and artificial bee colony algorithm [58], gravitational search technique [61]. These methods may do not necessarily find the global solution, but they are fast enough to be used in energy management systems.

Different optimisation algorithms have been used for PHS management. The sequential quadratic programming (SQP) is used in [62] to solve the optimisation problem by using the "fmincon" function in MATLAB. It scheduled the daily operation of a hybrid system consisting of PV, WT, PHS, and a diesel generator to minimise operating cost. It assumes that the daily operating costs of the PV, the WT, and the PHS are zero, so the optimiser minimises the usage of fuel. A stochastic optimisation method is proposed in [63] to schedule a hydropower plant, regulate reserve market and maximise its revenue. An evolutionary algorithm is also developed in [64] for optimal bidding strategy in PHS. Another article has used a GA to solve a multi-objective problem for optimising usages of a PHS [65].

Among presented optimisation methods, the GA is one of the best optimisers to find the optimum schedule in microgrids. It is able to solve a nonlinear and non-convex problem with an acceptable speed [65]. The GA is an optimisation algorithm inspired by Darwin's theory of evolution. The GA has numerous features, which make it a suitable optimiser for energy management in a microgrid [66, 67]. Several studies have used GA for scheduling microgrid units [68-71]. A GA is a powerful optimiser for

resource allocation and economic dispatch in the Smart Grid [72] and PHS systems [31]. This study uses GA for scheduling the microgrid

Genetic algorithm (GA) is a robust optimisation technique which is able to solve nonlinear and non-convex problems with an acceptable speed [66]. This optimisation algorithm is inspired by Darwin's theory of evolution. Several studies have used GA to schedule microgrid units where it is a powerful optimiser for resource allocation and economic dispatch [31, 69, 73]. GA has been tested for the proposed EMS, and it could determine the global solutions of the constrained optimisation problems of this study in less than the limited time of the system.

Because of the stochastic nature of renewable electricity generation, the scheduled program is not necessarily the optimum operation of the system. Thus, a real-time controller is needed to compensate the forecast data error. The next section will explain how a controller will be used to compensate this error.

2.6.4 Control methods

The optimisation part schedules the storage unit according to the forecast data, but in practice, managing the microgrid exactly according to the output of the optimisation is not efficient for two reasons. First, the forecast data is not 100% accurate. Hence, the generation of PV and energy consumption are not exactly as they are predicted. Secondly, the forecast data is the average of solar radiation at each time interval, so the optimisation is done according to the average generation during each time interval. Therefore, the power generation or consumption may be very different from the scheduled program, so the management system needs a controller to compensate mismatches between forecast and real-time data. This project designed two methods of real-time management to address this problem.

The fuzzy controller is one option to control the proposed PV-PHS system by receiving the PHS schedule and forecast error and adjust pump power and turbine flow rate efficiently. A fuzzy controller works like human logic. In this controller, there is no limitation for inputs and outputs [74]. All the

parameters of this controller can be designed by an expert, or they can be calculated optimally by an optimisation method [75].

Fig 2.11 shows the schematic of a fuzzy controller. In a fuzzy controller, there is no mathematical equation between inputs and outputs. Instead, the controller has three stages: fuzzification, fuzzy inference, and defuzzification. Inputs of the Fuzzy controller are data that are created by scheduling part and measurements. They are numbers, but fuzzy inference needs the membership value of each input for each membership function. The membership functions determine the membership value of the input data. The shape of the membership functions can be selected according to the application of the controller. In this project membership functions will be designed by the GA. The GA will assess possible states in a defined scenario and will find the optimum value of the variables. The rules of the fuzzy controller will be written in fuzzy inference. Finally, the output of the controller needs membership functions for defuzzification. All the membership functions and rules will be optimised by the GA.

A number of authors propose fuzzy inference systems as a supervisory control [13, 76]. When the power generation is equal to the forecast data, the supervisory control manages the microgrid units according to the scheduled power sets. However, when the generation or demand is different from the forecast data, this controller changes the power sets to compensate the forecast error.

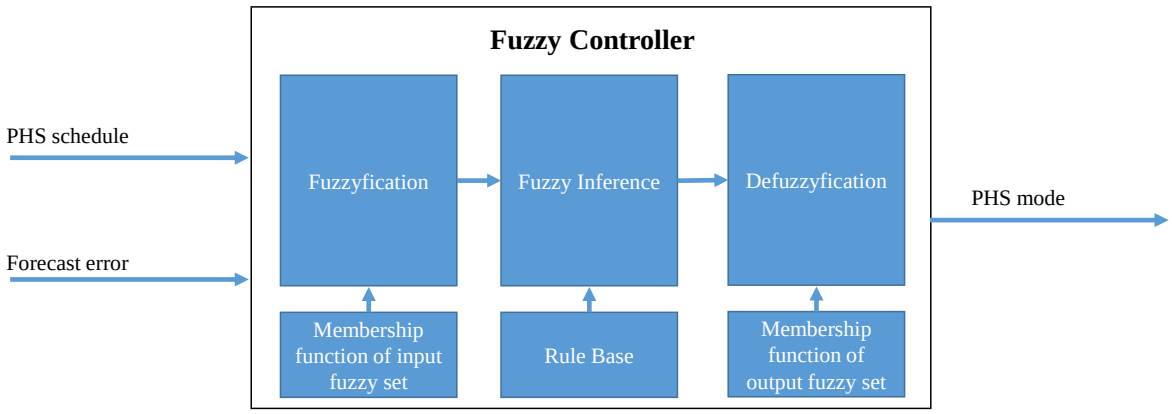

Fig 2.11**:** The schematic of the fuzzy controller

Another option to control the proposed system in real-time is an artificial neural network (ANN). In this method, the ANN is trained by optimal decisions for a large number of samples. ANN provides a complex decision-making network that can make efficient decisions. The main challenge of using ANN in this management system is producing target since there is no obvious answer for many conditions. This project presents a method to produce target data by a GA.

2.6.5 Experimental setup

Fig 2.12 shows the microgrid test site in the smart energy Lab at Edith Cowan University (ECU). It consists of four PV arrays, a pump, a hydro turbine, a reservoir, and a controllable load. This experimental setup is designed to simulate a microgrid with a PHS.

Fig 2.12**:** Microgrid test site in Edith Cowan university

Fig 2.13 depicts the components of the microgrid. The PV panels and the hydro turbine are connected to the AC bus with their inverters. The Pump is also connected to the AC bus via a variable-speed drive (VSD). The VSD can adjust the speed and power consumption of the pump. The load can be controlled to simulate a real energy demand in rural areas. Table 3.1 presents the details of the experimental setup devices.

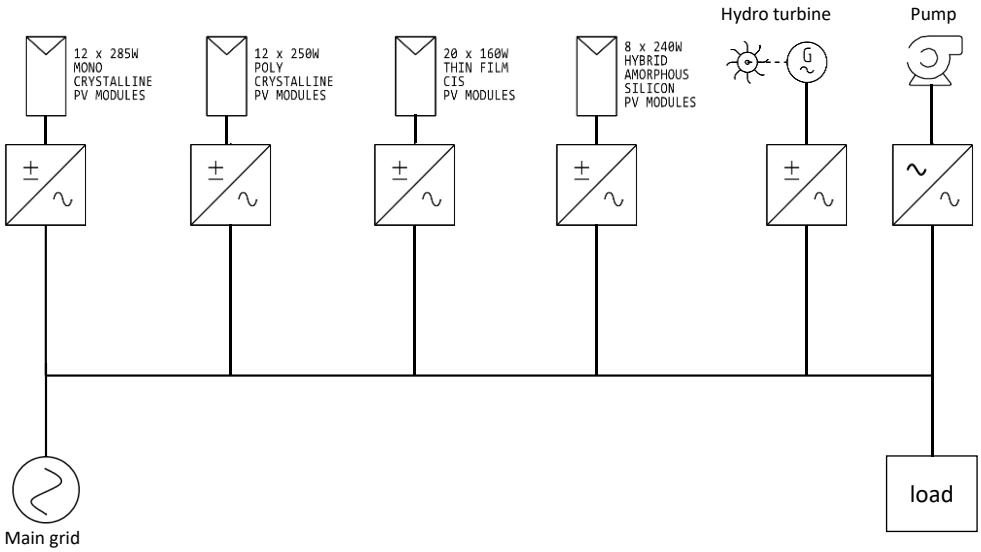

Fig 2.13**:** The schematic of the microgrid

Table 2.1: Smart Energy Lab components details

System	Type	Rated Power	Inverter	Details
Hydro Turbine	PowerSpout TRG 200	768W	Enasolar 2 kW Grid-tied inverter	Flow: 15.3 l/s Head:10 m
Pump	Southern Cross MFD	3000W	VLT HVAC Drive FC 102	Flow: 15-25 l/s Head:10-15 m
PV1	Monocrystalline	285W ×12	SMA 3000HF Grid-tied PV inverter	-
PV2	Polycrystalline	250W×12	Kaco 4202 Grid-tied PV inverter	-
PV3	Thin Film CIS	160W×20	Fronius Galvo 3.0 Grid-tied PV inverter	-
PV4	Amorphous Silicon	240W×8	Fronius Galvo 1.5 Grid-tied PV inverter	With solar tracker
AC Load	-	-	-	Max Load: 3100W×3, 240V
DC Load	-	-	-	Max Load: 3100W×3, 48V

During the pump mode, the water is pumped from the bottom of the reservoir into the top of the reservoir. During this mode, the turbine is off and does not generate energy. The hydraulic head of the test setup is two metres, but in a real water well, the head can be from 10 to 200 metres. To simulate the head of a real well, a valve is installed after the pump. By adjusting the valve handle the pressure and water flow rate will changes a result it can increase the head of the pump. In the turbine mode, the water is pumped through the turbine, but the pump power consumption will be ignored to simulate

releasing water from the ground into the well. There are also four valves before the turbine that can change the pressure of the water. These valves can simulate the head of a well for the turbine.

There are a data collection and controlling system implemented in the lab that measures all the voltages and currents of the components by national instrument DAQ cards. A designed LabVIEW program is shown in Fig 2.14 display and save the data. This data includes PV power generation, demand power, pump power, turbine power and weather parameters.

The irrigation mode of the system will be simulated in the LabVIEW. There is a flow meter in the lab, which measures the water flow rate and sends the data to the LabVIEW. The LabVIEW program will calculate the amount of the stored water in the reservoir by measuring the water flow rate in each operating mode. To simulate the irrigation mode, the LabVIEW program will subtract the amount of water that is required for irrigation from the stored water. Evaporation and precipitation are measured by the weather station installed in the lab, where it assists the reservoir model to accurately calculate the volume water in the reservoir.

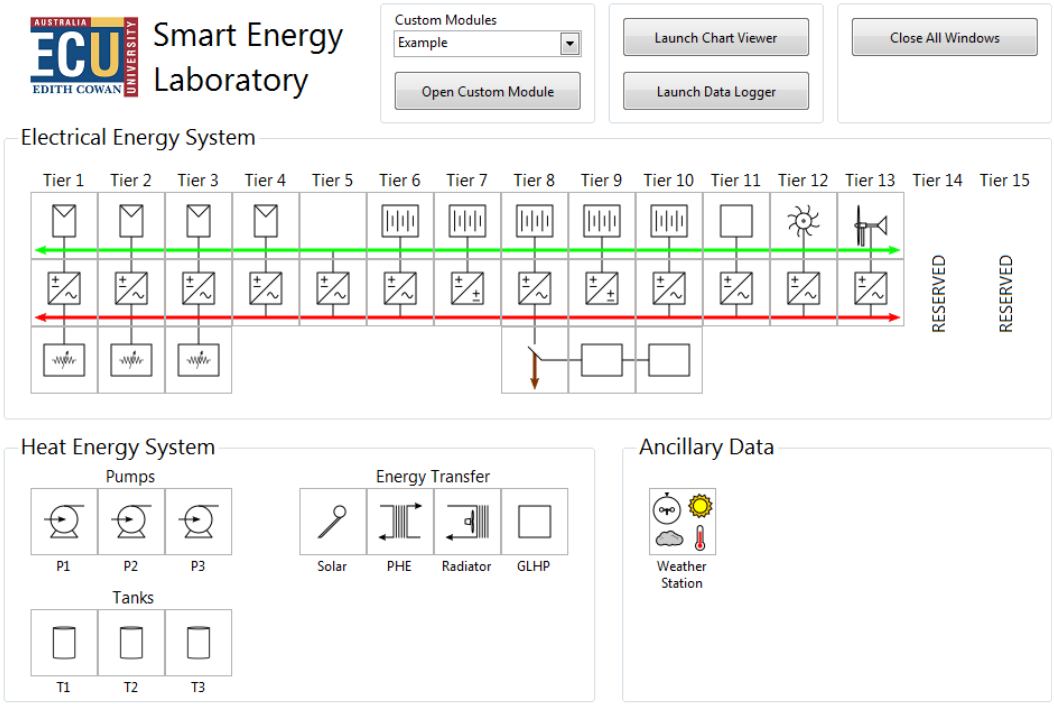

Fig 2.14**:** Smart energy LabVIEW software

2.7 Thesis format

This PhD project proposes a new type of PHS integrated into a farmhouse with a PV system. Both management and simulation require an accurate model of PHS, so in this project first, a comprehensive PHS model is developed. The model is presented in Chapter 3, where its accuracy is tested experimentally. Chapter 4 presents how the proposed PHS can be integrated into a farmhouse. Chapter 5 introduces a new scheduling method specifically designed for the proposed PV-PHS farmhouse which schedules PHS and irrigation. In Chapter 6, a real-time management system is suggested that can cost-effectively control the PHS considering both the current and future condition of the system. Through this project, the economic aspects of the proposed system are analysed for different configurations and management system. It is proved that with an accurate model and an efficient management system the proposed energy storage system can reduce the electricity costs of farmhouses significantly.

Chapter 3: **An improved mathematical model for pumped hydro storage systems** [1]

This chapter proposes a comprehensive pumped hydro storage model with applications in microgrids and smart grids. Existing models within current literature produce high error in calculating stored energy since some critical parameters are ignored. Thus, they are not suitable choices for energy management applications. Accordingly, the main objective of this study is to provide a more realistic model by estimating all the essential parameters in the system. First, all the losses due to the pump, pipes, and fittings are modelled. Next, a water balance approach is used to calculate the volume of water in the upper reservoir considering inflow, outflow, precipitation, and evaporation. Finally, the turbine power is calculated as a function of the water level in the reservoirs, considering the hydraulic losses of the turbine, pipes and fittings. The proposed model is validated using the experimental results of a physical system. The accuracy of the model is compared with other established models. The results demonstrate that the proposed model decreases the error of the estimated stored energy from 13.17% to 0.74%. Moreover, this study shows the capability of the model to simulate different configurations. The model provided in this chapter assists researchers in the field and is of benefit to engineers in designing, sizing, and managing pumped hydro storage systems.

---

[1]This chapter has been published as a full research paper:
N. Mousavi, G. Kothapalli, D. Habibi, M. Khiadani, and C. K. Das, "An improved mathematical model for a pumped hydro storage system considering electrical, mechanical, and hydraulic losses," Applied energy, vol. 247, pp. 228-236, 2019.

Whilst efforts were made to retain original content of the article, minor changes such as number formats and font size style were implemented in order to maintain the consistency in the formatting style of the thesis.

3.1 Introduction

A pumped-hydro storage (PHS) is comprised of two reservoirs, a pump, and a hydro turbine, storing electrical energy in the form of gravitational potential energy. When power generation is higher than demand, the water of the lower reservoir is pumped to the upper reservoir. When power generation is lower than demand, the stored water is released back into the lower reservoir through a hydro turbine in order to generate energy [77]. The capacity of a PHS depends on the volume of the upper reservoir and the height difference between the two reservoirs [78]. Therefore, a large reservoir at a height can form a PHS with lower cost and higher capacity compared to other ESSs. This method of energy storage has attracted much attention in recent years due to the fast growth of RESs in power systems [25, 79]. Ninety-four percent of energy storage projects in the world are PHS systems in terms of rated power [27], where they can be used for a variety of applications such as capacity firming, load levelling, peak shaving, power quality improvement, and spinning reserve.

Most research on PHS installation requires a model to accurately demonstrate the performance of a real PHS system [80, 81]. When sizing the pump, turbine, and reservoir, designers need a PHS model to optimally size the units [31, 37, 82], where a more accurate model produces a more realistic solution. Most energy management systems (EMSs) in this area require a PHS model with high accuracy in order to schedule the pump and turbine [62, 83-85]. The efficiency of these EMSs depends highly on the accuracy of estimated stored energy in the PHS. A model with low accuracy reduces the efficiency of EMSs by making wrong decisions. Accordingly, a model with high accuracy is necessary for both studying and managing PHS systems.

Current PHS models within the literature have high errors in calculating stored water. The simple PHS simulation model (model one) has two equations [31, 37, 51, 62, 80, 81, 83-91], including the pump equation and the turbine equation. Both equations consider the efficiency of the pump and the turbine, but hydraulic and mechanical losses of the system are not considered.

Some other studies [92, 93] have improved the accuracy of the PHS simulation model by considering hydraulic losses involved in pumping water (model two). Accordingly, the authors added a head loss to the static head of the pump to account for the hydraulic losses of the penstock due to friction. The authors calculated pipes and fittings losses, but some parameters such as friction factor, relative roughness, and Reynolds number were considered as fixed values. However, these parameters depend on water velocity, pipe diameter, and pipe material. In addition, this model does not calculate the hydraulic losses of the turbine mode. This model improved the accuracy of the PHS model compared to model one, but the error of model two is still high.

The next limitation of model two is that the weather effect on the water level of the reservoir has not been considered. Usually, upper reservoirs are open top, and they are exposed to the sun and wind, where water surface evaporates every day. This reduces the volume of water in the reservoir, which leads to a reduction in stored energy. Contrastingly during precipitation, rainwater is added naturally to the reservoir. Therefore, to obtain a complete PHS model the effect of weather on the volume of water in the reservoir should be considered.

Another problem with both established PHS models is that they ignore changes in water levels of the reservoirs. While a PHS is in pump mode or turbine mode water levels go up and down. These variations in water levels change the heads of the pump and the turbine.

This study proposes three major modifications to previous PHS models: (1) to reduce errors in flow rate calculation in the pump mode, the proposed model calculates the head loss of the penstock by calculating the friction factor, the relative roughness, and the Reynolds number according to the water velocity, pipe diameter, and pipe material; (2) to increase the accuracy of the water volume calculation, this model estimates the evaporation from the water surface of the upper reservoir; (3) to reduce errors in turbine power calculation, the turbine model calculates the head loss and the flow rate as a function of the water levels in both reservoirs. All these modifications help the model to calculate generated and stored energy with greater accuracy.

The chapter is organized as follows: Section 2 presents the proposed pump, reservoir, and turbine models. Section 3 validates the mathematical model by comparing the simulated model and experimental results. In Section 4.1, the proposed model is compared with other PHS models in different scenarios and weather conditions to show how much the modifications have increased the accuracy of the model. Section 4.2 shows the capabilities of the model in different configurations, and finally, Section 5 provides conclusions.

3.2 Pumped hydro storage model

This section presents mathematical models for different components of the proposed PHS model. The main focus here is to take account of all the losses of the three PHS components including the pump, the reservoir and the hydro turbine. The proposed model is designed in a way that all the required parameters can be found in the technical manuals of the components, so researchers are able to use this model without any further experiments.

3.2.1 Pump model

The pump model calculates the flow rate of the pump (Q_p) as a function of the input power (P_m). A pump unit includes a pump and an electric motor. The motor converts electrical energy into mechanical energy and drives the pump to deliver the water from the lower reservoir to the upper reservoir. The efficiency of the motor (η_m) represents how much of its input energy is wasted due to electrical and mechanical losses of the motor. In motors, η_m is a function of P_m (Eq. 3.2). This efficiency-power curve can be found in the technical manual of the motors. Thus, the input mechanical power of the pump (P_p) can be calculated from:

$$\mathrm{P_p} = \mathrm{P_m}\eta_\mathrm{m} \tag{3.1}$$

$$\eta_\mathrm{m} = \phi(\mathrm{P_m}) \tag{3.2}$$

In this model, Q_p is a function of P_p, the total head of the pump (H_p), and the pump efficiency (η_p) and defined as [94]:

$$\mathrm{Q_p} = \frac{\mathrm{P_p}\eta_\mathrm{p}}{\rho \mathrm{g H_p}} \tag{3.3}$$

$$\eta_\mathrm{p} = \phi(\mathrm{Q_p}) \tag{3.4}$$

Eq. (3.4) indicates that η_p is a function of Q_p. This efficiency-flow rate curve can be found in manufactures technical manuals. In Eq. (3.3), H_p is the sum of the static head (H_s) and the head loss of pump mode (H_{pl}):

$$\mathrm{H_p} = \mathrm{H_s} + \mathrm{H_{pl}} \tag{3.5}$$

H_s is the vertical distance between the water surface in the upper reservoir and the water surface in the lower reservoir. H_s changes as water levels rise and fall due to pumping and releasing water. H_{pl} changes when Q_p changes and represents the hydraulic losses of the pump mode due to friction between the water and the inner surface of the pipes and fittings. This model calculates H_{pl} as a function of Q_p using Darcy–Weisbach equation [95]:

$$\mathrm{H_{pl}} = \mathrm{K}\frac{\mathrm{v}^2}{2\mathrm{g}} \tag{3.6}$$

$$\mathrm{v} = \frac{\mathrm{Q_p}}{0.25\pi {\mathrm{D_p}}^2} \tag{3.7}$$

$$\mathrm{K} = \mathrm{K_{pipe}} + \mathrm{K_{fittings}} \tag{3.8}$$

$$\mathrm{K_{pipe}} = \frac{\mathrm{f\,L_p}}{\mathrm{D_p}} \tag{3.9}$$

$$f = \left[1.8 \log\left(\frac{6.9}{Re} + \left(\frac{\varepsilon/D_p}{3.7}\right)^{1.11}\right)\right]^{-2} \tag{3.10}$$

$$Re = \frac{\rho v D_p}{\mu} \tag{3.11}$$

The total resistance coefficient (K) is the sum of the resistance coefficient of the pipe (K_{pipe}) defined by Eq. (3.9) and the resistance coefficient of the fittings ($K_{fittings}$). Eq. (3.9) calculates the K_{pipe} as a function of the friction factor (f). Eq. (3.10) shows the relationship between friction factor (f), Reynolds number (Re), and the relative roughness of the pipe (ε/D). This equation is derived from the Moody chart in order to approximately calculate the friction factor (f) [36]. Eq. (3.11) calculates Reynolds number (Re) as a function of water velocity and pipe diameter. In penstocks, $K_{fittings}$ and absolute roughness (ε) depend on the fitting type and the pipe material, respectively.

3.2.2 Reservoir model

The reservoir model estimates the volume of the stored water in the upper reservoir ($\forall$) which is a function of the incoming flow, the outgoing flow, and losses due to evaporation assuming zero seepage. Evaporation depends on temperature (T_{hr}), relative humidity (RH), net radiation (R_n), and wind velocity at 2 m above the water surface (u_2). Hourly evaporation in this study is calculated by FAO Penman-Monteith equation [96]:

$$ET_\circ = \frac{0.408\Delta(R_n - G) + \gamma \frac{37}{T_{hr} + 273} u_2 (e^\circ(T_{hr}) - e_a)}{\Delta + \gamma(1 + 0.34u_2)} \tag{3.12}$$

$$\forall_{eva}(\Delta t) = ET_\circ \, A \, \Delta t \tag{3.13}$$

Precipitation is another parameter that influences $\forall$. Generally, upper reservoirs are open top, so precipitation adds water to the reservoir. For example, in tropical rainforest climate regions, the annual average rainfall is between 150 and 400 centimetres [97]. Failing to account for water added to the

reservoir due to precipitation considerably increases the error of the stored water calculation. Specifically, in energy management systems, calculating ∀ with high accuracy is critical since the management of the whole system depends on the volume of stored water. Therefore, the volume of precipitation ($\forall_{pre}$) and the volume of evaporation ($\forall_{eva}$) should be considered in the reservoir model. Accounting for evaporation and precipitation, the model of a reservoir may be expressed as Eq. (3.14) and Eq. (3.15):

$$\forall(\mathrm{t}) = \mathrm{Q_p}\,\Delta\mathrm{t} - \mathrm{Q_t}\,\Delta\mathrm{t} + \forall_{\mathrm{pre}}(\Delta\mathrm{t}) - \forall_{\mathrm{eva}}(\Delta\mathrm{t}) + \forall(\mathrm{t} - \Delta\mathrm{t}) \tag{3.14}$$

$$\forall_{\mathrm{pre}}(\Delta\mathrm{t}) = \mathrm{I\,A}\,\Delta\mathrm{t} \tag{3.15}$$

where the incoming flows are subtracted from the outgoing flows to calculate the amount of water that is added to the reservoir during one time interval. This amount of water is then added to the previous volume of water to calculate the current volume.

To calculate H_s the water levels in the reservoirs are required:

$$\mathrm{H_s} = \mathrm{H_r} + \mathrm{H_{uwl}} + \mathrm{H_{lr}} - \mathrm{H_{lwl}} \tag{3.16}$$

Water level in the lower reservoir (H_{lwl}) depends on the incoming and the outgoing water from the reservoir and can be calculated based on the geographical features of the area. The H_{lwl} is an input of the reservoir model. For PHS systems where water levels of the lower reservoir change during the day, the H_{lwl} needs to be estimated according to geographical features of the lower reservoir and added to this model.

The water level in the upper reservoir (H_{uwl}) can be calculated from Eq. (3.17) assuming the reservoir has a cuboid shape (Fig 3.4). This equation can be modified according to the shape of the reservoir.

$$\mathrm{H_{uwl}} = \frac{\forall}{\forall_{\mathrm{res}}} \times \mathrm{H_{ur}} \tag{3.17}$$

3.2.3 Hydro turbine model

The hydro turbine model calculates the output power of the hydro turbine unit (P_t) as a function of the flow rate (Q_t) and the turbine head (H_t). In this unit, kinetic energy is converted into electrical energy. Turbine efficiency (η_t) shows how much power is lost in the turbine due to mechanical and electrical losses and how much is converted to electrical energy. In turbines, η_t is a function of Q_t. Turbine manufacturers provide this efficiency-flow rate curve for each turbine they manufacture. The mathematical model of the hydro turbine is presented by [98]:

$$\mathrm{P_t} = \mathrm{Q_t H_t \rho g \eta_t} \tag{3.18}$$

$$\eta_\mathrm{t} = \phi(\mathrm{Q_t}) \tag{3.19}$$

The turbine head (H_t) equals H_s minus the head loss between the upper reservoir and the turbine outlet (H_{tl}). This head loss can be calculated from Eq 3.6 to Eq 3.11. Q_t depends on water levels in the reservoirs and can be obtained using Bernoulli equation defined as [99]:

$$\frac{\mathrm{P_1}}{\rho \mathrm{g}} + \frac{{\mathrm{v_1}}^2}{2\mathrm{g}} + \mathrm{h_1} = \frac{\mathrm{P_2}}{\rho \mathrm{g}} + \frac{{\mathrm{v_2}}^2}{2\mathrm{g}} + \mathrm{h_2} + \mathrm{H_{tl}} \tag{3.20}$$

In Eq. (3.19), the surface of the water in the upper reservoir is considered as point 1. Accordingly, the turbine outlet is considered as point 2 where the reference level is zero ($\mathrm{h_2} = 0$). At point 1, the pressure is atmospheric and v_1 is zero. The pressure at point 2 is equal to the height of the water in the lower reservoir (H_{lwl}). Therefore, Eq. (3.20) reduces to:

$$\mathrm{h_1} = \mathrm{H_{lwl}} + \frac{{\mathrm{v_2}}^2}{2\mathrm{g}} + \mathrm{H_{tl}} \tag{3.21}$$

The difference between $\mathrm{h_1}$ and H_{lwl} equals the vertical distance from the water surface in the upper reservoir to the water surface in the lower reservoir, which is defined in this study as H_s in Eq (16). Therefore, the water velocity at the turbine ($v_2 = v_\mathrm{t}$) is given by:

$$v_t = \sqrt{2g(Hs - H_{tl})} \tag{3.22}$$

By placing Eq. (3.7) into Eq. (3.22) and also considering the percent openness of the turbine valve (T_v), Q_t can be obtained from Eq. (3.23) and Eq. (3.24):

$$Q_t = \frac{T_v}{100} a\sqrt{2g(Hs - H_{tl})} \tag{3.23}$$

$$a = 0.25 \times \pi \times D_t^{\,2} \tag{3.24}$$

The turbine valve is located on the upper reservoir outlet in order to control Q_t. Another parameter that affects Q_t is the pipe diameter (D_t). Fig 3.1 shows all the equations for the proposed PHS model. This model first calculates Q_p during the pump mode. Next, ∀ is calculated. Finally, P_t is calculated during the turbine mode. The operating mode of this model can be controlled by adjusting P_m and T_v. In practice, P_m can be controlled by a variable speed drive, and T_v is the percent openness of a solenoid valve (where 0 means fully closed and 100 means fully open), which controls Q_t from zero to the maximum rate.

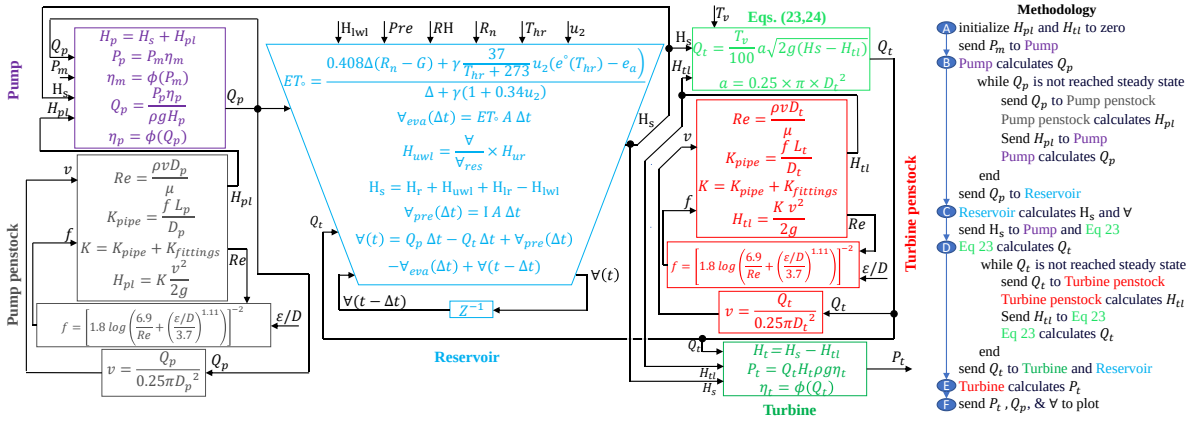

Fig 3.1: The proposed PHS model and the sequence of calculation

3.3 Simulation and experimental validation

This section compares the results of the proposed mathematical PHS model with the experimental results to verify the accuracy of the model. The proposed model is simulated in MATLAB Simulink (Fig 3.2). All the equations in Section 2 are written in the MATLAB function blocks and connected

together to simulate a PHS model. The experiments were conducted on an experimental setup, a physical PHS system installed at Edith Cowan University (Fig 3.3). Fig 3.4 depicts the PHS configuration, and Table. 3.1 represents the characteristics of the pump, turbine, reservoir, pipes, and fittings.

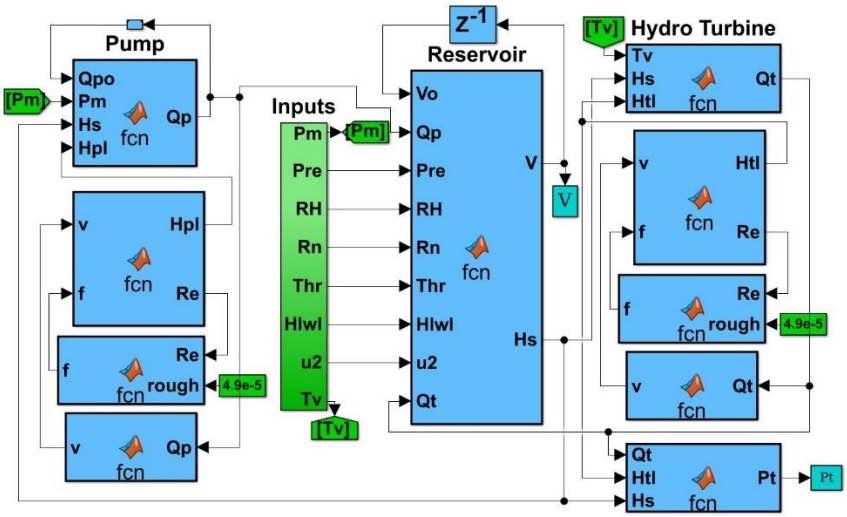

Fig 3.2: The PHS simulation in MATLAB Simulink

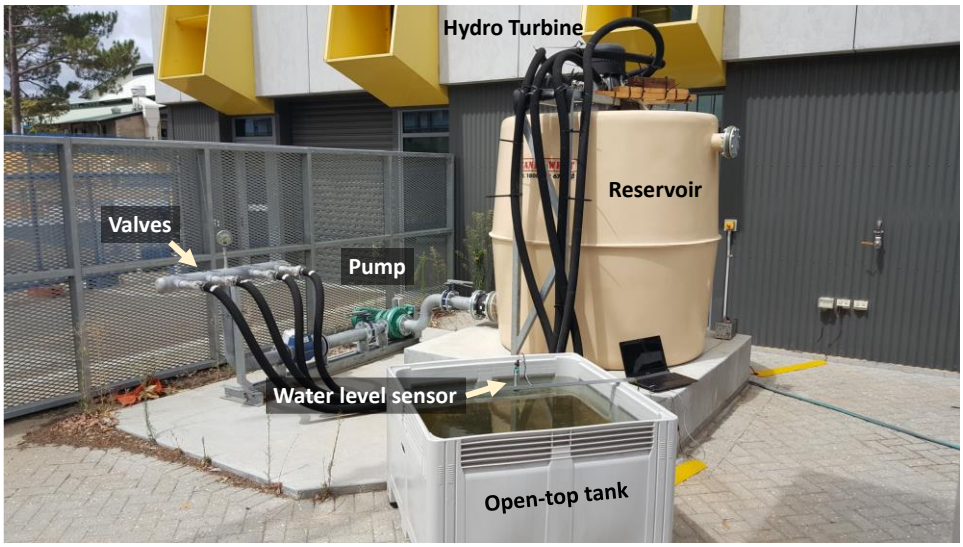

Fig 3.3: Experimental setup of the PHS system

The pump and turbine operating modes are simulated in the experimental setup. During the pump mode, the water is pumped from the bottom of the reservoir into the top of the reservoir to simulate pumping water from the lower reservoir to the upper reservoir. To simulate the static head (H_s) and the head loss (H_{pl}), four valves are installed after the pump. If the percent openness of these valves decreases, the

resistance coefficient of the valves (K) increases proportionally, so these valves can increase the total head of the pump (H_p). Thus, H_p is simulated in the experimental setup by adjusting the valves. In the turbine mode, the water is pumped through the hydro turbine to simulate releasing water from the higher reservoir into the lower reservoir. The pressure and the flow rate can be adjusted by controlling the pump speed and the pump valve to simulate the turbine head (H_t) in the experimental setup. The water level of an open-top tank was also continuously measured to determine the amount of evaporated water from the reservoir. In this experiment, it is assumed that the lower reservoir is considerably larger than the upper reservoir, and its water level change is negligible throughout the day.

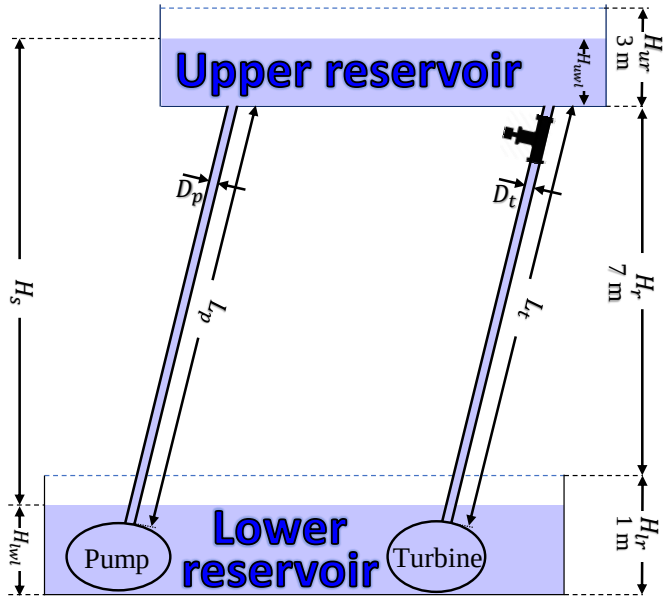

Fig 3.4: PHS configuration used in the simulation and the experiment

Table 3.1: Parameters of the PHS system.

Pump	Southern Cross, Type: MfD47A Impeller diameter: 211 mm	
Turbine	Power Spout, Type: TRG Rated: 768 w, 10 m, 15.3 L/s	
Pump Penstock	Material: carbon steel Inside diameter: 102.3mm Fittings resistance coefficient ($K_{fittings}$): 1	ε/D :0.000049 length:13 m
Turbine Penstock	Material: carbon steel Inside diameter: 102.3mm Fittings resistance coefficient ($K_{fittings}$): 1	ε/D :0.000049 length:13 m
Upper reservoir	$\forall_{res} = 1200\ m^3$	

3.3.1 Pump experiment

Fig 3.5 compares the results of the pump model with the experimental results in different input powers (P_m) and H_s. In the experiment, P_m was decreased from 3000 W (rated power) to 500 W using a drive, and the output flow rate (Q_p) was measured. In the simulation, the same amount of P_m was applied to the pump model to calculate Q_p. Results illustrate that the pump model can calculate Q_p with a low error over a wide range of P_m. The pump model error around the rated power is close to zero as the model accurately calculates the losses of the pump and the penstock. However, as the operating mode departs from the rated operating point, the error increases. This is due to the difference between the efficiency curve provided by the manufacturer and the efficiency of the pump in the experiment. Fig 3.5 shows the efficiency of the pump mode considering the losses of the motor, the pump, the pipes and the fittings for both the experiment and the mathematical model. In the mathematical model, the efficiency curve provided by the manufacturer is applied. In the experiment, the efficiency is calculated according to the measured flow rate and pressure.

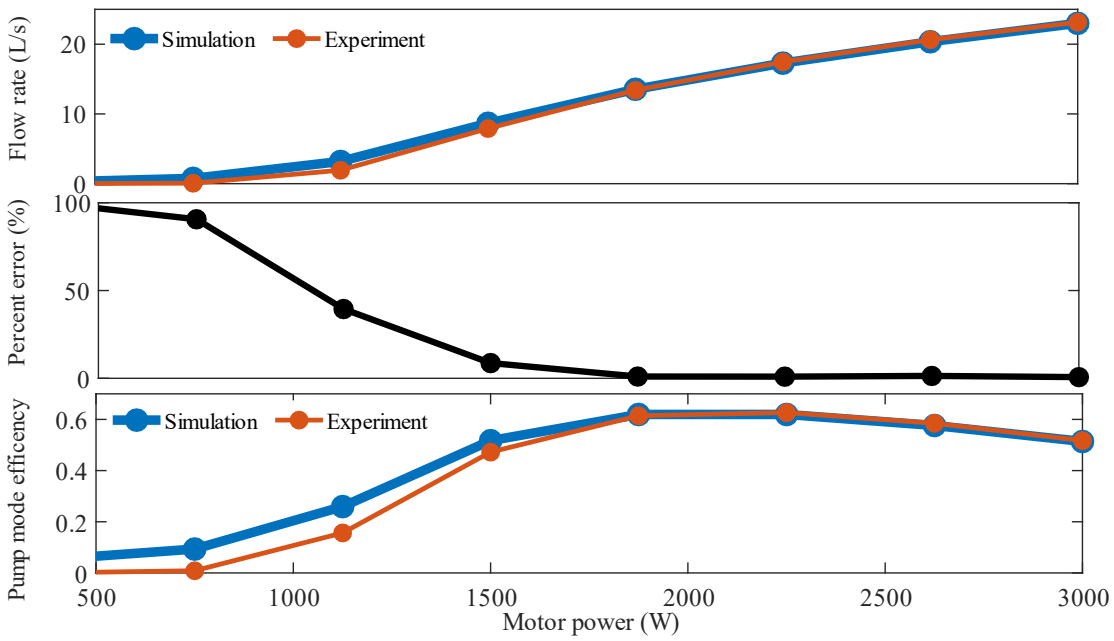

Fig 3.5: Simulation result of the pump model compared with the experimental result

3.3.2 Turbine experiment

Fig 3.6 shows the results of the turbine model and the experiment. It demonstrates that the calculated power is very close to the measured power at various turbine flow rates (Q_t) and H_s. H_s decreases as water is released down through the turbine. Results show that the error is small in the wide range of the operating points. The reason for this variation between the simulation and the experiment relates to the difference between the efficiency curve provided by the turbine manufacturer and the efficiency of the turbine in the experiment. This difference can be seen in the efficiency curves shown in Fig 3.6, which show the efficiency of the turbine mode considering the losses of the turbine, the pipes, and the fittings for both the simulation and the experiment.

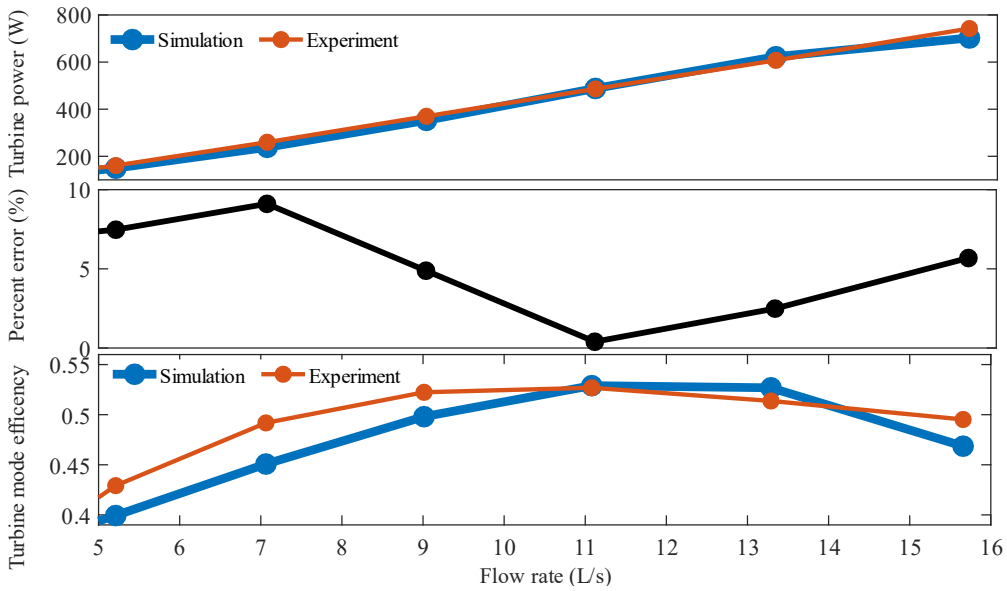

Fig 3.6: Simulation result of the turbine model compared with the experimental result

3.3.3 Reservoir experiment

This experiment compares the estimated evaporation with the measured evaporation. In this experiment, an open-top tank (Fig 3.3) was filled with water, and the level of the water was measured for 10 days to determine how much water evaporated each day from the upper reservoir. During the experiment, weather conditions were recorded and used in the simulation as the inputs of Eq. (3.12). The results of

the simulation and the experiment are presented in Fig 3.7, which shows daily evaporation rate per square metre. Results indicate that the error of the estimated evaporation is lower than 1 mm per day.

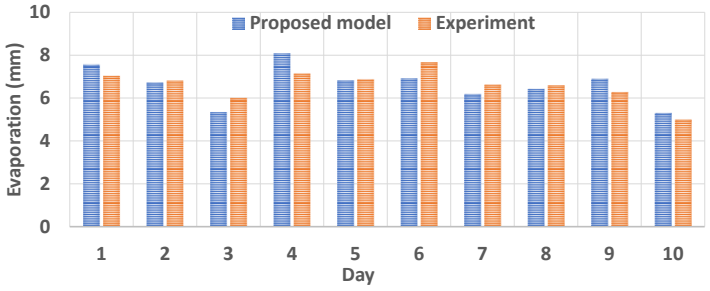

Fig 3.7: Simulation result of the evaporation model compared with the experimental result

3.4 Comparison of the PHS models

This section compares the results of the proposed model with model one [31, 37, 51, 62, 80, 81, 83-91] and model two [92, 93]. The operation of the physical PHS model was measured for 10 different days between August and December. In this experiment, 10 random scenarios were used for the operating mode of the PHS, and a weather station was installed near the experimental setup to measure temperature, humidity, wind speed, irradiance, and precipitation. The same scenarios and weather conditions were used for simulation of the models. Fig 3.8 presents the weather conditions on the first day.

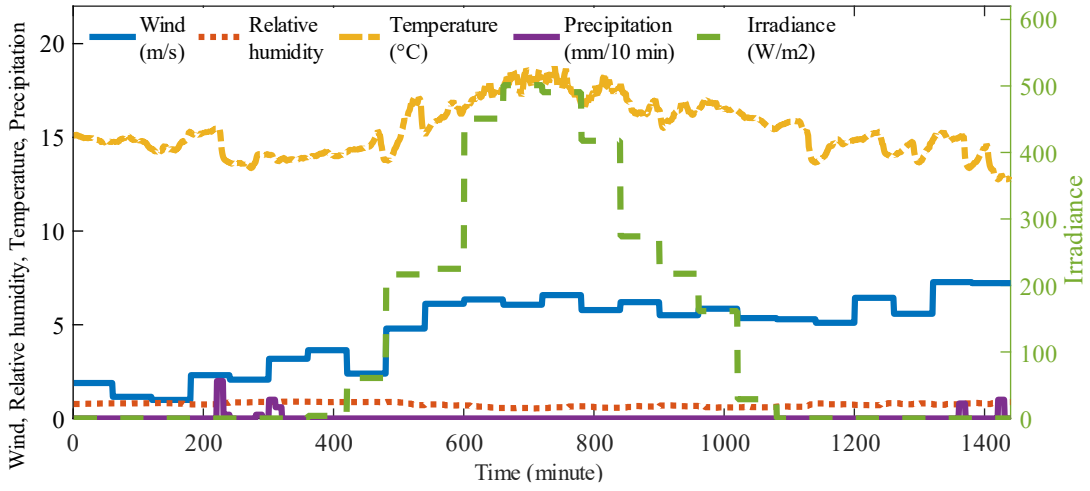

Fig 3.8: The weather condition on the first day

The accuracy of the model is presented by percent error. The percent error is the difference between estimated value by the model and the experimental value. Lower percent error means higher accuracy, which is calculated using Eq. (3.25) [100, 101].

$$\%\text{error} = \left|\frac{\text{Experimental value} - \text{Model value}}{\text{Model value}}\right| \times 100 \tag{3.25}$$

Fig 3.9 illustrates the performance of the PHS models on the first day. The input powers of the pump models (P_m) were changed during the day to show the error in different operating points. As illustrated in the results, the error in the proposed pump model is much smaller than other models since the head loss (H_{pl}) is estimated with relatively high accuracy. Model one has a high error in calculating the pump flow rate (Q_p) because it does not consider hydraulic losses. Although model two reduces the error by including the hydraulic losses of the penstock, the error is still high since the Reynolds number (Re) and the friction factor (f) are both constant numbers in this model. However, in the proposed model, f is calculated by Eq. (3.10), and Re is calculated as a function of Q_p.

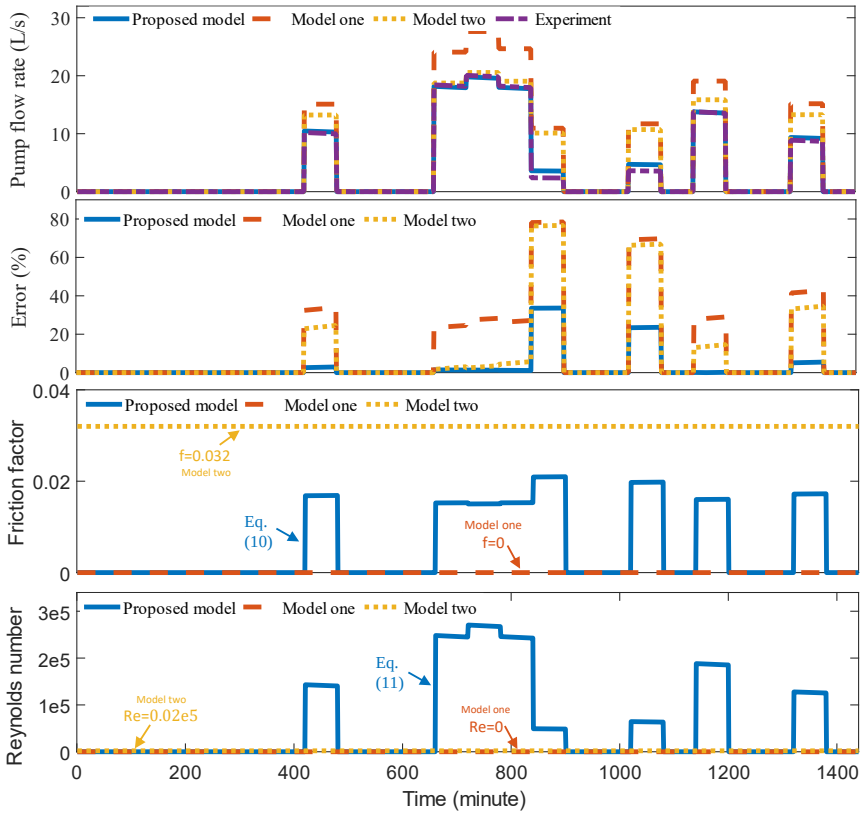

Fig 3.9: Pump performance in different PHS models

Fig 3.10 presents the error of the turbine power calculation in different PHS models on the first day. It demonstrates that the errors are not constant; they change with increases and decreases in the flow rate (Q_t) and the head (H_t) during the day. The comparison of these results reveals that both model one and model two have an equal error in turbine power calculation (P_t) as these models do not consider the H_t variations, Q_t variations, and the penstock losses (H_{tl}). However, the proposed model could reduce the error significantly by estimating both H_t and Q_t considering the water levels in the reservoirs and calculating the head loss in the penstock by Eq 3.6 to Eq 3.11.

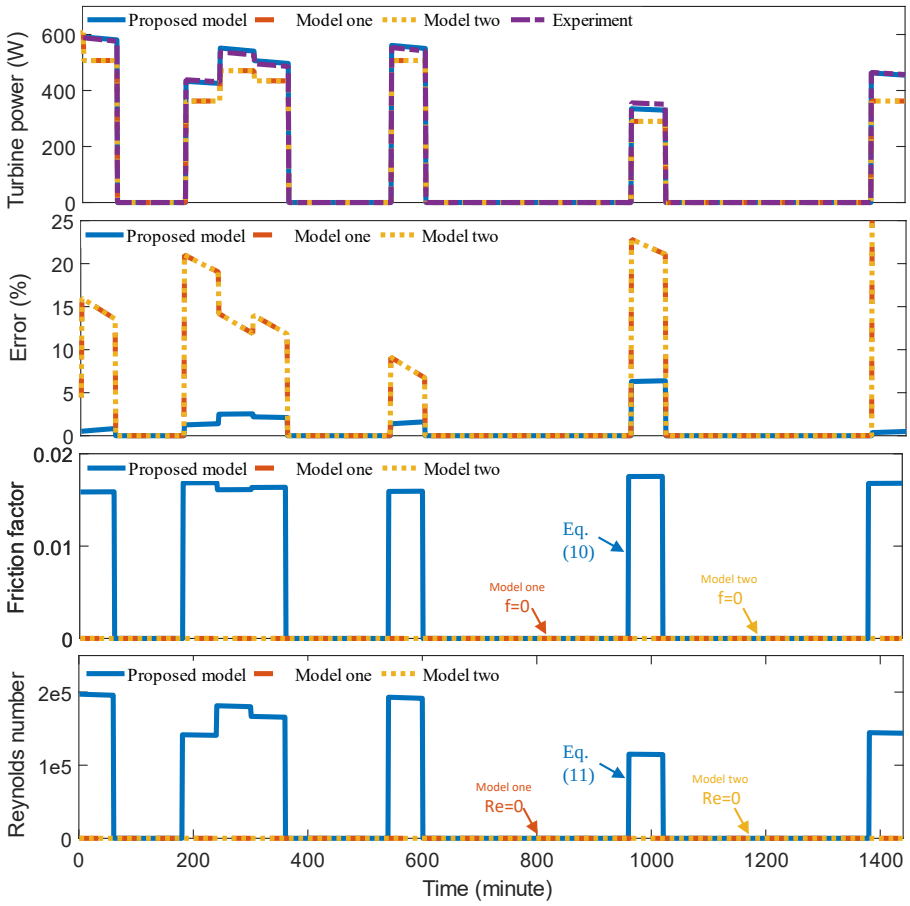

Fig 3.10: Turbine performance in different PHS models

Fig 3.11 compares the percent error of the PHS models in calculating the volume of water in the upper reservoir (∀) on the first day. It is apparent from the chart that the error of the proposed model is much smaller than both model one and model two due to the high accuracy of calculating the hydraulic losses, evaporation, precipitation, and water levels.

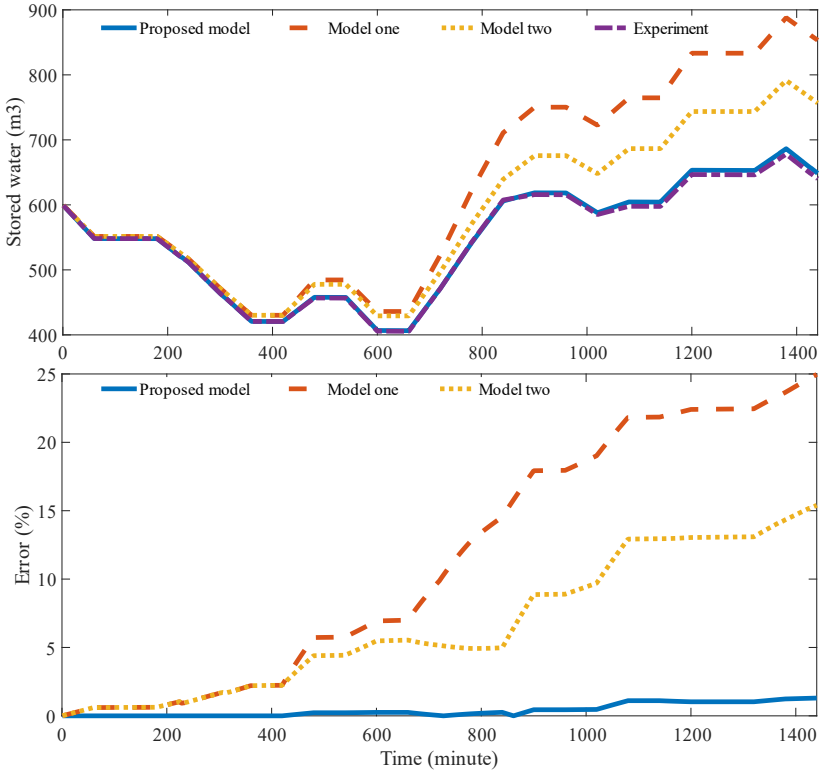

Fig 3.11: The error of the stored water calculation in different PHS models

Model one has a high error since Q_p and Q_t are calculated with a large error. Model two has a lower error than model one because it calculates Q_p including the hydraulic losses, but still, the error is significant. As shown in Fig 3.9, the proposed model more accurately calculates Q_p than model two, where the proposed model estimates the volume of pumped water to the reservoir more precisely which increases the accuracy of calculating ∀.

Another system parameter is precipitation. The proposed model added the precipitation to ∀, whereas established models have not considered this incoming water to the reservoir.

Another parameter that influences the accuracy of the reservoir model is the consideration of water level and H_{tl} in Q_t calculation. Model one and two have not considered these two parameters to calculate the outgoing flow rate. However, the proposed model calculates Q_t by Eq. (3.23) considering the water level in both reservoirs and H_{tl}. This calculation has helped the proposed model to calculate the amount of outgoing water from the reservoir more accurately within the turbine mode.

Evaporation is another water loss from the reservoir that both model one and two have ignored. However, the proposed model calculates evaporation considering temperature, relative humidity, irradiance, and wind speed.

Fig 3.11 also illustrates that the small error of model one and two in calculating incoming and outgoing water can make a large error over a long period of time. At the beginning of the simulation, the error of all the three models are zero; however, after 24 hours, model one has 25% error, and model two has 15% error. This shows that these two models are not appropriate for scheduling and energy management of a PHS over a long period of time since there are significant differences between the estimated stored water and reality.

So far, this section has focussed on the results of the first day. The following discussion will concentrate on the overall results of the experiments throughout the 10 days of observation.

Fig 3.12 presents the percent error of each unit over the 10 days. Numbers written on each group in the figure indicate the average percent error for the 10 days.

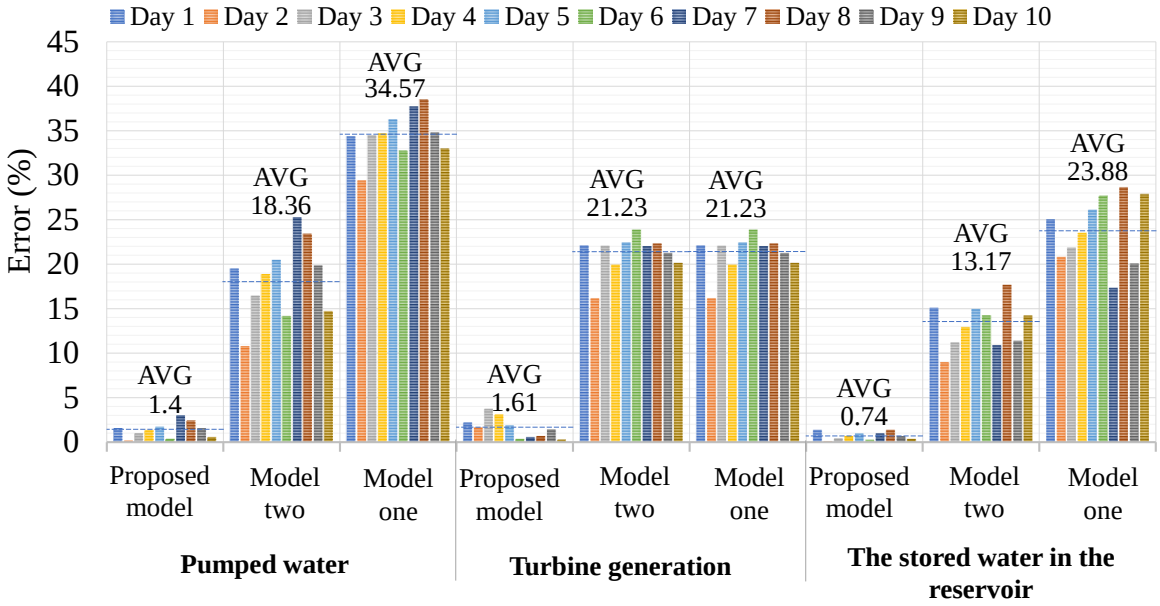

Fig 3.12: Percent error of each unit of the model (pump, turbine, and reservoir) for 10 days

The results illustrate a 16.96% reduction in average pump model error in the proposed model compared to model two because of: (1) calculating the hydraulic losses in the penstock according to Q_p and (2) considering the water level in the reservoirs.

The percent error of the turbine generation shows the error in the total amount of calculated energy generation compared to the experiment results within 24 hours. In the turbine model, the error is dropped by 19.62% on average mainly because of considering water levels and H_{tl} in calculating the turbine power.

The third part of Fig 3.12 presents the error of the calculated stored water in the upper reservoir at the end of the day. The results show a 12.43% reduction in the percent error of the reservoir model compared to model two due to consideration of all incoming and outgoing water in the upper reservoir.

These experiments have tested the PHS models in a variety of operating modes and weather conditions to evaluate the accuracy of the PHS models. The results indicate a substantial reduction in the error of the three units.

3.5 The effect of the ageing of the equipment on the model

Ageing would affect the pump, penstocks, and turbine. Ageing would increase the head loss by effecting the friction factor (f) of the penstocks. The friction factor is a function of roughness (ε) where roughness is the amount of surface roughness that exists inside the pipe. Roughness increases with time due to encrustations and biofouling. This increase in roughness depends on the type of pipe and its diameter. Ageing also has effects on the pump efficiency (η_p) and the turbine efficiency (η_t). Efficiency curves may change by ageing, but they depend on how the pump and the turbine were operated and maintained. There would not be any effect on the reservoir due to ageing since it has no effect on the evaporation rate.

3.6 Proposed model performance in different cases

This section presents the performance of the proposed model in seven cases as an example that shows the capability of the model in different configurations. In each case, there is one difference compared to Case 1. Table 3.2 shows the characteristics of these cases. Fig 3.13 (a) shows the pump flow rate during pump mode while the pump powers are gradually increasing. Whilst the powers increase, H_{uwl} also rises due to the pumping water. Fig 3.13 (b) shows the turbine power as the turbine flow rate gradually increases; where because of this outflow of water, $\forall_{res}$ gradually reduces.

In Case 2, the vertical distance between the two reservoirs (H_r) is increased by 5%, which raises the pump static head (H_s). As a result, the pump power is decreased by 2.2% at rated power. This decline is non-linear since H_{pl} has a nonlinear relationship with the pump power, and the pump power is a function of H_s and H_{pl}. This increase in H_r increases turbine flow rate by 5%. This shows the linear relationship between H_r and P_t.

Table 3.2: PHS characteristics used in various cases

Case	Reservoir			Pump & turbine		Penstock				Change
	H_r (m)	H_{ur} (m)	$\forall_{res}$ (m^3)	Pump	Turbine	D_p & D_t (m)	ε (mm)	$K_{fittings}$	L (m)	
1	380	90	4.5e6	Single-pump	Single-turbine	5	0.8	10	1152	-
2	400	90	4.5e6	Single-pump	Single-turbine	5	0.8	10	1152	Reservoir height
3	380	70	6e6	Single-pump	Single-turbine	5	0.8	10	1152	Reservoir dimensions
4	380	90	4.5e6	Multi-pump	Multi-turbine	5	0.8	10	1152	Pump & Turbine
5	380	90	4.5e6	Single-pump	Single-turbine	3	0.2	10	1152	Pipe type
6	380	90	4.5e6	Single-pump	Single-turbine	5	0.8	50	1152	Fittings type
7	380	90	4.5e6	Single-pump	Single-turbine	5	0.8	10	23040	Pipe length

Case 3 demonstrates the effect of the volume of the upper reservoir ($\forall_{res}$) and the height of the upper reservoir (H_{ur}) on the pump mode performance. Fig 3.13 (a) shows 33.3% rise in $\forall_{res}$ increases the pump flow rate by 4.5% at rated power. It can be seen that the pump flow rate drop is lower than Case

1 due to the lower increase of H_s while pumping. The reason for this is that the reservoir has a greater area. In low turbine flow rate, the turbine power in Case 3 is lower than Case 1 since the reservoir height is 22.2% lower. However, in high turbine flow rate, the power is 3% higher than Case 1 since the reservoir is larger, and H_{uwl} does not drop as much as Case 1.

In Case 4, instead of a single pump-single turbine, five pumps and turbines are used to increase the efficiency of the PHS in a wide range of input and output powers. Pumps are modelled separately using Eq 3.1 to Eq 3.5, and then the pump outputs are added and sent to the penstock Eq 3.6 to Eq 3.11. The results show that in a multi-pump PHS the flow rate increases in a more linear manner as at each step one pump is added to the system, where each pump works at their rated operating points. To model a multi-turbine PHS, each turbine is modelled by Eq. 3.18 and Eq. 3.19. When the turbine flow rate is low, one turbine works in its rated operating point. Then in each step, one turbine is added to the system. This continues until all the turbines work together. It can be seen that in a multi-turbine PHS, the turbine power increases in a more linear manner than in a single turbine.

Case 5 shows the effect of pipe characteristics on PHS performance. Although absolute roughness (ε) is less than Case 1, 40% reduction in pipe diameter (D_p) decreased the pump flow rate by 10% at rated power. The reason for this is that the reduction in D_p increases H_l significantly, and higher H_l reduces Q_p. This reduction in the pipe diameter reduced the turbine power by 28% at rated flow. It is apparent from this curve that the pipe diameter effect on the turbine power is higher in high flow rates and less in low flow rates.

Case 6 shows the effect of the fitting resistance coefficient ($K_{fittings}$) on the PHS performance. In this case, $K_{fittings}$ is five times greater than Case 1. This can be due to a greater number of fittings being applied or using different types of fittings. This increased H_l, so the pump flow rate declined by 5% at rated power. This increase in $K_{fittings}$ reduced the power by 11% at rated flow.

The pips length depends on the geographical condition of the site. Case 7 illustrates that a pipe that is 20 times longer decreased pump flow rate by 6.8% and increased the head loss in turbine mode. As a result, the output power was reduced by 16%.

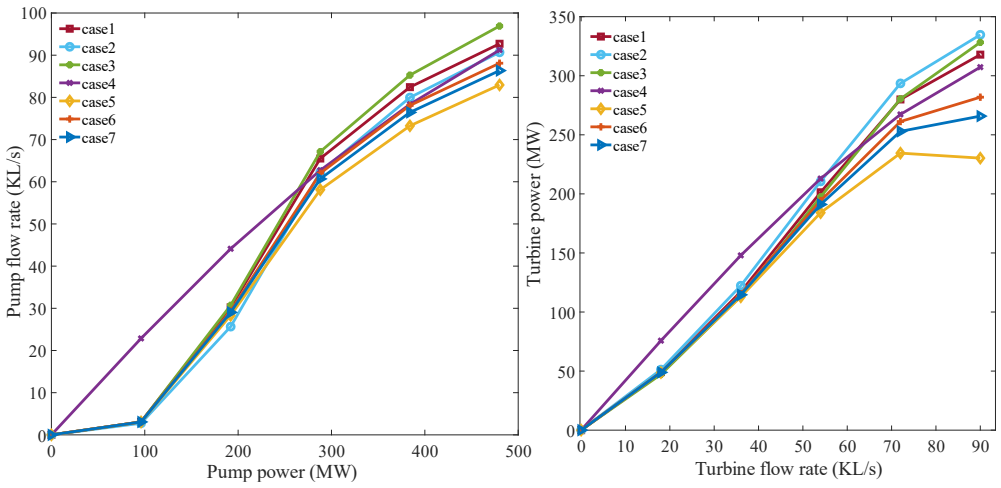

(a) (b)

Fig 3.13: Variations in the PHS model performance by changing the model parameters: (a) Pump, (b) Turbine

Fig 3.13 illustrates that the characteristics of the pump, the turbine, the reservoirs, and the penstocks have significant effects on the performance of the PHS. In addition, these effects vary at different operating points. Thus, it is important to take into account all these parameters in modelling a PHS.

3.7 Conclusion

This study has improved the mathematical models of pumped hydro storage systems to calculate stored water volume and power generation with higher accuracy. The results of the proposed model are compared with the results of established models presented in other papers. The results of this study indicate that both model one and two significantly overestimate the volume of water. However, the proposed model has reduced this error from 13.17% to 0.74%. The error of the proposed model in the pump mode is reduced from 18.36% to 1.4% and the error in the turbine mode is reduced from 21.23% to 1.61%. Although using another experimental setup may change the error, the experiments are conducted in different scenarios and weather conditions to determine the average error of the model.

Finally, the effects of the model parameters on the model performance are studied. These results suggest that consideration of the losses of the system delivers a more practical model. This model is recommended for energy management applications since it estimates the system performance more accurately.

Chapter 4: **A novel pumped hydro storage system** [2]

This chapter investigates the value of using existing irrigation infrastructure to store surplus photovoltaic energy in a farmhouse. The irrigation system includes a reservoir and a water well. The depth of the water well is used to store energy in the form of gravitational potential energy. Throughout the day, photovoltaic energy is used to pump water from the bottom of a well to the reservoir at ground level, where this stored water is then used to meet demand by releasing the water back to the well through a hydro turbine. A controller is designed to manage the pump and the turbine efficiently to reduce daily electricity costs of the farmhouse. The proposed method is validated experimentally with a real pump and a turbine. The controller manages the pump power and turbine flow rate considering the losses of storage, the feed-in income, and the cost-saving for each decision. The proposed system is also simulated in MATLAB for a whole year using real data to investigate the economic aspects of this storage in different seasons with different irradiance, weather, energy demand, and water demand profiles.

4.1 Introduction

Nowadays, photovoltaic (PV) systems are common in agricultural areas due to their clean and cost-effective energy production. However, one major issue of PV systems is in meeting dynamic energy

[2] This chapter has been published as a full research paper:
N. Mousavi, G. Kothapalli, D. Habibi, C. K. Das, and A. Baniasadi, "Modelling, design, and experimental validation of a grid-connected farmhouse comprising a photovoltaic and a pumped hydro storage system," Energy Conversion and Management, vol. 210, p. 112675, 2020.

Whilst efforts were made to retain original content of the article, minor changes such as number formats and font size style were implemented in order to maintain the consistency in the formatting style of the thesis.

demand with their intermittent power generation [102, 103]. An energy storage system can address this issue by storing surplus PV energy and returning it at night times or on cloudy days [104, 105]. Batteries, as conventional energy storage systems, are not an eco-friendly option due to their high carbon footprint [106-108]. Therefore, this study proposes a cleaner energy storage system to be used instead of batteries to store surplus PV power.

Adding batteries to PV systems increases capital costs by more than double [109, 110], where many users prefer to install a PV system without storage. The rapid growth of PV systems raises a timing imbalance between PV generation and peak demand known as the duck curve problem [111, 112]. Dynamic retail pricing plans like critical peak pricing, real-time pricing, and time-of-use have been suggested to increase the economic benefits of self-consumption [113]. In a dynamic pricing environment, a cost-effective energy storage system can reduce electricity prices significantly. Therefore, this study presents a new type of pumped hydro storage (PHS) system utilising existing infrastructure in farms to store energy.

Most research on PHS systems has been conducted in relation to large scale storage which requires special geographical features. The aim of these studies has been related to power balancing in power systems. The size of reservoirs, pumps and turbines are critical in the design of PHS systems, so some papers have focused on sizing [114]. Several studies have developed optimal scheduling technics to dispatch power flow economically [62, 115]. Multiple papers have investigated control strategies to regulate voltage and frequency by PHS systems [85, 116]. A PHS system is recommended for the generation of continuous power at a constant voltage for islanded areas in [88], where the authors propose an off-grid wind-PHS microgrid to meet the demand. Results show that a PHS can keep the microgrid voltage constant even when the wind does not blow. A recent study has developed a hybrid PHS-Battery storage system for an off-grid microgrid [114]. The performance of the energy storage system is evaluated by storage overall performance (SOP) and storage usage factor (SUF) parameters. In this system, a battery meets the demand when deficit energy is low, where a PHS meets the demand when the deficit energy is high.

There are limited papers examining the integration of small scale PHS systems into microgrids. It has been claimed that a small PHS reduced fuel consumption in a PV-diesel microgrid by 4% [50]. The authors in [51, 53] have investigated adding PHS systems to standalone microgrids to reduce the size of the battery in an islanded microgrid. Ref. [51] utilised a PHS to minimise monthly electricity costs in a grid-connected microgrid with dynamic electricity pricing. These papers have studied sizing, management and economic aspects of PHS systems in rural areas but have only used pumped water to generate energy. However, pumped water can be used for irrigation as well. Thus, the common critical gap of these research studies is that irrigation, which is the primary purpose of storing water in rural areas has been neglected.

Another limitation of these papers is that they do not account for hydraulic losses, rainfall, and evaporation in PHS systems. PHS losses are a function of pump power, turbine flow rate, and weather. To schedule a PHS, it is essential to estimate the volume of the stored water accurately since a small error in estimation reduces management efficiency in the long term. The authors in [117] have reported that the inaccuracy of previous models causes more than 13.17% error in water level estimation after 24 hours. Consequently, a comprehensive model is necessary to manage the system and schedule the PHS efficiently.

This study develops a new type of PHS and an energy management system (EMS) to address the above gaps in the literature. The main contributions of this chapter are listed below:

- An existing irrigation system is used to develop a low-cost and eco-friendly energy storage system suitable for rural areas.
- An EMS is designed to minimise electricity costs of the farmhouse by controlling the pump power and the turbine flow rate.
- A comprehensive PHS model is applied to improve the EMS performance by providing a more accurate prediction of the PHS losses in different conditions.

- The proposed system is tested with an experimental setup, where the EMS receives forecast data, and the microgrid runs with real PV power generation, and PHS operates in a real weather condition.
- The economic aspects of the proposed system are evaluated by calculating its payback period and lifetime benefit.
- The proposed system uses the stored water for both irrigation and electricity generation.

This chapter is organised as follows. Section 2 presents the proposed PHS system which uses an irrigation infrastructure to store energy. Section 3 presents the PHS model, PV power prediction method, energy demand prediction method, and irrigation requirement. In Section 4, the proposed PHS management system is presented to optimally schedule the PHS operating point without disturbing the irrigation functionality. In Section 5, the proposed method is experimentally tested to practically validate the performance of the management system. In Section 6, the system is simulated for one year in MATLAB to calculate annual electricity bill reduction. In Section 7, the effect of the aquifer and the PHS on the water level in the well is described. In Section 8, the economic aspects of the proposed storage are discussed.

4.2 Proposed System

A farmhouse is an ideal place to implement a pumped hydro storage (PHS) system. A PHS needs two reservoirs with different heights, where the lower reservoir is connected to a source of water. In farmhouses, there are water wells connected to aquifers and open-top reservoirs at ground level to store pumped water from a well. Adding a hydro turbine to this system, as in Fig 4.1, would convert the irrigation system to a PHS. In this system, the pump consumes the PV power to store water in the reservoir when there is surplus energy in the microgrid. When this stored energy is needed, the water will be released back to the well through a hydro turbine in order to generate electricity. In this system, the stored water can be used for both irrigation and electricity generation. The power generation of the turbine is directly proportional to the depth of the well and water flow rate, where the size of the

reservoir determines the capacity of the storage system. Since there is no space limitation in farmhouses, this energy storage can be implemented with a very high capacity.

The main difference of the proposed energy storage system and conventional PHS systems is that the proposed system store water not only for electricity generation but also for irrigation. Using this system for two applications make the system efficient and cost-effective on the one hand but more complex to manage on the other hand. This novel PHS is specifically designed for farmhouses that have water wells.

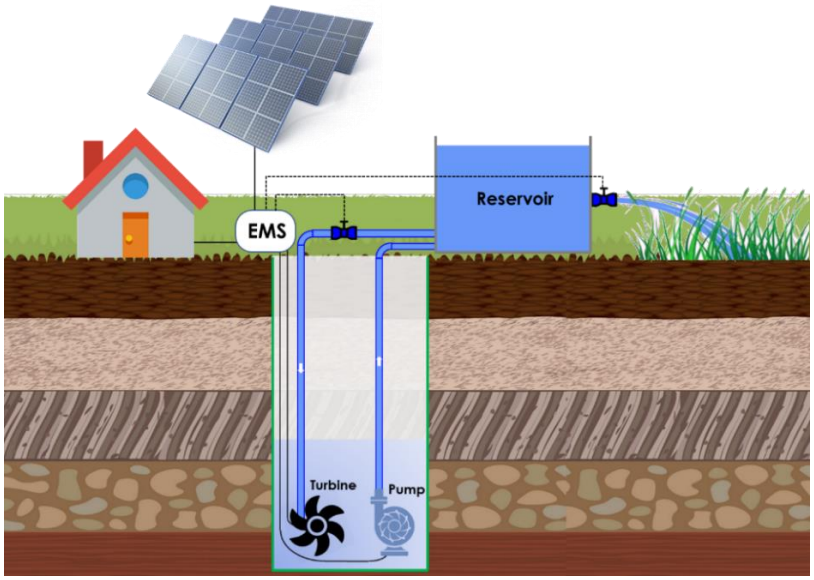

Fig 4.1: The proposed PV-PHS microgrid for farmhouses.

4.3 System modelling

The efficiency of the management system highly depends on the accuracy of the model used to estimate the system's parameters. This section presents a comprehensive PHS model and the methods of PV and load prediction.

4.3.1 PHS model

This study has applied the PHS model presented in Chapter 3 [117], which considers electrical, mechanical, and hydraulic losses of the PHS with a flexible water flow rate (Fig 4.2). In this model

pump power (P_p) and the percent openness of the turbine valve (T_v) are inputs, where stored water (∀) and turbine power (P_t) are outputs. This model can estimate the stored water with a very low error (0.73%), which assists the management system to make more accurate decisions. The model calculates evaporation and precipitation to estimate the stored water level more accurately for open top reservoirs. In closed tanks, evaporation and precipitation would be zero in the model. The model calculates water level according to the dimension of the reservoir, where the effect of water level on water flow rate and output power is considered in the model.

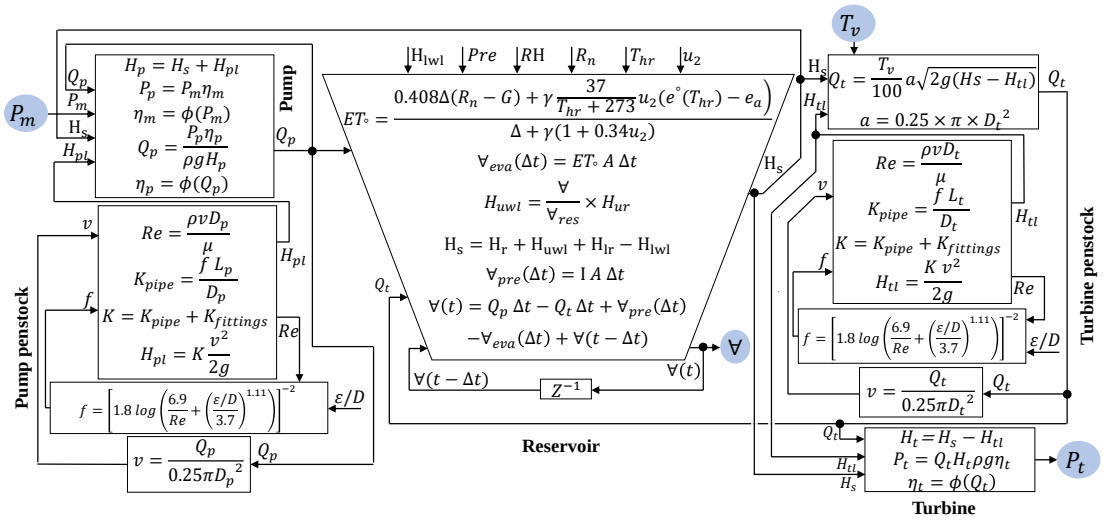

Fig 4.2: PHS model

The water level in the well should be maintained in a limited range otherwise the well overflows during turbine mode, or water goes down during pump mode. To keep the water level in a limited range, pump and turbine flow rate must be less than the flow rate between the well and aquifer. Therefore, the aquifer can feed the well at the same flow rate of pumping, and the well can inject water to the aquifer at the same flow rate of releasing water to the well. The flow rate between well and aquifer (Q_w) can be calculated by Dupuit equation [118]:

$$Q_w = \pi K_h \times \frac{{h_1}^2 - {h_w}^2}{\ln(r_1/r_w)} \tag{4.1}$$

where K_h is hydraulic conductivity of aquifer, h_1 is aquifer head, h_w is well head, r_w is well radius, and r_1 is the radius of influence. r_1 can be expressed by Sichardt equation [119]:

$$r_1 = 3000 \times s_w \times \sqrt{K_h} \tag{4.2}$$

where s_w is drawdown at the well (m).

4.3.2 Solar power prediction

PV power is a function of irradiance and temperature. Two mathematical models are suggested to estimate the output the power of PV systems: one-diode model [120] and two-diodes model [121]. Some studies have presented new artificial methods to predict PV power with high accuracy. In this study, an artificial neural network (ANN) method presented in [122] is trained to predict PV power. The MATLAB Neural network training tool is used to train the ANN with 10 hidden neurons and recurrent neural network (RNN) architecture. Eq 3 and Eq 4 represent a neuron model. Each neuron receives inputs (x_j) which are connected to a summing junction by adjustable synaptic weights (ω_{kj}). The ANN is trained by a Levenberg-Marquardt (LM) learning algorithm to adjust the synaptic weights.

The ANN was trained by real data, including clear sky irradiance, cloud cover percentage, and temperature as inputs; and PV power as the target. Clear sky irradiance was collected from [123] and cloud cover percentage was provided by [124]. The temperature was measured by the weather station installed near the PV system. PV power was obtained by measuring the output voltage and current of the PV. These data were collected for one year to train the ANN, then the ANN was used to forecast PV power.

$$u_k = \sum_{j=1}^{m} \omega_{kj} x_{kj} \tag{4.3}$$

$$y_k = \varphi(u_k + b_k) \tag{4.4}$$

4.3.3 Energy demand

In this study, energy demand is the energy consumption in the farmhouse including the electric devices in the house and farm, such as lights, heating and cooling systems, cooking elements, laundry machines, irrigation components, personal items, and so on. In this study the ANN presented in [125] is trained to forecast energy demand. The ANN structure is similar to Section 3.2, but the hidden neurons are 40. In this study, the ANN is trained by a household energy demand model presented in Section 5. Inputs of the ANN are month of the year, day of the week, and hour of the day where the output is hourly average demand power.

4.3.4 Irrigation demand

Irrigation schedule depends on the type of the crop and season and is given as the volume of water that needs to be supplied for each month of the year. The irrigation times and the duration of each irrigation can be determined by knowing the water flow rate. The irrigation plan used in this study is provided by the website of The Department of Primary Industries and Regional Development [126]. Table 4.1 shows the irrigation requirement of a 3-hectare Avocado farm used for one-year simulation in Section 6. Each irrigation takes 6 hours with 122 m^3/h flow rate.

Table 4.1: Irrigation requirement of a 3-hectare Avocado farm

	Jan	Feb	Mar	Apr	May	Jun	Jul	Aug	Sep	Oct	Nov	Dec
Volume (m^3)	6588	6588	5124	2196	0	0	0	0	1464	3660	5124	6588
Number of Irrigation	9	9	7	3	0	0	0	0	2	5	7	9

4.4 System design

This PHS system is proposed for farmhouses with PV pumping system, so the PV and pumping system is already installed. The capacity of PV systems should be around the power of pumps to meet the energy required for pumping during the day. The only component that is needed to be selected is the turbine. Selecting the capacity of the turbine depends on the demand profile. The turbine rated power should be selected around the average demand power during peak hours since the most saving happens

during peak hours; thus, it is essential to choose a turbine that is able to meet the demand at peak hours. A larger turbine would increase the operating costs of the system since the efficiency of turbine significantly drops in lower than half of the rated power. Operation with low efficiency would increase the loss of saved energy which could be used to save money during deficit energy.

4.5 PHS management system

The aim of using a PHS is to receive less energy from the grid and utilise more clean energy generated inside the microgrid. Since the energy tariff, PV power, demand and PHS losses are not constant, the proposed management system estimates all these parameters to control the PHS efficiently. Since there is an energy storage system, any action will change the future condition of the system. Consequently, in each hour, the proposed controller receives current water volume and forecast data to schedule the PHS until the end of the day to find the best PHS mode for the next hour.

The amount of energy received from the grid for each hour can be calculated by:

$$E_{Grid\ t} = E_{Dt} + E_{Pt} - E_{PVt} - E_{Tt} \tag{4.5}$$

Energy demand (E_{Dt}) is the forecast of the farmhouse energy consumption. Pump energy (E_{Pt}) is the energy consumption of the pump in the well. PV energy (E_{PVt}) is the forecast of the energy generation by PV. Turbine energy (E_{Tt}) is the energy generation of the hydro turbine.

In this equation, demand and PV are not controllable; however, the pump and the turbine are under the control of the PHS management system. To determine the pump power and the turbine flow rate an optimisation algorithm is required. There are various dispatch algorithms used in microgrids [127-129]. Genetic algorithm (GA) is a robust optimisation technique for economic dispatch, which can solve complex and nonlinear problems with an adequate speed [66]. This optimisation technique is inspired by the theory of evolution, where it has been applied in several papers to schedule the microgrids [73, 130, 131]. The proposed system has been tested experimentally with GA, where it could determine the optimal schedule of the pump power and the turbine flow rate in the limited time of the system. The

objective of GA is minimising electricity costs receiving from the grid. To take into account the energy tariff of each hour (λ), electricity costs are calculated for each solution by:

$$E\_Cost = E_{Grid}\ \lambda_t \tag{4.6}$$

To minimise electricity costs, the objective function is given as follows:

$$minimise \quad F = \left[\sum_{t=1}^{T}(E_{Dt} + E_{Pt} - E_{PVt} - E_{Tt})\lambda_t\right] \tag{4.7}$$

This objective function calculates electricity costs for H hours which H is the following hours until the end of the day. In each iteration, GA generates a population where each individual composed of H number of variables. Each variable represents the PHS mode for one hour, where it can be a number between -1 and +1 (-1 means E_{Tt} is at its maximum, and +1 means E_{Pt} is at its maximum). GA calculates the costs of schedules by the objective function and generates the next population. The output of the GA is the schedule with the lowest costs. The following constraints are applied in the GA.

$$\forall_{min} < \forall < \forall_{max} \tag{4.8}$$

$$E_{Tt} = \begin{cases} E_{Tt}, & \text{if } \forall > \forall_{min} \\ 0, & \text{if } \forall = \forall_{min} \end{cases} \tag{4.9}$$

$$E_{Pt} = \begin{cases} E_{Pt}, & \text{if } \forall < \forall_{max} \\ 0, & \text{if } \forall = \forall_{max} \end{cases} \tag{4.10}$$

$$\forall_{t=0} = \forall_{t=24} = 40\% \tag{4.11}$$

$$T_{v\_min} < T_v < T_{v\_max} \tag{4.12}$$

$$P_{p\_min} < P_p < P_{p\_max} \tag{4.13}$$

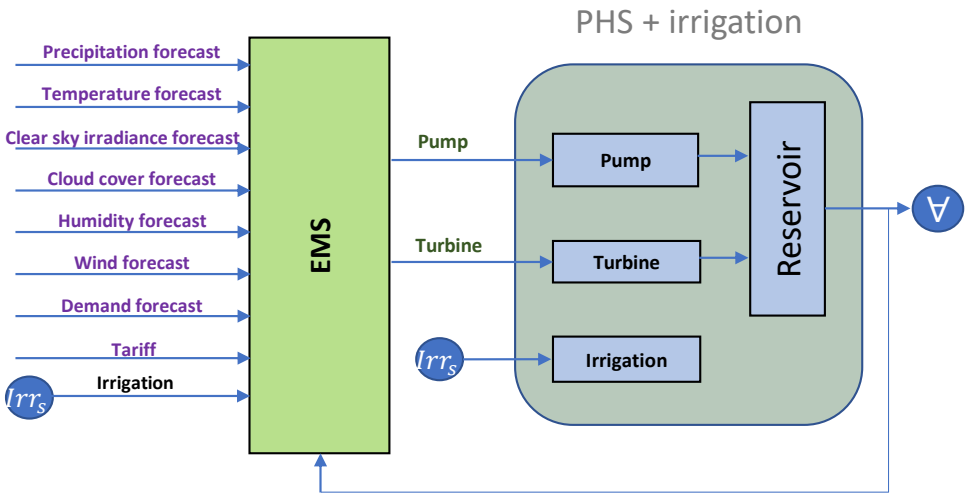

Fig 4.3: Schematic diagram of the proposed PHS management system

The water volume in the reservoir is limited by the reservoir size. When the reservoir is empty ($\forall = \forall_{min}$), the turbine energy (E_{Tt}) must be zero since there is no stored water to spin the turbine blades. When the reservoir is full ($\forall = \forall_{max}$) the pump energy (E_{Pt}) must be zero since the pump will be mandatorily turned off.

The volume of the reservoir at the beginning of each day is set at 40% of its full capacity, where it should have the same amount of 40% at the end of each day to be prepared for the next day [51].

The outputs of the EMS are the pump power (P_p) and the percent openness of the turbine valve (T_v) for the next hour, where they are calculated by the following function:

$$\begin{aligned} &if \quad PHS\ mode < 0 \\ &\qquad T_v = PHS\ mode \times 100; \\ &\qquad P_p = 0; \\ &else \\ &\qquad P_p = PHS\ mode \times Pump\ rated\ power \\ &\qquad T_v = 0; \\ &end \end{aligned} \tag{4.14}$$

Pump power can be any value between zero to its rated power. A variable-speed drive (VSD) connected to the pump controls its power. VSD receives P_p from the EMS and controls the pump power by adjusting its frequency and voltage. The turbine valve (Fig 4.1) controls the turbine flow rate, where $T_v = 0\%$ means the turbine flow rate is zero, and $T_v = 100\%$ means the flow rate is at the maximum flow rate of the turbine.

The schematic diagram of the proposed PHS management system is shown in Fig 4.3. Inputs of the management system are weather forecast, energy tariff, irrigation schedule, and the volume of the stored water. This schedules the pump and the turbine for the next hours until 12 AM to determine the next pump power and turbine flow rate. The reservoir model receives the pump and turbine flow rate to calculate the volume of stored water. The scheduling process updates hourly to reduce the effect of prediction error.

4.6 Experimental validation

The proposed PHS management system was examined in the experimental setup shown in Fig 4.4 to verify the performance of the system with a real pump and a real turbine. The proposed system was physically modelled to measure the pump flow rate and the turbine power for each PHS mode. The details of the experimental setup, the pump efficiency curve, and the turbine efficiency curve are presented in [117]. The parameters of the components used in the experiment are noted in Table 4.2.

The household energy demand model suggested in [132] is used to simulate the energy consumption of a family of three. The model has 25 appliances composed of lighting, laundry machines, cooking devices, entertainment devices, personal items, and cleaning devices. Fig 4.5 shows the demand profile for one year, where the resolution is one minute. To calculate electricity costs, this study has used a time of use tariff from Synergy Smart Home Plan (Fig 4.6) [133].

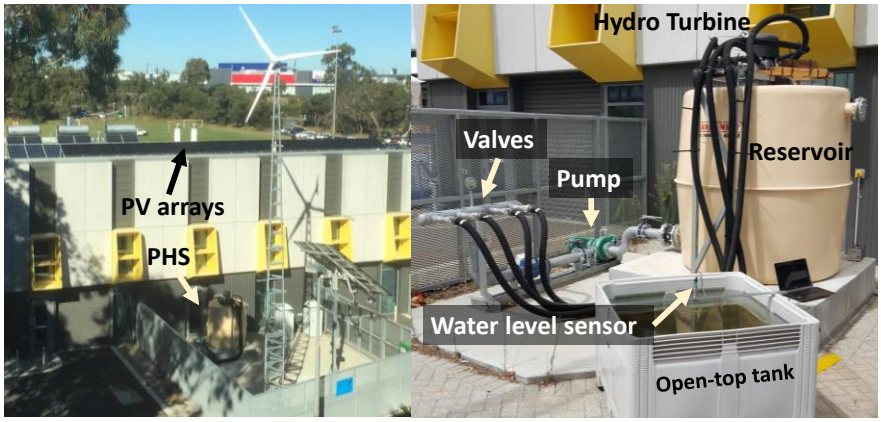

Fig 4.4: Smart Energy Laboratory at Edith Cowan University, Western Australia.

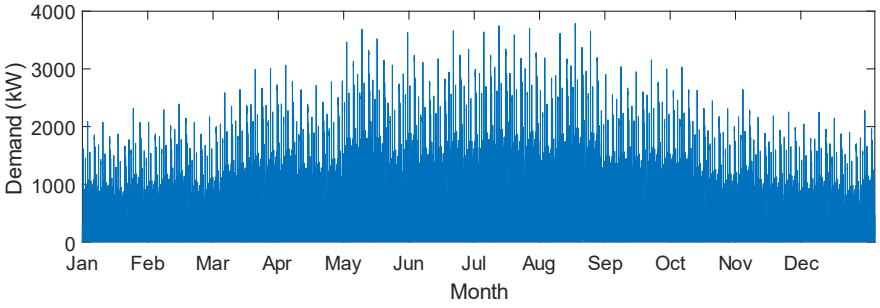

Fig 4.5: Demand profile for one year with 1-min resolution

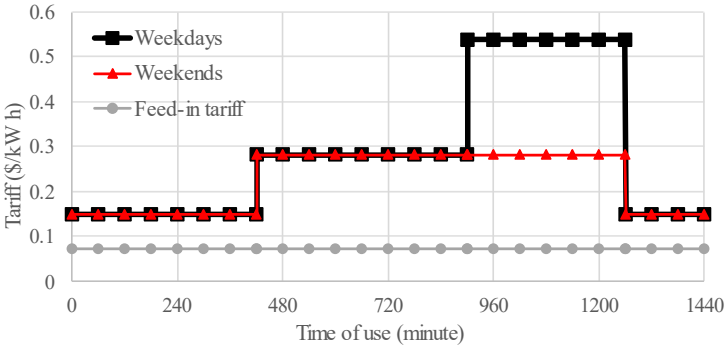

Fig 4.6: Time of use tariff [133].

Table 4.2: Parameters of the microgrid in the experiment.

Pump	Southern Cross, Type: MfD47A	Impeller diameter: 211 mm
Turbine	Power Spout, Type: TRG	Rated: 768 w, 10 m, 15.3 L/s
Pipe	Diameter: 102.3mm	
PV	LG280/285S1C-L4, Monocrystalline, 12 modules, Power:$12 \times 285\ W$	
Reservoir	600 m^3	

Fig 4.7 illustrates the results of the experiment. In this experiment, the management system is tested to investigate how efficiently it can manage the pump, the turbine, and stored water to reduce electricity costs. The stored water was managed to return 40% of the water to the reservoir at the end of the day. The pump and the turbine were scheduled to have the highest cost-saving for this day.

The results show that the turbine had worked when both tariff and demand were high. The turbine flow rate was optimally determined to minimise electricity costs by the limited stored water. For one hour it

worked with low flow rate since there was small deficit energy in the microgrid. Then for three hours, the turbine operated with its highest efficiency.

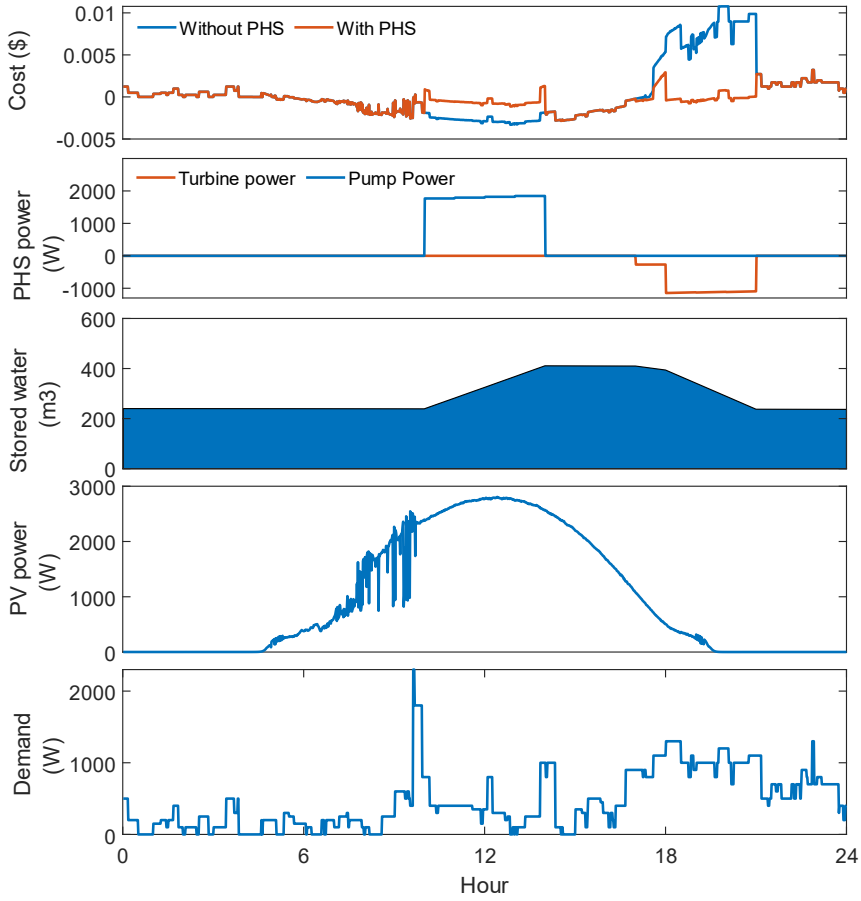

Fig 4.7: Experimental results.

The pump worked for 4 hours when there was high surplus energy generated by PV. In the morning, the PHS management system did not pump water in order to meet the demand by PV power directly. Pumping at this time would increase the losses since the pump efficiency drops when the pump works in low power. The management system decided not to pump more than 4 hours since it was enough to cover peak hours and high demand period. Then for 3 hours, the cost is negative, which means the PHS management system decided to send the energy to the grid. The feed-in income of this decision was more than cost-saving of storing more energy for the night. In this system, feed-in income is equal to PV energy fed back to the grid times feed-in tariff, where cost-saving is equal to energy generation by

the turbine times grid energy tariff. The designed optimisation algorithm determines which one reduces costs more and decides to run the pump or send energy to the grid.

The PHS model presented in Section 3.1 assisted the PHS management system to accurately estimate the pump flow rate and stored water, which increased the efficiency of the management. In an experiment, the system was tested with two different PHS models to investigate the effect of the proposed PHS model on the PHS management system decisions. The simple PHS model presented in [50, 51, 53, 88] had 18% error in stored water estimation for a period of 24 hours. However, this error was reduced with the proposed model to 2%. With the simple PHS model, high overestimation in stored water caused pumping less than enough water to cover peak hours and high demand period, which led to less cost-saving. The PHS needs to store enough water to meet the demand at peak hours, so any error in the calculation of the pump flow rate or stored water reduces the efficiency of the management system.

4.7 Simulation results

The proposed system was simulated in MATLAB for one year to calculate the cost-benefit of the proposed storage. The simulated farm covers 3 hectares with a reservoir which occupies 1.7% of the farm area. Most of the data used in the simulation was measured data in order to produce a realistic estimation of the cost reduction of the proposed storage.

Weather data used in the simulation, including temperature, rainfall, humidity, irradiance, and wind speed were measured by the weather station installed at Edith Cowan University. Weather forecast data are also collected hourly from a weather forecast website [124] for the same period.

PV power was measured from the installed PV system shown in Fig 4.4. Energy demand was generated by the suggested model in [132] for one year. The demand profile was generated for ten houses in rural areas. This model is also used to generate data to train the ANN that forecasts energy demand, which has a 10% error on average within a year. The forecasted energy demand is given to the EMS and energy

demand is used in costs calculation. Table 4.3 presents the characteristics of the components used in this simulation.

Table 4.3: Parameters of the PHS components used in the simulation.

Pump	100 ANZE	30 kW Head:40m, Water Flow: 0.06 m3/s
Turbine	XJ40-L-10DCT4	10 kW, Head:30~40m, Water Flow: 0.048~0.05 m3/s
Reservoir	length: 25 m, Width: 20 m, depth: 2m	
Water well	Diameter: 1 m, depth: 40 m	

Fig 4.8 shows one week of the simulation results as an example. The PHS management system has controlled the PHS to reduce daily operational costs considering the losses of the storage, feed-in income, and cost-saving for each decision.

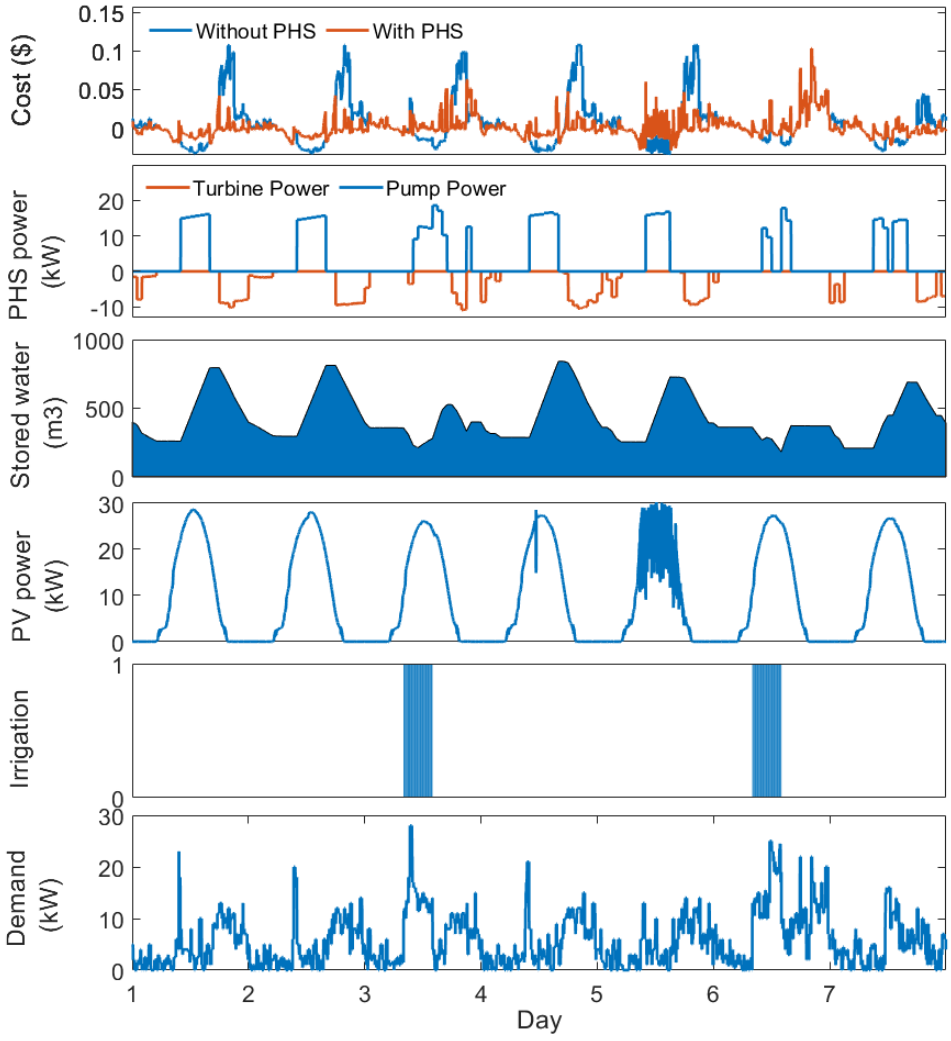

Fig 4.8: One week of the one-year simulation results.

The first and second day were sunny days, so the pump used the PV power to store water during the day, and the stored water was used by the turbine to reduce costs during not only peak hours but also off-peak hours.

On the third day from 10 a.m. to 2 p.m., the pump power was low due to high energy demand. At these hours, the surplus PV power was not enough for the pump, so the remainder should be met by the grid. Receiving energy from the grid increases costs, and on the other hand, reducing the pump power increases the pumping losses. Thus, the PHS management system determined the optimal powers to make a balance between pumping costs and cost-saving of the PHS. Since the stored water was used more for irrigation, the turbine only covered the peak hours and high demand hours. At night, the management system ran the pump during the off-peak hours to reach 40% water in the reservoir.

The fifth day was cloudy, so the pump and the turbine were used less. On this day, less energy was generated by the PV, so the management system decided to pump less water to the reservoir. Consequently, the turbine worked for fewer hours.

On the sixth day, there was a six-hour irrigation and energy demand was high. Thus, PV power was used to meet the demand, and the pump worked only to provide water for irrigation. Consequently, the turbine could generate energy only for one hour.

Although the seventh day was as sunny as the first day, the PHS was used less since energy demand was high during the day, so there was less surplus energy.

4.8 hydrogeology of the aquifer

As mentioned in Section 3.1, the water level in the well should be kept in the limited range to be able to operate the proposed PHS. In this study, it is assumed that water level changes in the range of 1% of the well depth do not interrupt the PHS operation. The water level in the well depends on the water flow rate of the PHS and the hydraulic conductivity of the aquifer (K_h). K_h mainly depends on the type of aquifer; where it can range from 1 m/s for good aquifers with well-sorted gravel to 10^{-5} m/s for poor

aquifers with very fine sand [134]. The highest PHS flow rate that can keep the water level in the limited range can be calculated by Eq 4.1. In aquifers with high K_h, a high water flow rate can be pumped and discharged to the well; however, when the aquifer has low K_h, more than one well can be used to keep the water level in the limited range. In the case of requiring more than one well, the hydraulic interference of wells should be evaluated, and the costs of extra wells would be added to the capital costs of the system.

Table 4.4 shows the characteristic of the aquifer and the well modelled in the simulation. In this system, the water level in the well can change in the range of ±0.4 m (1% of the well depth). Using Eq 4.1, the water flow rate should be less than 0.0908 m3/s to keep the water level in the limited range. In the simulation, the maximum PHS flow rate is 0.06 m^3/s, which is in the limited range.

Table 4.4: Parameters of the aquifer and the well modelled in the simulation

Well depth	40 m
Hydraulic conductivity of aquifer (K_h)	0.01 m/s [134]
Aquifer head (h_1)	20 m
well head (h_w)	20±0.4 m
Radius of influence (r_1),	120 m
Well radius (r_w)	0.5 m

4.9 Economic aspects

Cumulative electricity costs over a year are shown in Fig 4.9. The proposed PHS could reduce electricity costs from $7586 to $1523, which is 80% reduction in the annual electricity costs of the farmhouse. The operation costs were reduced more in summer than winter. During winter there was less PV generation due to a higher number of cloudy days, so less water is stored to be used for electricity generation.

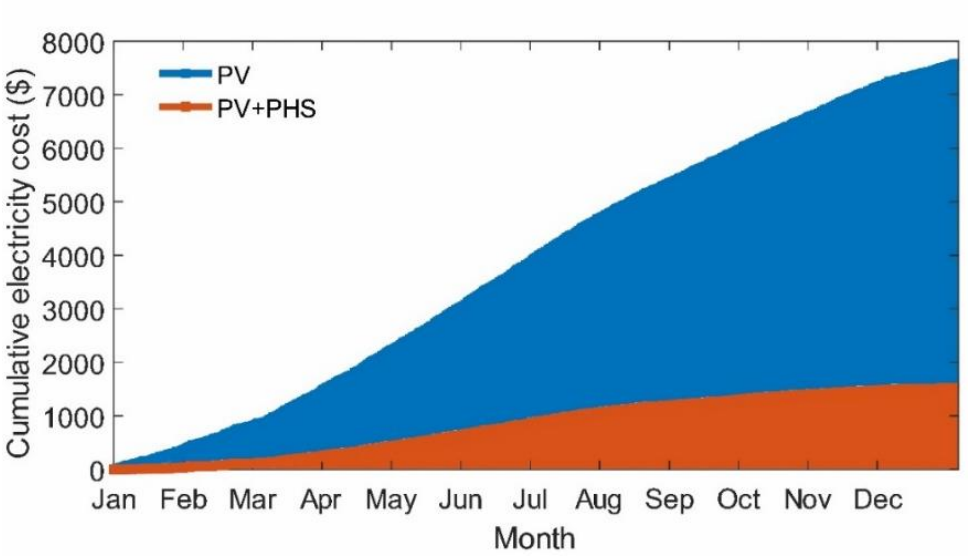

Fig 4.9: Cumulative electricity costs of the microgrid for one year

The payback period and lifetime benefit of the proposed energy storage system are calculated to evaluate its economic aspects. The details of the proposed system costs are indicated in Table 4.5. Installation costs include costs of pipes, valves and labour costs of installing the turbine in the well. The hydro turbine life span is estimated at 20 years [135], so lifetime benefit is calculated for 20 years. Operation and maintenance costs of the system are estimated at $8.02/kW on average for 20 years [135]; and annual water treatment costs of the system are assumed on average at $150 for a 1000 m^3 reservoir to remove water contamination. Results shown in Fig 4.9 demonstrated that adding a turbine to the existing irrigation infrastructure provides an annual saving of $5983 on the electricity bill. The payback period (PP) of the proposed storage system can be calculated by Eq 15.

$$PP = \frac{CC}{EBS - O\&M - WT} \tag{4.15}$$

Where CC is capital casts including turbine price and installations costs, EBS is annual saving on the electricity bill, $O\&M$ is annual operation and maintenance costs, and WT is annual water treatment costs. The payback period of the proposed energy storage system is 8 months, and it saves $121,260 on electricity bill over its lifetime.

Table 4.5: System costs and payback period estimation

Turbine	$3410
Installation	$500
Annual EBS	$6063
Annual O&M	$80.2
Annual WT	$150
Payback period (month)	8
Lifetime benefit	$112,746

In rural areas, reservoirs are available in the majority of farmhouses, so the proposed system can use the existing reservoir to store water. If a farmhouse does not have a reservoir or the size of the reservoir is not enough for the proposed PHS, the costs of building or expanding the reservoir would be added to capital costs. For the case study here, the construction costs of a plastic-lined reservoir with 1000 m^3 volume is estimated at $4000 including earthworks and lining costs. Therefore, if the reservoir is not already available in the farmhouse, capital costs would increase to $7910, where the payback period of the system would increase to 16 months.

4.10 Conclusion

This chapter has proposed a new type of PHS system designed for farmhouses to reduce electricity costs. A simple management system was designed to control the pump power and the turbine flow rate taking into account PV power generation, energy demand, water demand, PHS losses, and grid tariff. The proposed system is tested experimentally in lab environment. The simulation results show that this system can store energy without interrupting irrigation. The results demonstrate that the annual electricity cost of the farmhouse is significantly reduced by the integration of the proposed PHS system into the PV system. The comprehensive PHS model has assisted the management system to optimally select the pump power and the turbine flow rate by determining the efficiency of the PHS at different conditions. Consequently, the designed management system takes into account not only generation and demand but also the efficiency of the PHS to make a decision. This system is recommended for farmhouses that have water wells and reservoirs.

Chapter 5: **A new scheduling method** [3]

This Chapter proposes a new scheduling method for PV-PHS farmhouses. It takes into account energy generation, energy demand, water demand, energy tariff, and system losses to determine the pump power, the turbine flow rate, and irrigation times. The proposed scheduling method compares cost-saving and feed-in income for each decision by using two forecasting methods and a multi-level optimisation algorithm. The performance of the system using this scheduling method is experimentally verified on a real pump and turbine. The objective of this study is not only to manage pump power and turbine flow rate but also to manage irrigation times and water volume. The results show that adding irrigation and water management assist the energy management system in using stored water more efficiently. As a result, electricity costs are reduced by more than 31% compared to existing management methods. The proposed system is simulated in MATLAB to calculate annual electricity costs. The payback period and lifetime benefit of the proposed storage are calculated to investigate the economic aspects of the system.

5.1 Introduction

Pumped hydro storage (PHS) is a clean and sustainable energy storage system that uses water to store energy. This storage system does not require any chemical substances and can store energy in a wide range of capacities. This storage system requires two reservoirs with different heights. During the day when the PV generates surplus energy, the water is pumped to the upper reservoir to store energy

[3] This chapter has been published as a full research paper:
N. Mousavi, G. Kothapalli, D. Habibi, C. K. Das, and A. Baniasadi, "A novel photovoltaic-pumped hydro storage microgrid applicable to rural areas," Applied Energy, vol. 262, p. 114284, 2020.

Whilst efforts were made to retain original content of the article, minor changes such as number formats and font size style were implemented in order to maintain the consistency in the formatting style of the thesis.

coming from PV in the form of gravitational potential energy. When power is required, the water flows down to the lower reservoir through a turbine and potential energy converts to electrical energy. PHS systems with high efficiency and a long lifetime [136] can be a suitable alternative storage option.

Most studies on PHS systems have been conducted on large-scale ESSs; however, many aspects of integrating small-scale PHS systems into microgrids have not been studied. Two studies have reported that introducing a PHS system into a microgrid comprising of a diesel generator, a PV system, and a battery, ultimately decreases fuel consumption by 4% [137]. Ref [89] has compared the operational cost of a 4 kW diesel generator microgrid with a 4 kW grid-connected PHS microgrid. The results have shown that the daily costs of the grid-connected PHS are 71.3% less than the diesel generator microgrid.

Ref [135] has studied the electricity cost reduction of a PHS in a dynamic electricity pricing environment. The paper has modelled a small grid-connected farm with an 8 kW PHS using a water well in South Africa. It is reported that this system can reduce 68.44% of electricity costs, and its payback period is 5.9 years.

In another study, a PV-PHS system has been suggested to reduce the electricity costs of a grid-connected microgrid [51]. This study demonstrated that the depth of well could be used to store the electrical energy in the form of gravitational potential energy. The payback period of this suggested system was determined to be 15 years, including the total hydraulic system cost and digging costs. This study focused on PHS management, where irrigation was not accounted for. However, pumping systems and reservoirs exist in many farms for the primary purpose of irrigation, and therefore the above-suggested management system may interrupt the primary function of the irrigation system.

To prevent disruption of irrigation functionality, a recent study has developed an energy management system (EMS) for a PV/PHS system [138]. This system manages the PHS operating mode to both reduce operational costs and provide water for irrigation as needed. The limitation of this study is that the suggested EMS does not manage the irrigation times, where irrigation accrues at certain times according to a fixed irrigation schedule. However, scheduling irrigation times according to the future state of the system may further reduce operational costs.

To date, suggested EMSs [49-51, 89, 135, 138, 139] have not optimised the amount of water in the reservoir at the end of the day. An optimiser that schedules the PHS needs to know the desired volume of water at the end of the day ($\forall_{24}$). In these articles, $\forall_{24}$ is arbitrarily selected to be 40% of maximum reservoir volume. However, $\forall_{24}$ has a substantial impact on the performance of the system over the following days. For instance, maybe the next day is a cloudy day where storing more water on the current day would be beneficial to reduce the total operating costs of the microgrid. On the other hand, if the next day is sunny, not as much energy may be required for storage. Therefore, neglecting to determine optimum $\forall_{24}$ would reduce the efficiency of the system.

Another research study has integrated a PHS to a stand-alone microgrid to reduce battery usage [53]. This study also maintains $\forall_{24}$ at an arbitrary value of 40% of maximum reservoir volume.

Another weakness of the current management methods is that they do not accurately take into account the PHS losses. A PHS system has hydraulic, mechanical, and electrical losses, which are mainly a function of pump speed, turbine flow rate, stored water and weather conditions [117]. PHS losses are not calculated in the simulation-based studies [49-51, 53, 89, 135, 139], so the results are not accurate for systems in which losses are not fixed. In practice, the losses of PHS highly depend on the EMS decision. Consequently, the EMS would manage the PHS more efficiently if it could calculate the losses for each decision to make a balance between pumping costs and PHS losses, and this would lead to more electricity costs reduction.

The gaps within the literature demonstrate that there is a need to develop an EMS that manages both the PHS system and the irrigation system at the same time. The main contributions of this chapter are:

- Irrigation times are scheduled to assist the EMS in using the stored energy more efficiently.
- The required volume of water for the next day is determined in order to store sufficient energy before cloudy days.
- A comprehensive PHS model is applied in the management system to reduce both PHS losses and electricity costs.

Recently, different management strategies have been proposed for residential microgrids. A flexible communication control strategy has been proposed in [140] which uses an optimisation approach to minimise the cost of energy from the grid. A closed-loop optimal control strategy has been presented in [141], which manages energy flow in a microgrid composed of PV and wind generators that are connected to the grid with battery storage. These authors reported that the initial value of energy storage plays a significant role in the control strategy. Mixed-integer-linear-programming (MILP) optimisation combined with a fuzzy controller method is presented in [13] to manage a hybrid PV-wind-battery microgrid. In this method, the optimisation program schedules battery charging and discharging current, where then the fuzzy controller adjusts the scheduled current of the battery to compensate any mismatch between the real power generation and forecasted power generation. Another management strategy suggested for microgrids is model predictive control (MPC). In [142, 143] an MPC algorithm is developed to manage energy in a real-time pricing environment. Some other studies have proposed demand-side management strategies to use renewable energy power generation more efficiently [144, 145]. This method manages shiftable and interruptible loads to balance power generation and demand.

Lifetime benefit and payback period are two key parameters of the economic feasibility study of microgrids. Payback period is the time that it takes for the microgrid to earn equal to capital and operating costs. Capital costs include components' prices, installation costs, labour costs, and balance of system costs. Operating costs include maintenance and services costs during operation [146]. Lifetime benefit is the profit after reducing the capital and operating costs from savings of the microgrid for its lifetime [147]. The payback period and lifetime benefit of microgrids with energy storage systems highly depend on the electricity pricing mechanism [148]. Time of use is a common method of pricing. In this method, different tariffs are applied for different times of the day. Some power policies have a great difference between peak tariff and off-peak tariff, where reduces payback periods to encourage more investments in microgrids [149]. This chapter evaluates the feasibility of the proposed system by calculating the payback period and lifetime benefits at different capacities.

5.2 Proposed microgrid

In most agricultural lands, there are pumps that transport water from wells to reservoirs that is then used to irrigate land. This study suggests adding a turbine to this irrigation system in order to institute a pumped hydro storage (PHS) system, as shown in Fig 5.1. Following this, the PHS is then able to pump water to the reservoir in order to store energy in the form of gravitation potential energy, and when this stored energy is needed, it releases water down to the well through the turbine to generate electricity. This eco-friendly energy storage system can be used to manage surplus PV power. The challenge of implementing this system, however, is managing stored water for both irrigation and electricity generation.

Fig 5.2 shows the schematic diagram of the proposed system, where PV and grid are sources of energy and PHS is the energy storage of the microgrid. The PHS consists of a pump and a turbine, where the pump stores water, and the turbine generates electricity from the stored water. Demand is power consumption in the farmhouse and the irrigation pump. The EMS controls the pump power, the turbine flow rate, and irrigation times.

To manage the proposed microgrid, all of the components are modelled to possess an accurate estimation of the system's behaviour. There are four components in this system: PHS, PV, energy demand and the irrigation system.

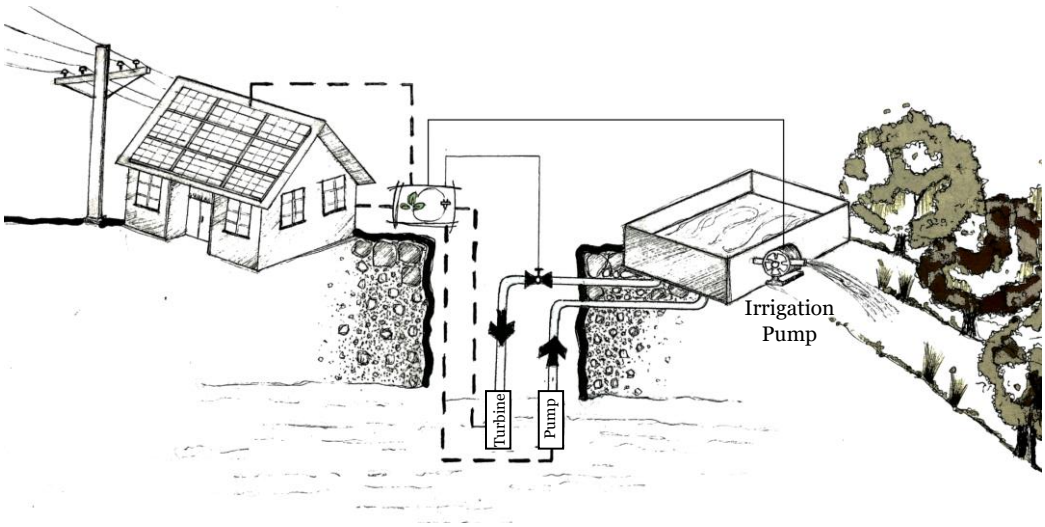

Fig 5.1: Proposed microgrid configuration

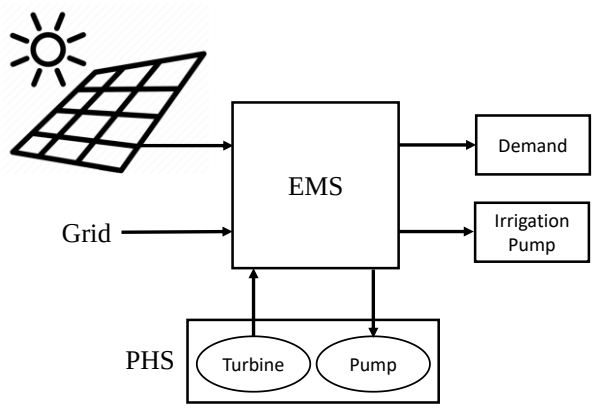

Fig 5.2: Schematic diagram of the proposed microgrid

5.2.1 PHS Model

A comprehensive PHS model [117] shown in Fig 5.3 has been applied in this study. This model receives pump power (P_p) and the percent openness of the turbine valve (T_v) in order to calculate stored water (∀) and turbine power (P_t). This model requires knowledge of weather conditions in order to estimate variation in ∀ caused by evaporation and precipitation. This PHS model can calculate the losses of the system for any pump power and turbine flow rate, where it assists the EMS to determine the optimum operating point of the PHS for each condition.

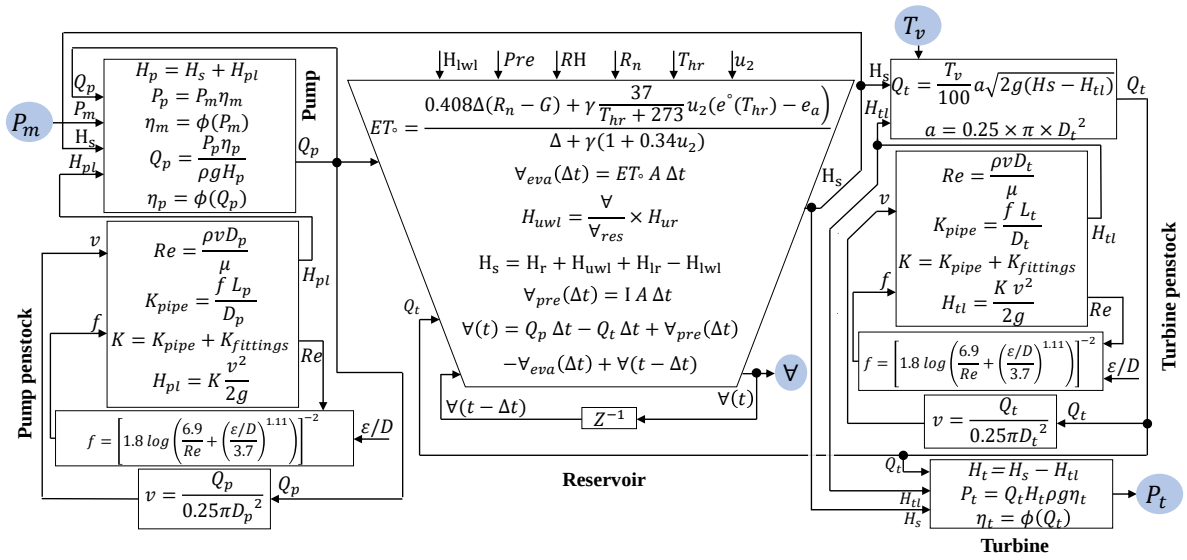

Fig 5.3: Comprehensive PHS model considering electrical, mechanical, and hydraulic losses

5.2.2 PV Power Forecast

The conventional methods to estimate PV power use a one-diode PV model [120] or two-diodes PV model [121]. These models calculate the output power of PV by receiving irradiance and temperature. Recent studies have applied artificial neural networks (ANNs) to forecast PV power with higher accuracy [122, 150, 151]. This method simulates a human brain process and can be trained by a set of input and output data. Recent studies have demonstrated that ANN is a powerful method to predict renewable energy sources [152]. To predict PV power, we have used the method suggested in [122].

An ANN consists of several layers of neurons which act as nonlinear summing junctions connected by adjustable synaptic weights. Fig 5.4 represents an artificial neuron model. This neuron model can be expressed as Eq 5.1 and Eq 5.2 below:

$$u_k = \sum_{j=1}^{m} \omega_{kj} x_j \tag{5.1}$$

$$y_k = \varphi(u_k + b_k) \tag{5.2}$$

where k is neuron number, x_j are inputs, ω_{kj} are synaptic weights, y_k are activation values, φ is activation function, and b_k are bias units. In the training of ANNs, synaptic weights are adjusted to minimise error. In this study, a recurrent neural network (RNN) architecture is used, where it is trained by a Levenberg-Marquardt (LM) learning algorithm. The trained ANN receives clear sky irradiance, temperature, and cloud cover percentage to forecast PV power. MATLAB Neural network training tool is used to train the ANN with 10 hidden neurons.

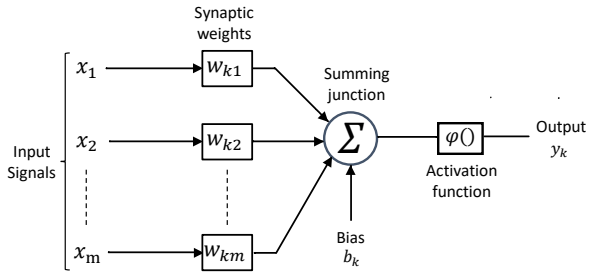

Fig 5.4: Artificial neural model.

5.2.3 Demand Forecast

ANN is the most popular method for electricity demand forecasting due to its higher accuracy compared to statistical methods [153]. This study has used the forecasting approach presented in Ref [125] which presents an ANN, designed in MATLAB, to predict home energy consumption at different times of the day. The same ANN structure mentioned in section 2.2 is used to predict demand but with 40 hidden neurons. The input data used in the ANN are month of the year, day of the week, and hour of the day.

5.2.4 Irrigation Pump

To irrigate the land, there is an irrigation pump where its power consumption (P_{IP}) can be calculated by [94]:

$$P_{IP} = \frac{Q_{IP}\rho g H_{Ip}}{\eta_{Ip}} \tag{5.1}$$

where Q_{IP} is the pump flow rate, H_{Ip} is the total head of the pump, η_{Ip} is the efficiency of the pump, ρ is density of water, and g acceleration due to gravity.

5.3 Proposed Energy Management System

This section presents an EMS which takes into account energy generation, energy demand, energy tariff, system losses and water demand to optimally use the energy sources. Before managing the PHS system to improve microgrid operation, the EMS should determine irrigation times and the required volume of water at the end of the next day ($\forall_{24}$). These two parameters should be optimally determined every day according to the demand and generation of the following days. In the absence of this, these parameters must be arbitrarily selected [49-51, 89, 135, 138, 139]. Therefore, to determine these parameters first and then manage the PHS, the proposed EMS has the following layers:

- Irrigation and water management layer
- Pump and turbine management layer

Fig 5.5 illustrates the proposed EMS. The process of these two layers is explained in Sections 3.1 and 3.2.

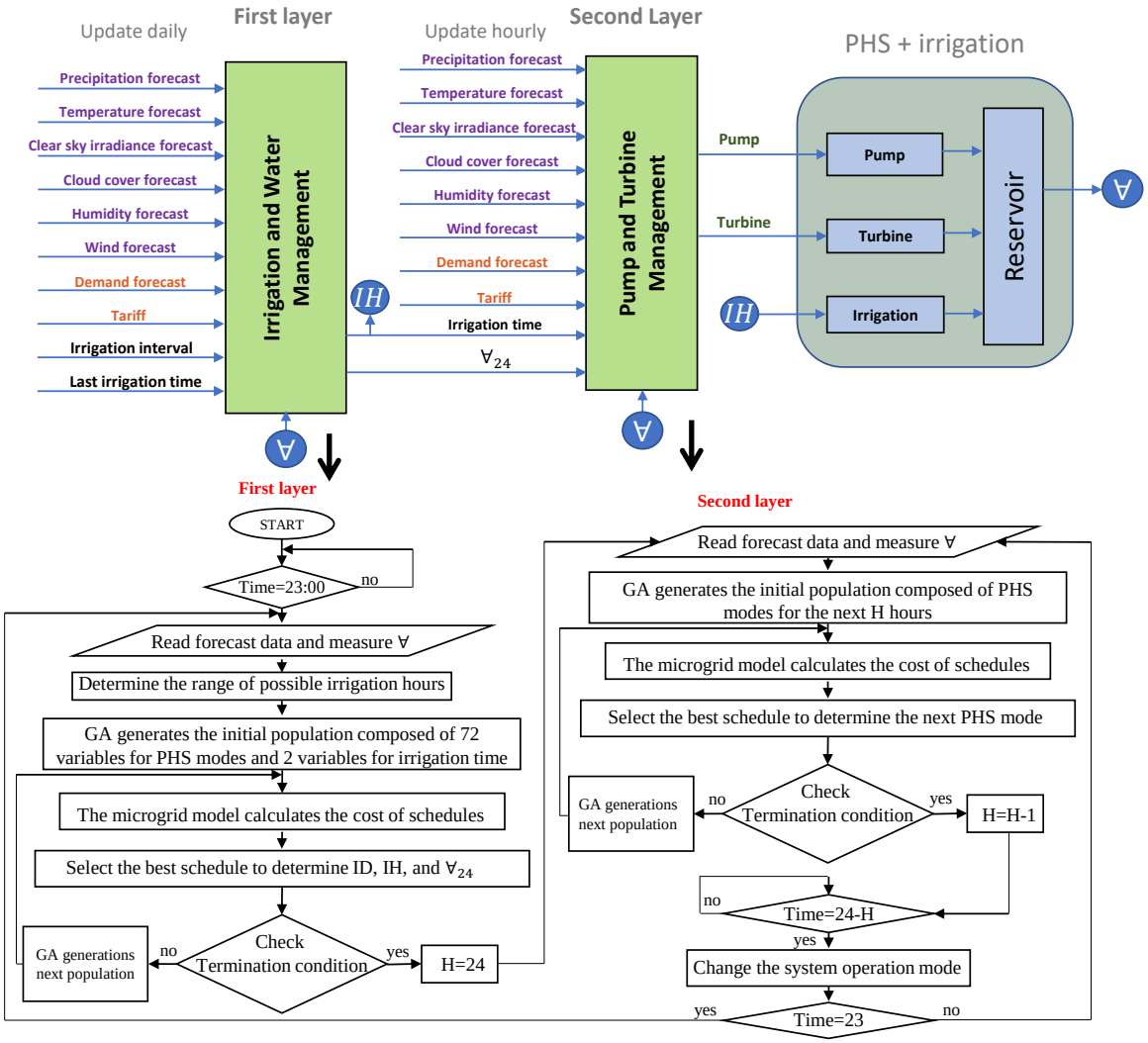

Fig 5.5: Proposed energy management system, block diagram and flowchart algorithm

5.3.1 Irrigation and Water Management Layer

Irrigation and water management layer accrues every day at 23:00, receiving irrigation interval, last irrigation times, and water volume in the reservoir (∀), and forecast data. The trained ANNs mentioned in sections 2.2 and 2.3 receive forecast data to predict PV power and energy demand. All these forms of data in addition to the range of possible irrigation times are then sent to an optimisation algorithm to schedule the system for the next three days.

In this system, it is assumed that irrigation has three days of flexibility, meaning that the EMS can irrigate the land one day before or after the given irrigation time interval. In this situation, there are 72 hours of possible irrigation times. The range of the possible irrigation day may be expressed as:

$$FPID = LI + II - 1 \tag{5.2}$$

$$LPID = LI + II + 1 \tag{5.3}$$

where $FPID$ is the first possible irrigation day, $LPID$ is the last possible irrigation day, LI is last irrigation day, and II is irrigation interval. Since there are three days of flexibility for irrigation, the first layer schedules the system for the next three days.

Irrigation day (ID) can be any day from $FPID$ to $LPID$ and Irrigation hour (IH) can start at any hour from the beginning of the day until IL hours before the end of the day, where IL is irrigation length. ID and IH will be determined by the optimisation algorithm in the possible irrigation time range.

Both layers of the EMS require an optimisation algorithm. There are several heuristic algorithms and advanced methods used in renewable energy technologies [109, 113, 154-156]. Genetic algorithm (GA) is able to solve nonlinear and non-convex problems with an acceptable speed [66]. This optimisation algorithm is inspired by Darwin's theory of evolution. Several studies have used GA to schedule microgrid units where it is a powerful optimiser for resource allocation and economic dispatch [31, 69, 73]. GA has been tested for the proposed EMS, and it could determine the global solutions of the constrained optimisation problems of this study is less than the limited time of the system.

To determine irrigation times and $\forall_{24}$, a genetic algorithm (GA) schedules the system. In each generation, the GA generates possible solutions composed of 72 variables for the PHS operating points, 1 variable for irrigation day (ID), and 1 variable for irrigation hour (IH). The model calculates the pump power, turbine power and ∀ for the next 72 hours for each solution. Then the fitness function calculates the electricity costs of each solution. The GA generates the next generations through cross over and

mutation. The iteration process continues until the minimum cost does not change. The fitness function (FF) has been defined to minimise the operation cost:

$$FF = min\left[\sum_{t=1}^{T}(E_{Dt} + E_{Pt} + E_{IPt} - E_{PVt} - E_{Tt})\lambda_t\right] \quad (5.4)$$

where E_{Dt} is the energy consumption of demand at interval t, E_{Pt} is the energy consumption of the pump at interval t, E_{IPt} is the energy consumption of the irrigation pump at interval t, E_{PVt} is the energy generation of the PV at interval t, and E_{Tt} is the energy generation of the turbine at interval t. In order to determine optimal solutions, the following constraints are applied in the optimisation algorithm:

$$E_{Pt\_min} < E_{Pt} < E_{Pt\_max} \quad (5.5)$$

$$E_{Pt} = \begin{cases} E_{Pt}, & \text{if } \forall < \forall_{max} \\ 0, & \text{if } \forall = \forall_{max} \end{cases} \quad (5.6)$$

$$E_{Tt\_min} < E_{Tt} < E_{Tt\_max} \quad (5.7)$$

$$E_{Tt} = \begin{cases} E_{Tt}, & \text{if } \forall > 0 \\ 0, & \text{if } \forall = 0 \end{cases} \quad (5.8)$$

$$0 < \forall < \forall_{max} \quad (5.9)$$

$40\% < \forall_{t=72} <100\%$ [51] (5.10)

$$FPID < ID < LPID \quad for\ FPID \geq D \quad (5.11)$$

$$D < ID < LPID \quad for\ FPID < D \quad (5.12)$$

$$1 < IH < (24 - IL) \quad (5.13)$$

where D is the current day. The PHS operating point can be a number between -1 and +1 (-1 means the turbine energy generation (E_{Tt}) is at its maximum, and +1 means the pump energy consumption (E_{Pt})

is at its maximum). During turbine mode, the pump does not operate; during pump mode, the turbine does not operate.

The volume of water in the reservoir (∀) is limited by the maximum volume of the reservoir. Consequently, when ∀ is at its maximum, the pump stops operating since the reservoir is full. When ∀ is zero, the turbine stops operating since there is no water in the reservoir.

5.3.2 Pump and Turbine Management Layer

The second layer manages the PHS hourly, receiving irrigation times, $\forall_{24}$, and forecasts data to determine the pump power or turbine flow rate for the next hour. This layer schedules the PHS for the following hours until the end of the day (H), but the schedule updates hourly. Thus, the decision made in each hour is based on the current and future state of the system. This layer manages stored water to ensure enough water for irrigation and to retain at least $\forall_{24}$ water in the reservoir at the end of the day.

The fitness function and constraints of the second layer are the same as Eq. 5.4 to Eq. 5.9. Since minimum $\forall_{24}$ is produced by the first layer, water volume constraint is:

$$\forall_{24} < \forall_{t=24} < 100\% \tag{5.14}$$

The output of the optimisation algorithm is a PHS operating point which controls the pump power and the turbine flow rate. If PHS operating point is a positive number, it indicates the pump power in percentage, whereas if PHS operating point is a negative number, it indicates the percent openness of the turbine valve. By controlling the turbine valve, the EMS controls turbine power generation.

5.4 Results and Discussion

5.4.1 Experimental Verification

The proposed PHS management system was examined in the experimental setup shown in Fig 5.6 to verify the performance of the system with a real pump and a real turbine. The proposed system was

physically modelled to measure the pump flow rate and the turbine power of each PHS mode. In this experimental setup, the pump circulates the water, where the valves placed after the pump can change the total head of the pump. Reducing the percent openness of these valves increases their resistance coefficients. Increases in their resistance coefficient increase the total head of the pump. These valves were adjusted to simulate the total head of the pump in the proposed system. In the turbine mode, the pumped water through the turbine spins the turbine blades to generate electricity. The head and flow rate of water can be controlled by the pump speed and the valves placed before the turbine. During the experiment, the valves and pump speed were adjusted to simulate water flowing from the reservoir to the well through the turbine. To measure evaporation and precipitation, the water level of an open-top tank was measured continuously during the experiment. The parameters of the components used in the experiment are mentioned in Table 5.1.

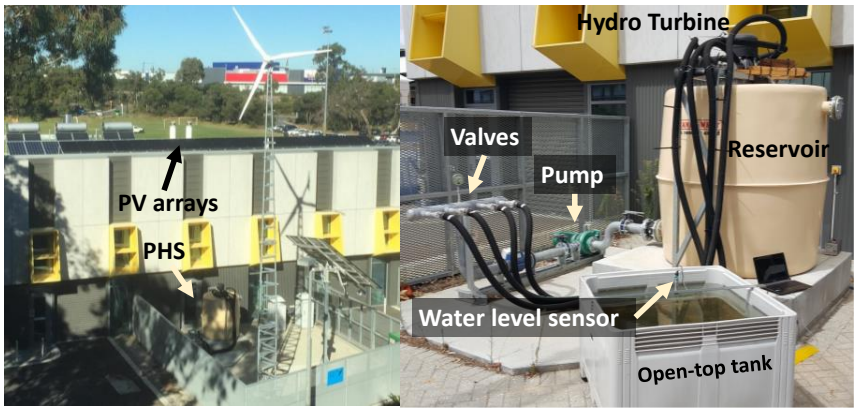

Fig 5.6: Experimental setup installed at Edith Cowan University composed of a PV system and a PHS

Table 5.1: Parameters of the Experimental setup components.

Turbine	Power Spout, Type: TRG	Rated: 768 w, 15.3 L/s
Pump	Southern Cross, Type: MfD47A	3 kW Motor, Impeller diameter: 211 mm

In the experiment, two types of data were applied: measured data and forecast data. Measured data includes PV power generation, pump flow rate, pump power, turbine flow rate, turbine power, precipitation, and evaporation. These parameters were measured in the Smart energy lab of Edith Cowan University. Load demand data was generated by a high-resolution household electricity demand

model presented in Ref [132] for three households. Forecast data including temperature, clouded cover percentage, relative humidity, wind speed, precipitation was received from an online weather service named "Yr" [124]. This online data is received hourly since the forecast data time interval is one hour. The forecast of clear sky irradiance was provided by the Australian PV Institute Solar Map [123]. The price of energy received from the grid is according to the local time-of-use tariff (Synergy Smart Home Plan) presented in Table 5.2 [133].

Table 5.2: Local time-of-use tariff

	Time of use (Hour)		Tariff ($/kWh)
Weekdays	21 – 7	Off-peak	0.148405
	7– 15	Shoulder	0.282139
	15– 21	Peak	0.538714
Weekends	21 – 7	Off-peak	0.148405
	7– 21	Shoulder	0.282139
Feed-in tariff			0.071350

Fig 5.7 shows the results of the experiment for two days. The proposed EMS controlled the pump power and the turbine flow rate considering PHS losses, PV power, energy demand, water demand, energy tariff, and the future state of the system.

The proposed EMS determined that the required volume of water for the end of the first day was $\forall_{24} = 440\ m^3$, where the weather prediction forecasts cloudy weather for the following two days. Hence, the turbine and the pump were managed to retain $440\ m^3$ in the reservoir for the second day. This stored water is then managed to reduce costs on the next days.

As shown in Fig 5.7, the turbine flow rate was managed during the experiment to reduce electricity costs. At minutes 1080-1260, the turbine worked with 92% of its full capacity since both demand and tariff were high. At minutes 1980-2040, the turbine was used to meet the demand, when the PV could not generate enough power due to cloudy weather. On the afternoon of the second day, the turbine started working one hour earlier than the previous day since the PV power was not enough to meet the demand.

It can be seen from the results that the proposed EMS ran the pump efficiently. When the surplus energy was high, the pump worked at 70% of its full rated power since its highest efficiency is at this point. However, when the surplus energy was not high, but enough to run the pump, the EMS has found an optimum pump power to reduce both PHS losses and electricity cost. In this case, the deficit energy to run the pump should be taken from the grid, thus increasing the pump power increases the electricity cost; on the other hand, reducing pump power increases the losses of pumping since the efficiency of the pump drops as the operating power departs from the rated power. The EMS made a balance between pumping costs and PHS losses to determine the pump power.

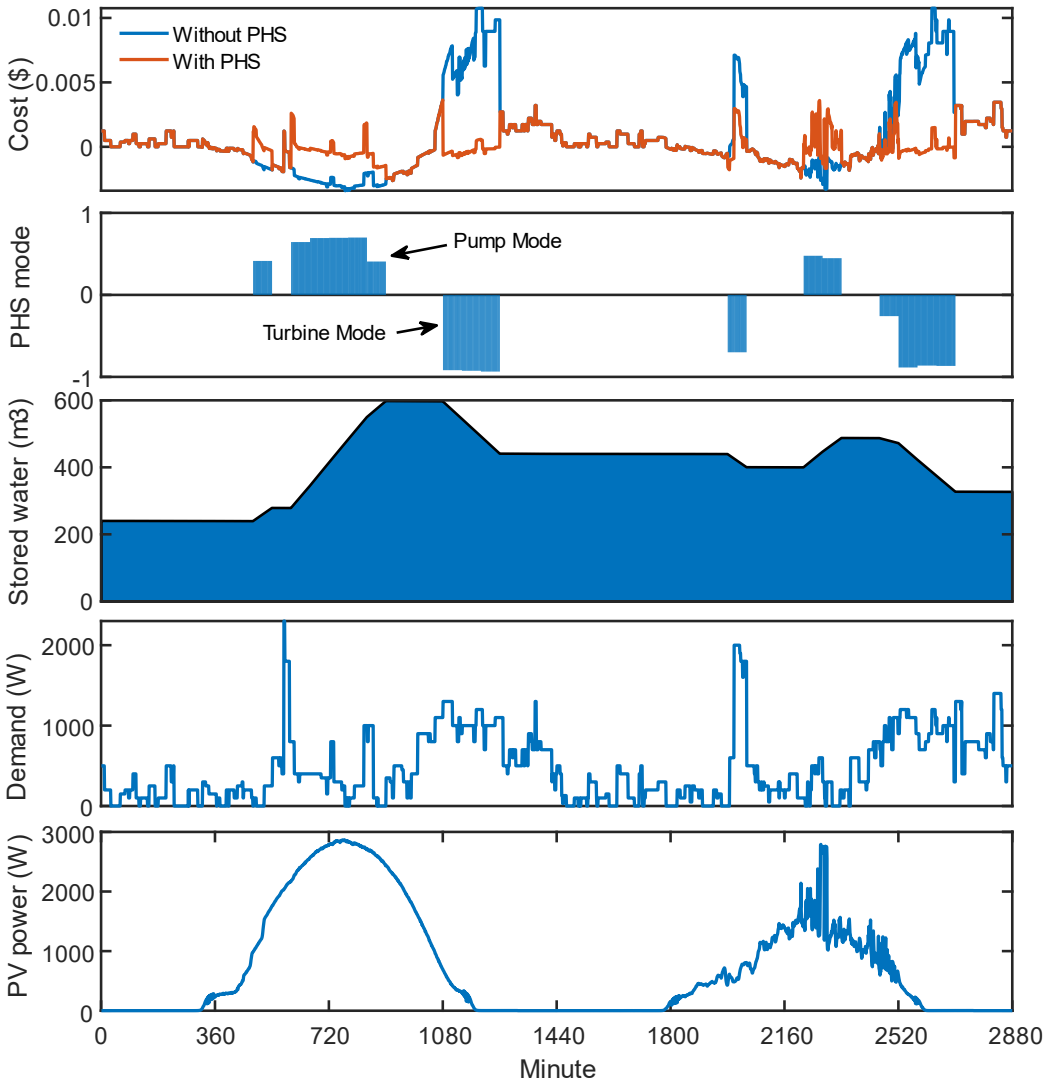

Fig 5.7: Electricity costs, PHS mode, stored water in the reservoir, energy demand, and PV power of the proposed system for 2 days of the experiment.

To make this balance for each decision, the EMS looks at the current and future state of the system and compares three costs: 1) pumping costs: the electricity costs of pumping water to the reservoir; 2) cost-saving: the cost-saving of generating energy later by that pumped water considering the losses of the PHS; 3) feed-in income: the feed-in income from the export of the surplus energy to the grid. If cost-saving minus pumping cost is less than feed-in income, the EMS does not run the PHS. Otherwise, the EMS determines the pump power and the turbine flow rate to increase cost-saving minus pumping cost to its highest.

When the demand was at its peak (M:580), the EMS decided not to pump. Consequently, the PV system could directly supply the demand instead of storing energy. The EMS decided not to pump water in this condition because cost-saving minus pumping cost was less than the feed-in income from the export of the surplus PV energy to the grid.

5.5 Simulation Results

The proposed system is simulated for one year in MATLAB to calculate the annual cost reduction. An irrigation plan shown in Table 5.3 is used in this simulation. This plan is provided by the Department of Primary Industries and Regional Development and is for a 1-hectare apple garden in Western Australia [126]. The irrigation pump has a 1 KW motor which works 6 hours during each irrigation with 28 m^3/h flow rate. The pump and the turbine types used for the PHS is mentioned in Table 5.4.

Table 5.3: Irrigation requirement used in the simulation

	Jan	Feb	Mar	Apr	May	Jun	Jul	Aug	Sep	Oct	Nov	Dec
Volume (m^3)	1575	1350	1050	525	0	0	0	0	0	525	1050	1575
Number of Irrigation	9	8	6	3	0	0	0	0	0	3	6	9

Table 5.4: The pump and the turbine used in the simulation

Element	Type	power	Water head	Water Flow
Turbine	XJ12-1.0DCTH4	1000W	7 ~ 12m	0.010~0.012 m3/s
Pump	6VP 60-2B	3000W	20 m	0.02 m3/s

Fig 5.8 compares the performance of the proposed EMS with the conventional EMS presented in [51, 135, 138]. In the conventional method, the irrigation times were fixed; however, in the proposed EMS, the irrigation times were managed. The proposed model determined the fourth day to be the best day of irrigation as it was a sunny day and the irrigation pump could directly consume clean electricity coming from the PV system. The next irrigation was on the seventh day because the sixth and eighth days were both cloudy and irrigating on the seventh day reduced pumping operation costs.

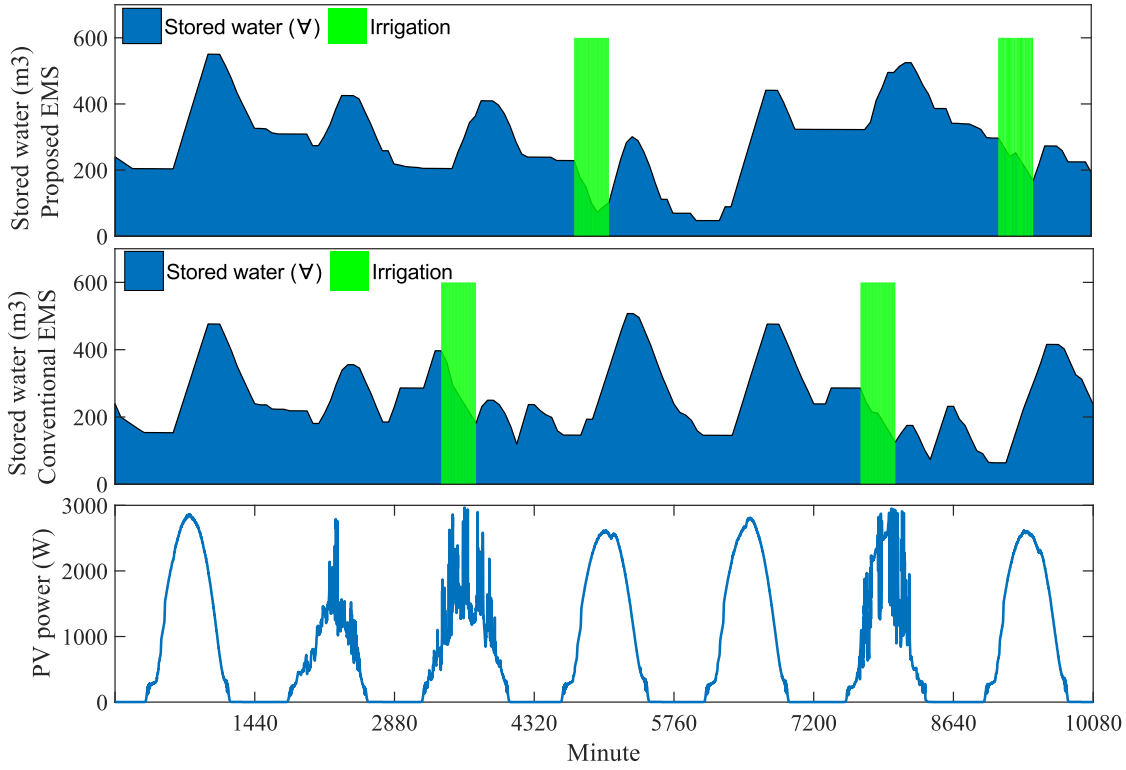

Fig 5.8: Volume of stored water and irrigation times for the proposed system and conventional EMS

Fixed irrigation times in the conventional EMS causes two problems: 1) It may run the pump when there is no PV power. After both irrigation times, the submerged pump compulsory worked consuming grid electricity to increase stored water to the arbitrary level of 40%; 2) It may run the irrigation system on cloudy days. The irrigation system has a pump which consumes electricity, so if PV does not generate energy, the energy will come from the grid, which increases electricity costs. Therefore, scheduling the time of irrigation can lead to managing the surplus PV power more effectively.

Fig 5.9 illustrates the effect of determining the required volume of stored water for the end of the day ($\forall_{24}$) on PHS management. On this day, the EMS decided to store more water in the reservoir ($\forall_{24} = 326\ m^3$). Consequently, there was more limitation in releasing water through the turbine. The proposed EMS decided to run the turbine less at the beginning of the day since both demand and tariff were low. However, the conventional EMS generated surplus energy by the turbine and sent it to the grid. Although the conventional EMS could save more money on this day, the amount of money that the proposed EMS could save on the next cloudy days is much more.

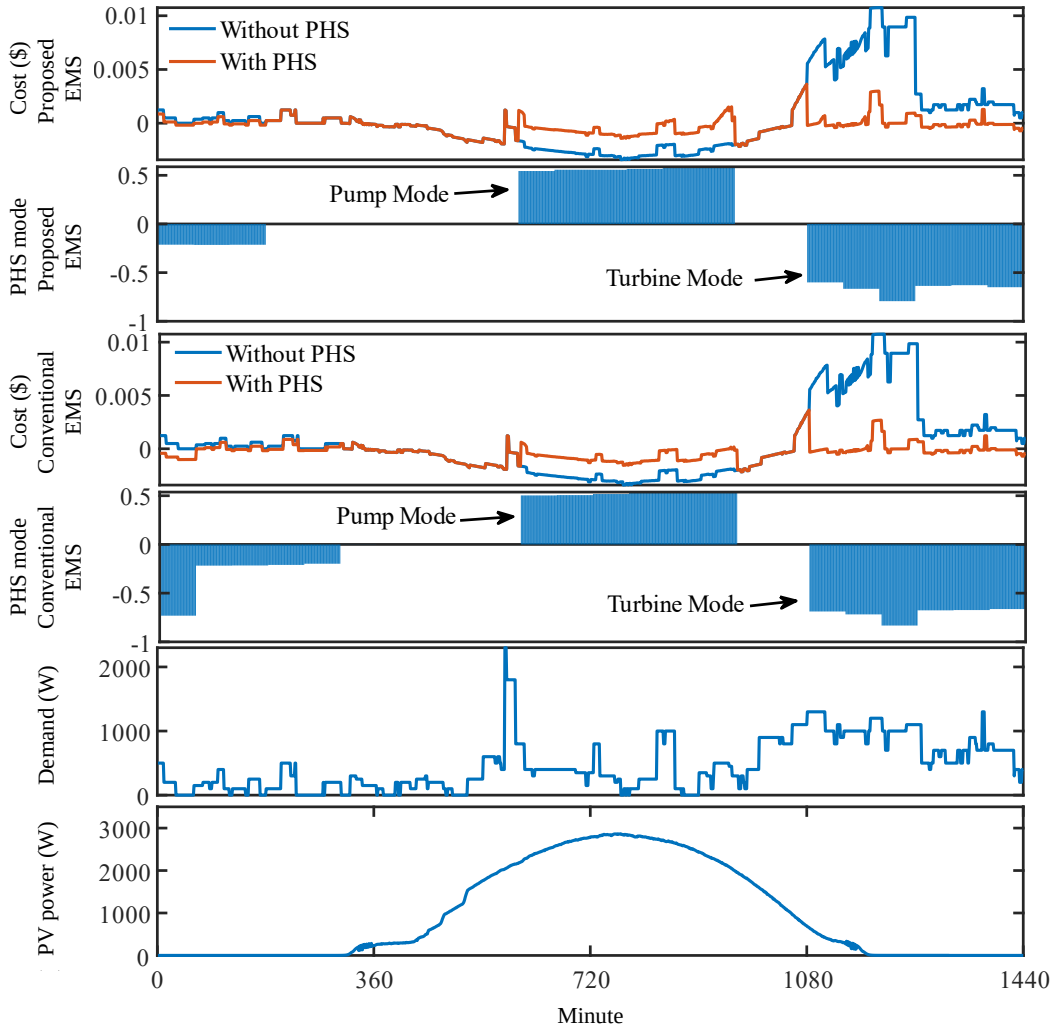

Fig 5.9: Comparison of proposed EMS and conventional EMS in electricity costs and PHS mode.

The results demonstrate that the proposed EMS takes into account the losses of the system due to using a comprehensive PHS model [117]. At night, even when the tariff was low, the EMS tried to meet the demand using the turbine, which did not happen in the experiment. The EMS made this decision since

the efficiency of the PHS was high enough to save money by using the turbine at this time. The turbine and the pump type used in the simulation have higher efficiency compared to the experiment. The proposed EMS can calculate the losses of the system and determine whether generating energy by the turbine is more cost-effective or buying energy from the grid. However, in the experiment, the proposed EMS decided to not use the turbine after the peak-period, since getting energy from the grid was more cost-effective.

5.6 Economic Analysis

5.6.1 Annual Electricity Cost Reduction

The proposed system is simulated for one year in different capacities from 300 W to 40 kW. The results of the simulation are given in table 5.5. These results indicate how much electricity costs will be reduced by adding a turbine to a farmhouse which already has a PV system. In each case, the capacities of other components of the microgrid are also changed relatively with the turbine capacity.

For each capacity, the annual electricity costs of the proposed EMS are compared with conventional EMS and without PHS. In "Without PHS", there is a PV system which generates power during the day, and when there is no sunshine, the grid meets the demand. In "conventional EMS", the turbine is added to the system to have a PHS, and the EMS presented in [51, 135, 138] is applied to manage the system.

Table 5.5: Annual electricity cost of the proposed system in a variety of capacities

Turbine capacity (kW)	Turbine	Storage capacity (kWh)	Annual electricity cost (AUD)		
			Without PHS	Conventional EMS	Proposed EMS
0.3	XJ14-0.3DCT4	4.2	183	46	30
0.5	XJ18-0.5DCT4	6.9	213	77	49
0.75	XJ18-0.75DCT4	10	351	118	81
1	XJ12-1.0DCTH4	14	652	175	99
1.5	XJ25-1.5DCTH4	21	720	292	116
2	XJ30-2.0DCT4-Z	28	1352	361	178
3	XJ13－L－13/1x3	42	1494	536	297
5	XJ13－L－18/1x5	69	3291	885	393
10	XJ40-L-10DCT4	139	7650	1487	959
15	XJ13-L-20/1*5	208	9701	3159	1602
20	XJ13-W-25/1*6	278	11200	3717	1757
30	XJ13-W-25/1*7/30	417	14410	5735	1852
40	XJ13-W-25/1*7/40	556	24194	6655	2100

Comparing the annual electricity costs of the microgrid without PHS with the conventional EMS illustrates how adding a turbine to the microgrids could significantly reduce electricity costs. Moreover, the proposed EMS could reduce electricity costs from 31% in small capacities to 68% for large capacities compared to the conventional EMS (Fig 5.10). Although both EMSs manage the system hourly, the proposed EMS considers the effect of each decision on the subsequent days as well. That is why the proposed EMS could manage the microgrid more efficiently.

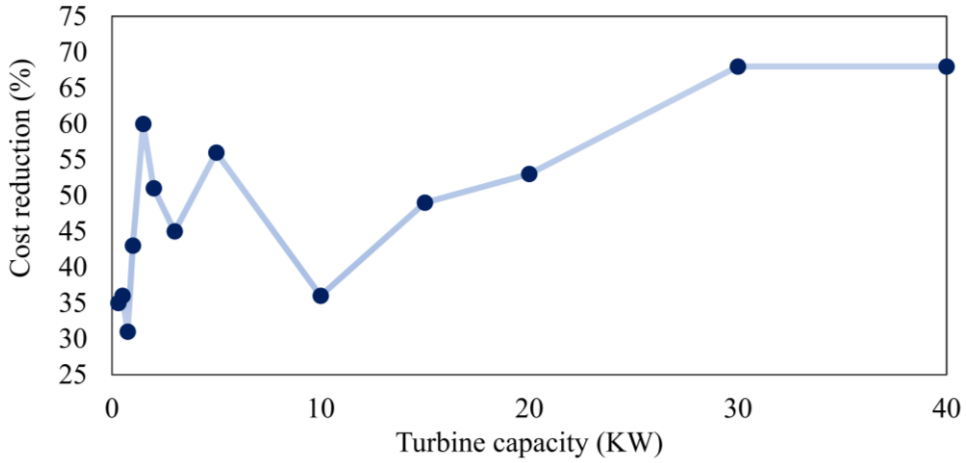

Fig 5.10: Percentage of electricity costs reduction by using the proposed EMS instead of the conventional method.

5.6.2 Payback Period

Table 5.6 indicates the payback period and lifetime benefit of implementing PHS systems into farmhouses managed with the proposed EMS. The capital cost includes the turbine price and balance of system (BOS). BOS includes the costs of pipes, fittings, cables, valves, and installation. The lifetime cost is calculated for each capacity for a duration of 20 years. The lifetime costs include capital, operation, and maintenance costs. A hydro turbine lifespan is estimated 20 years with the average annual operation and maintenance costs of 8.02 $/kW [135]. Annual saving is calculated by deducting the electricity, operation and maintenance costs of the proposed PHS from the electricity costs of the microgrid without PHS. The average residential electricity price has increased by 56% over the last

decade in Australia [157]. Assuming that the same trend continues, it is taken into account that the electricity price has an increase of 5.6% annually.

The results demonstrate that the proposed storage is profitable in all the cases where the lifetime benefits are from 4 to 29 times more than lifetime costs. The computed payback period shows that the proposed clean storage is an economical option for microgrids. The payback period of the proposed system is from 5 months to 3.2 years depending on the size of the system.

When comparing the proposed energy storage to batteries, the efficiency of batteries is higher. The efficiency of Li-ion batteries is about 81 to 98% [136], but the efficiency of the proposed storage is about 50 to 75%. However, the capital and maintenance costs of batteries are much higher than the proposed energy storage. A Li-ion battery costs around $600–3800/kWh [158] but the proposed energy storage costs $10-65/kWh (table 5.6). The lifetime of the proposed energy storage is much greater than batteries. The lifetime of Li-ion batteries is 5 to 15 years [158]; however, the lifetime of the proposed storage is around 20 to 50 years. Lower capital and maintenance costs of the proposed storage have made this storage more cost-effective than batteries. The payback period of a battery storage installed in Australia with an existing PV system is about 4 to 25 years for the range of 20 kWh to 3 kWh [159, 160]. However, the payback period of the proposed storage for the same capacity range is 1 to 3 years. This is shorter than one-fourth of battery payback period with the same capacities.

Table 5.6: Payback period and lifetime benefit of the proposed storage system

Storage capacity (kWh)	Turbine Price (AUD)	BOS (AUD)	Capital cost (AUD)	Lifetime cost (AUD)	Annual saving (AUD)	lifetime benefit (AUD)	Payback period (Year)
4.2	276	200	476	524.1	150.6	2487.8	3.2
6.9	292	220	512	592.2	160	2607.6	3.2
10	301	220	521	641.3	264	4638.4	2
14	344	250	594	754.4	545	10145	1.1
21	346	300	646	886.6	592	10953	1.1
28	350	300	650	970.8	1158	22188	0.6
42	430	300	730	1211	1173	22248	0.6
69	803	300	1103	1905	2858	55253	0.4
139	3410	500	3910	5514	6611	126702	0.6
208	3740	500	4240	6646	7979	152928	0.5
278	8130	700	8830	12038	9283	173614	1
417	9100	700	9800	14612	12317	231736	0.8
556	9750	1000	10750	17166	21773	418298	0.5

5.7 System design

The purpose of installing PV systems in farms is to supply power for irrigation systems. The capacity of PV systems should be selected around the power of pumps to meet the energy required for pumping during the day. In the experiment, the pump is 3 kW, so a 3 kW PV system is connected to the microgrid.

The results of the economic analysis show that turbines with large capacities have a lower payback period which has two reasons. First, larger turbines have higher efficiency comparing to small turbines; Second, large turbines have a lower price per kW. Selecting the capacity of the turbine depends on the demand profile. The turbine rated power should be selected around the average demand power during peak hours since the most saving happens during peak hours; thus, it is essential to choose a turbine that is able to meet the demand at peak hours. In the experiment, average demand in peak hours is around 726 W, so a 768 W turbine is selected for the PHS. A larger turbine would increase the operating costs of the system since the efficiency of turbine significantly drops in lower than half of the rated power. Operation with low efficiency would increase the loss of saved energy which could be used to save money during deficit energy.

Pump and turbine flow rate must be less than the flow rate between the well and aquifer to make sure the water level in the well is kept constant. If the aquifer feeds the well at the same rate of pumping, the water level in the well does not go down in the pump mode. In the turbine mode, if water releases through the turbine at the same rate of flowing water between well and aquifer, the water level in the well does not rise. Therefore, the PHS can operate according to the schedule without interruption.

5.8 Conclusion

This chapter developed a new type of PHS system applicable to farmhouses with PV systems. The proposed storage can store energy and irrigate land at the same time. Using existing irrigation infrastructure for storing energy makes this system a cost-effective option compared to other types of energy storage systems. The designed energy management system takes into account PV power, energy

demand, water demand, energy tariff, PHS losses, and the future state of the system to determine the pump power and the turbine flow rate. The experimental test showed that the proposed management system is able to efficiently control the pump power and the turbine flow rate during the day with different energy tariff and power generation to minimise operating costs. This study demonstrates that managing irrigation times and $\forall_{24}$ assists the system to use stored energy more efficiently. The proposed system can consider the losses of the energy storage system for each decision by using a comprehensive PHS model. The simulation results indicate that the PHS can reduce electricity costs not only during peak hours but also during off-peak hours. It was found that the cost-saving by the PHS is much more than feed-in income without PHS, even during off-peak hours, although the PHS configuration used in the simulation has 40% energy losses on average. The proposed system could reduce electricity costs by more than 31% compared to the conventional energy management system. The payback period of the proposed system is less than 3.2 years, which encourages industry to use this clean energy storage as an alternative to batteries in rural areas.

Chapter 6 is not included in this version of the thesis

Chapter 7: **Conclusion**

This study proposed a new type of pumped hydro storage system applicable in rural areas. This storage uses existing irrigation infrastructure to store energy as the form of gravitational potential energy. It uses the available pumping system, water well, and reservoir to build a pumped hydro storage (PHS) system. It is very low-cost energy storage since the capital cost would be installing a turbine. It has a long life span, 20 to 50 years, where maintenance costs are low as well. This energy storage does not have any chemical substances; water is the only material that it needs to work, which makes it eco-friendly energy storage. Therefore, this project focused deeply on how this energy storage can be implemented. The first step was modelling the system as the model is required in both management and simulation.

Chapter 3 presented a comprehensive mathematical PHS model that can calculate pump flow rate, stored water, and turbine generation taking into account losses of the system as well as precipitation and evaporation. The results of the proposed model are compared with the results of established models presented in other papers. The results of this study indicated that the proposed model has reduced the stored water error from 13.17% to 0.74%. The accuracy of calculating stored water has a key role in scheduling as any error can cause inefficient decisions. In this model, the effects of water level and flow rate on the head loss of the penstock are deeply studied to reduce errors in flow rate calculation in both pump mode and turbine mode. The error of the proposed model in the pump mode is reduced from 18.36% to 1.4% and the error in the turbine mode is reduced from 21.23% to 1.61%. This model is useful for scheduling since it predicts the performance of the PHS in any conditions. The significant assistance of the proposed model is that it can calculate losses in any pump power or turbine rate. This helps the scheduling part to select the optimum turbine flow rate and pump power.

Chapter 4 described the idea of using irrigation components to store energy without interrupting their primary functions. A turbine is placed in a farmhouse to build a low-cost and eco-friendly energy storage system. The stored water in the reservoir is used for both irrigation and electricity generation.

The effect of PHS operation and aquifer type on the water level in the well is studied to calculate the maximum flow rate that the PHS is allowed in both pump and turbine mode. The comprehensive PHS model presented in chapter 3 is applied in the scheduling part to increase the efficiency of pump and turbine management by takes into account not only generation and demand but also the efficiency of the PHS at different conditions. The idea is tested with the experimental setup installed at smart energy lab at Edith Cowan University. The proposed PHS system could reduce the annual electricity costs of the farmhouse significantly.

Chapter 5 introduced a new method of scheduling designed especially for the proposed PV-PHS system. This developed scheduling method manages not only the pump and turbine but also irrigation times and stored water by using two forecasting methods and a multi-level optimisation algorithm. It takes into account energy generation, energy demand, water demand, energy tariff, and system losses to determine the pump power, the turbine flow rate, and irrigation times. In this method, the required volume of water for the next day is determined in order to store sufficient energy before cloudy days. The proposed method compares cost-saving and feed-in income for each decision and decides to store surplus energy or sell it to the grid. The results showed that adding irrigation and water management assisted the energy management system in using stored water more efficiently. Therefore, the electricity costs are reduced by more than 31% compared to the previous scheduling methods.

Chapter 6 proposed a real-time management system to solve the forecast error problem in scheduling methods. Scheduling methods suffer from the error of forecast data, as a result, any difference in forecast data and actual data would cause not efficient decisions. This problem is addressed by a real-time management system that receives PHS schedule and forecast error to make more efficient decisions. The novelty of Chapter 6 is that the pump and turbine are controlled on real-time considering both current and future conditions of the system. From the two controllers designed for this purpose, the artificial neural network (ANN) method had better performance. The results show that real-time management was very useful in cloudy days as fluctuations are high. A big challenge of designing the proposed real-time management was producing target data to train the ANN network. An innovative approach is suggested to produce target data to reduce training time. Economic analysis with real data

showed a major reduction in the annual electricity bill of the farmhouse after adding the real-time management to the scheduling method.

Another contribution of this project is its focus on the practical examination of PV-PHS microgrids. The microgrid is tested in a laboratory environment, where real data was used in both experiments and simulations. PV power data used in this project was measured in the lab in order to evaluate the performance of the system with real PV power fluctuation in cloudy days. Weather data including evaporation, rainfall, irradiance, temperature, and wind speed were measured by a weather station installed in the place. The proposed management system was receiving forecast data from a powerful online weather service every hour for the scheduling part. Both forecast and actual data were collected at the same time to experience real forecast error with current predicting technology. Therefore, the results of this project can be an accurate prediction of real implementations.

Another very important aspect of this project is designing a variable-speed pumped hydro storage system, where both pump power and turbine flow rate are adjustable. The developed model in Chapter 3 can calculate the performance of PHS systems in a wide operation range, where it accurately calculates the losses depending on the flow rate. The designed management system in chapter 5 and Chapter 6 are able to optimise the pump power and turbine flow rate considering the power generation, demand, and the losses of storage. This model and management system provide a wider operating range which assist the pump and turbine to operate more efficiently.

Costs of the proposed energy storage system are calculated for different cases to produce a useful economic analysis for farmers to have a better understanding about the costs of implementing this system in their land. This system is cost-effective in a wide range of farmhouses with different sizes of reservoir and water well depth. The results in Section 6.4 showed that adding the turbine to the farmhouse with the proposed management system saved 90% of the annual electricity bill for the tested microgrid. The proposed idea is a very cost-effective energy storage system for farms with water wells. Capital costs limit to a turbine that has made its payback period in most cases around one year. The

results in Section 5.6 and Section 6.6 proved that any investment in this storage is highly profitable as lifetime benefits are tens of times more than capital costs.

Future work may look at the technical and economic feasibility study of the proposed system in remote areas. The proposed PHS can be used to store surplus energy in a stand-alone PV system to meet the demand when there is no sunshine. A small battery bank can also be included to assist the system during transients. Future study may also consider using the proposed real-time energy management for other configurations such as PV-Battery or Wind-PHS microgrids. The designed energy management system is capable of controlling any microgrids with energy storage systems. It uses forecast data to schedule the amount of energy that is required to be sent or received by the energy storage system. Then, it applies actual measurements to control the microgrid on real-time.

References

[1] Ş. E. C. Şener, S. Julia L, and A. Annick, "Factors impacting diverging paths of renewable energy: A review.," *Renewable and Sustainable Energy Reviews*, 2017.

[2] X. Liang, "Emerging power quality challenges due to integration of renewable energy sources," *IEEE Transactions on Industry Applications* vol. 53, no. 2 pp. 855-866, 2017.

[3] L. Wang, Q. S. Vo, and A. V. Prokhorov, "Dynamic Stability Analysis of a Hybrid Wave and Photovoltaic Power Generation System Integrated Into a Distribution Power Grid," (in English), *Ieee Transactions on Sustainable Energy*, vol. 8, no. 1, pp. 404-413, Jan 2017, doi: 10.1109/Tste.2016.2602370.

[4] C. Mejia and Y. Kajikawa, "Emerging topics in energy storage based on a large-scale analysis of academic articles and patents," *Applied Energy*, vol. 263, p. 114625, 2020.

[5] E. Chemali, M. Preindl, P. Malysz, and A. Emadi, "Electrochemical and electrostatic energy storage and management systems for electric drive vehicles: State-of-the-art review and future trends," *IEEE Journal of Emerging and Selected Topics in Power Electronics*, vol. 4, no. 3, pp. 1117-1134, 2016.

[6] Y. Karimi, H. Oraee, M. S. Golsorkhi, and J. M. Guerrero, "Decentralized method for load sharing and power management in a PV/battery hybrid source islanded microgrid," *IEEE Transactions on Power Electronics*, vol. 32, no. 5, pp. 3525-3535, 2017.

[7] H. Hao, Z. Mu, S. Jiang, Z. Liu, and F. Zhao, "GHG Emissions from the Production of Lithium-Ion Batteries for Electric Vehicles in China," *Sustainability*, vol. 9, no. 4, p. 504, 2017.

[8] D. W. Gao, *Energy Storage for Sustainable Microgrid*. Academic Press, 2015.

[9] Siemens. "Microgrids." www.siemens.com (accessed.

[10] Z. Zhao, "Optimal energy management for microgrids," Ph.D. dissertation, Clemson University, 2012.

[11] Z. Zhou *et al.*, "Game-Theoretical Energy Management for Energy Internet With Big Data-Based Renewable Power Forecasting," *IEEE Access*, vol. 5, pp. 5731--5746, 2017.

[12] W. Shi, N. Li, C.-C. Chu, and R. Gadh, "Real-Time Energy Management in Microgrids," *IEEE Transactions on Smart Grid*, vol. 8, no. 1, pp. 228-238, 2017.

[13] A. C. Luna, N. L. Diaz, M. Graells, J. C. Vasquez, and J. M. Guerrero, "Mixed-integer-linear-programming-based energy management system for hybrid PV-wind-battery microgrids: Modeling, design, and experimental verification," *IEEE Transactions on Power Electronics*, vol. 32, no. 4, pp. 2769--2783, 2017.

[14] P. Malysz, S. Sirouspour, and A. Emadi, "An optimal energy storage control strategy for grid-connected microgrids," *IEEE Transactions on Smart Grid*, vol. 5, no. 4, pp. 1785--1796, 2014.

[15] T. Strasser *et al.*, "A review of architectures and concepts for intelligence in future electric energy systems," *IEEE Transactions on Industrial Electronics*, vol. 62, no. 4, pp. 2424--2438, 2015.

[16] A. A. S. de la Nieta, J. Contreras, and J. P. Catalão, "Optimal Single Wind Hydro-Pump Storage Bidding in Day-Ahead Markets Including Bilateral Contracts," *IEEE Transactions on Sustainable Energy*, vol. 7, no. 3, pp. 1284-1294, 2016.

[17] K. Bruninx, Y. Dvorkin, E. Delarue, H. Pandzic, W. D'haeseleer, and D. S. Kirschen, "Coupling Pumped Hydro Energy Storage With Unit Commitment," (in English), *Ieee Transactions on Sustainable Energy*, vol. 7, no. 2, pp. 786-796, Apr 2016, doi: 10.1109/Tste.2015.2498555.

[18] A. Helseth, A. Gjelsvik, B. Mo, and Ú. Linnet, "A model for optimal scheduling of hydro thermal systems including pumped-storage and wind power," *Helseth, Arild and Gjelsvik, Anders and Mo, Birger and Linnet, {\'U}lfar*, vol. 7, no. 12, pp. 1426--1434, 2013.

[19] A. B. T. Attya and T. Hartkopf, "Utilising stored wind energy by hydro-pumped storage to provide frequency support at high levels of wind energy penetration," *Attya, Ayman Bakry Taha and Hartkopf, Thomas*, vol. 9, no. 12, pp. 1485-1497, 2015.

[20] C. G. Baslis and A. G. Bakirtzis, "Mid-term stochastic scheduling of a price-maker hydro producer with pumped storage," *IEEE Transactions on Power Systems*, vol. 26, no. 4, pp. 1856-1865, 2011.

[21] Y. Zhang, Y. Zhang, and Y. Wu, "A review of rotating stall in reversible pump turbine," *Journal of Mechanical Engineering Science*, vol. 231, no. 7, pp. 1181-1204, 2017.

[22] E. C. Walseth, "Dynamic Behavior of Reversible Pump-Turbines in Turbine Mode of Operation," Ph.D. dissertation, Norwegian University of Science and Technology, Norway, 2016.

[23] T. Kousksou, P. Bruel, A. Jamil, T. El Rhafiki, and Y. Zeraouli, "Energy storage: Applications and challenges," *Solar Energy Materials and Solar Cells*, vol. 120, pp. 59-80, 2014.

[24] R. Amirante, E. Cassone, E. Distaso, and P. Tamburrano, "Overview on recent developments in energy storage: mechanical, electrochemical and hydrogen technologies," *Energy Conversion and Management*, vol. 132, pp. 372--387, 2017.

[25] M. Chazarra, J. I. Pérez-Díaz, and J. García-González, "Optimal energy and reserve scheduling of pumped-storage power plants considering hydraulic short-circuit operation," *IEEE Transactions on Power Systems*, vol. 32, no. 1, pp. 344-353, 2017.

[26] ABB. "Energy storage systems, Keeping smart grids in balance." www.abb-energystoragesolutions.com (accessed.

[27] DOE. "Global Energy Storage Database." http://www.energystorageexchange.org/projects/data_visualization (accessed 2018.

[28] M. Rossi, M. Righetti, and M. Renzi, "Pump-as-Turbine for energy recovery applications: the case study of an aqueduct," *Energy Procedia*, vol. 101, pp. 1207-1214, 2016.

[29] E. C. Walseth, T. K. Nielsen, and B. Svingen, "Measuring the Dynamic Characteristics of a Low Specific Speed Pump-Turbine Model," *Energies*, vol. 9, no. 3, p. 199, 2016.

[30] T. Ma, H. Yang, and L. Lu, "Feasibility study and economic analysis of pumped hydro storage and battery storage for a renewable energy powered island," *Energy Conversion and Management*, vol. 79, pp. 387--397, 2014.

[31] T. Ma, H. Yang, L. Lu, and J. Peng, "Pumped storage-based standalone photovoltaic power generation system: Modeling and techno-economic optimization," *Applied energy*, vol. 137, pp. 649-659, 2015.

[32] A. Alhamali, M. E. Farrag, G. Bevan, and D. M. Hepburn, "Review of Energy Storage Systems in Electric Grid and their potential in Distribution Networks," in *Power Systems Conference (MEPCON), 2016 Eighteenth International Middle East*, 2016.

[33] H. Hahn, D. Hau, C. Dick, and M. Puchta, "Techno-economic assessment of a subsea energy storage technology for power balancing services," *Energy*, vol. 133, no. 15, pp. 121-127, 2017.

[34] D. Connolly, "A review of energy storage technologies: for the integration of fluctuating renewable energy," 2010.

[35] X. Luo, J. Wang, M. Dooner, and J. Clarke, "Overview of current development in electrical energy storage technologies and the application potential in power system operation," *Applied Energy*, vol. 137, pp. 511-536, 2015.

[36] K. Kusakana, "Feasibility analysis of river off-grid hydrokinetic systems with pumped hydro storage in rural applications," *Energy Conversion and Management*, vol. 96, pp. 352-362, 2015.

[37] T. Ma, H. Yang, L. Lu, and J. Peng, "Technical feasibility study on a standalone hybrid solar-wind system with pumped hydro storage for a remote island in Hong Kong," *Renewable Energy*, vol. 69, pp. 7-15, 2014.

[38] H. Chen, T. N. Cong, W. Yang, C. Tan, Y. Li, and Y. Ding, "Progress in electrical energy storage system: A critical review," *Progress in Natural Science*, vol. 19, no. 3, pp. 291-312, 2009.

[39] D. Connolly, H. a. F. Lund, P, B. V. Mathiesen, and M. Leahy, "Practical operation strategies for pumped hydroelectric energy storage (PHES) utilising electricity price arbitrage," *Energy Policy*, vol. 39, pp. 4189-4196, 2011.

[40] M. Obi, S. M. Jensen, J. B. Ferris, and R. B. Bass, "Calculation of levelized costs of electricity for various electrical energy storage systems," (in English), *Renew Sust Energ Rev*, vol. 67, pp. 908-920, Jan 2017, doi: 10.1016/j.rser.2016.09.043.

[41] J. K. Kaldellis and D. Zafirakis, "Optimum energy storage techniques for the improvement of renewable energy sources-based electricity generation economic efficiency," (in English), *Energy*, vol. 32, no. 12, pp. 2295-2305, Dec 2007, doi: 10.1016/j.energy.2007.07.009.

[42] S. Rehman, L. M. Al-Hadhrami, and M. M. Alam, "Pumped hydro energy storage system: A technological review," *Renewable and Sustainable Energy Reviews*, vol. 44, pp. 586-598, 2015.

[43] K. Ghaib and F.-Z. Ben-Fares, "A design methodology of stand-alone photovoltaic power systems for rural electrification," *Energy Conversion and Management*, vol. 148, pp. 1127-1141, 2017.

[44] J. P. Deane, B. Ó. Gallachóir, and E. McKeogh, "Techno-economic review of existing and new pumped hydro energy storage plant," *Renewable and Sustainable Energy Reviews*, vol. 14, no. 4, pp. 1293-1302, 2010.

[45] M. J. Severson, "Preliminary Evaluation of Establishing an Underground Taconite Mine, to be Used Later as a Lower Reservoir in a Pumped Hydro Energy Storage Facility, on the Mesabi Iron Range, Minnesota," 2016.

[46] B. Parkin. "How to Make Electricity in a Disused Coal Mine." www.bloomberg.com (accessed.

[47] J. Olsen, K. Paasch, B. Lassen, and C. T. Veje, "A new principle for underground pumped hydroelectric storage," *Journal of Energy Storage,* vol. 2, pp. 54-63, 2015.

[48] C. Gopal, M. Mohanraj, P. Chandramohan, and P. Chandrasekar, "Renewable energy source water pumping systems-A literature review," *Renewable and Sustainable Energy Reviews,* vol. 25, pp. 351--370, 2013.

[49] A. Stoppato, G. Cavazzini, A. Benato, N. Destro, and G. Ardizzon, "Optimum design and management of a hybrid photovoltaic-pump hydro energy storage system," in *Proceedings of the ASME 2014 12th Biennial Conference on Engineering Systems Design and Analysis*, Copenhagen, 2014.

[50] A. Stoppato, G. Cavazzini, G. Ardizzon, and A. Rossetti, "A PSO (particle swarm optimization)-based model for the optimal management of a small PV(Photovoltaic)-pump hydro energy storage in a rural dry area," (in English), *Energy,* vol. 76, pp. 168-174, Nov 1 2014, doi: 10.1016/j.energy.2014.06.004.

[51] T. T. Anilkumar, S. P. Simon, and N. P. Padhy, "Residential electricity cost minimization model through open well-pico turbine pumped storage system," *Applied Energy,* vol. 195, pp. 23-35, Jun 1 2017, doi: 10.1016/j.apenergy.2017.03.020.

[52] H. Zhu, X. Li, Q. Sun, L. Nie, J. Yao, and G. Zhao, "A power prediction method for photovoltaic power plant based on wavelet decomposition and artificial neural networks," *Energies,* vol. 9, no. 1, p. 11, 2015.

[53] A. T. Thankappan, S. P. Simon, P. S. R. Nayak, K. Sundareswaran, and N. P. Padhy, "Pico-hydel hybrid power generation system with an open well energy storage," *IET Generation, Transmission & Distribution,* vol. 11, no. 3, pp. 740-749, 2017.

[54] E. Pujades, T. Willems, S. Bodeux, P. Orban, and A. Dassargues, "Underground pumped storage hydroelectricity using abandoned works (deep mines or open pits) and the impact on groundwater flow," *Hydrogeology Journal,* vol. 24, no. 6, pp. 1531-1546, 2016.

[55] N. Kannan, J. Jeong, and R. Srinivasan, "Hydrologic modeling of a canal-irrigated agricultural watershed with irrigation best management practices: Case study," *Journal of Hydrologic Engineering,* vol. 16, no. 9, pp. 746-757, 2010.

[56] A. J. Wood and B. F. Wollenberg, *Power generation, operation, and control*. John Wiley & Sons, 2012.

[57] A. Arabali, M. Ghofrani, M. Etezadi-Amoli, M. S. Fadali, and Y. Baghzouz, "Genetic-algorithm-based optimization approach for energy management," *IEEE Transactions on Power Delivery,* vol. 28, no. 1, pp. 162-170, 2013.

[58] S. Singh and S. C. Kaushik, "Optimal sizing of grid integrated hybrid PV-biomass energy system using artificial bee colony algorithm," *IET Renewable Power Generation,* vol. 10, no. 5, pp. 642-650, 2016.

[59] G. Tian, Y. Ren, and M. Zhou, "Dual-objective scheduling of rescue vehicles to distinguish forest fires via differential evolution and particle swarm optimization combined algorithm," *IEEE Transactions on Intelligent Transportation Systems,* vol. 17, no. 11, pp. 3009-3021, 2016.

[60] N. H. Saad, A. A. El-Sattar, and M. E. Marei, "Improved bacterial foraging optimization for grid connected wind energy conversion system based PMSG with matrix converter," *Ain Shams Engineering Journal,* 2017.

[61] H. M. Hasanien, "Gravitational search algorithm-based optimal control of archimedes wave swing-based wave energy conversion system supplying a DC microgrid under uncertain dynamics," *IET Renewable Power Generation,* vol. 11, no. 6, pp. 763-770, 2016.

[62] K. Kusakana, "Optimal scheduling for distributed hybrid system with pumped hydro storage," *Energy Conversion and Management,* vol. 111, pp. 253-260, 2016.

[63] M. Chazarra, J. García-González, J. I. Pérez-Díaz, and M. Arteseros, "Stochastic optimization model for the weekly scheduling of a hydropower system in day-ahead and secondary regulation reserve markets," *Electric Power Systems Research,* vol. 130, pp. 67-77, 2016.

[64] C.-C. Tsai, Y. Cheng, S. Liang, and W.-J. Lee, "The co-optimal bidding strategy of pumped-storage unit in ERCOT energy market," in *North American Power Symposium (NAPS), 2009*, 2009: IEEE, pp. 1-6.

[65] M. A. Hozouri, A. Abbaspour, M. Fotuhi-Firuzabad, and M. Moeini-Aghtaie, "On the use of pumped storage for wind energy maximization in transmission-constrained power systems," *IEEE Transactions on Power Systems,* vol. 30, no. 2, pp. 1017-1025, 2015.

[66] A. Panday and H. O. Bansal, "Energy management strategy for hybrid electric vehicles using genetic algorithm," *Journal of Renewable and Sustainable Energy,* vol. 8, no. 1, p. 015701, 2016.

[67] C. Desai and S. S. Williamson, "Comparative study of hybrid electric vehicle control strategies for improved drivetrain efficiency analysis," in *Electrical Power & Energy Conference (EPEC), 2009 IEEE*, 2009: IEEE, pp. 1-6.

[68] S. Golshannavaz, S. Afsharnia, and F. Aminifar, "Smart distribution grid: optimal day-ahead scheduling with reconfigurable topology," *IEEE Transactions on Smart Grid,* vol. 5, no. 5, pp. 2402-2411, 2014.

[69] F.-L. Meng and X.-J. Zeng, "A profit maximization approach to demand response management with customers behavior learning in smart grid," *IEEE Transactions on Smart Grid,* vol. 7, no. 3, pp. 1516-1529, 2016.

[70] M. Alamaniotis, D. Bargiotas, N. G. Bourbakis, and L. H. Tsoukalas, "Genetic optimal regression of relevance vector machines for electricity pricing signal forecasting in smart grids," *IEEE Transactions on Smart Grid,* vol. 6, no. 6, pp. 2997-3005, 2015.

[71] S. Yue, Q. Xuesong, and G. Shaoyong, "Genetic algorithm-based redundancy optimization method for smart grid communication network," *China Communications,* vol. 12, no. 8, pp. 73-84, 2015.

[72] T. M. Hansen, R. Roche, S. Suryanarayanan, A. A. Maciejewski, and H. J. Siegel, "Heuristic optimization for an aggregator-based resource allocation in the smart grid," *IEEE Transactions on Smart Grid,* vol. 6, no. 4, pp. 1785-1794, 2015.

[73] R. Zafar, A. Mahmood, S. Razzaq, W. Ali, U. Naeem, and K. Shehzad, "Prosumer based energy management and sharing in smart grid," *Renewable and Sustainable Energy Reviews,* vol. 82, pp. 1675-1684, 2018.

[74] N. Denis, M. R. Dubois, and A. Desrochers, "Fuzzy-based blended control for the energy management of a parallel plug-in hybrid electric vehicle," *IET Intelligent Transport Systems,* vol. 9, no. 1, pp. 30-37, 2014.

[75] F. Valencia, J. Collado, D. Sáez, and L. G. Marín, "Robust energy management system for a microgrid based on a fuzzy prediction interval model," *IEEE Transactions on Smart Grid,* vol. 7, no. 3, pp. 1486-1494, 2016.

[76] Y.-K. Chen, Y.-C. Wu, C.-C. Song, and Y.-S. Chen, "Design and implementation of energy management system with fuzzy control for DC microgrid systems," *IEEE Transactions on Power Electronics,* vol. 28, no. 4, pp. 1563-1570, 2013.

[77] W. Wang, C. Li, X. Liao, and H. Qin, "Study on unit commitment problem considering pumped storage and renewable energy via a novel binary artificial sheep algorithm," *Applied Energy*, vol. 187, pp. 612-626, 2017.

[78] A. S. Kocaman and V. Modi, "Value of pumped hydro storage in a hybrid energy generation and allocation system," *Applied Energy*, vol. 205, pp. 1202-1215, 2017.

[79] A. Blakers, B. Lu, M. Stocks, K. Anderson, and A. Nadolny, "Pumped hydro storage to support 100% renewable power," *Energy News*, vol. 36, no. 1, p. 11, 2018.

[80] S. Koko, K. Kusakana, and H. Vermaak, "Energy flow modeling between grid and micro-hydrokinetic-pumped hydro storage hybrid system," in *Industrial and Commercial Use of Energy (ICUE), 2017 International Conference on the*, 2017, pp. 1-7.

[81] I. Mougharbel, Z. Shehab, and S. Georges, "Simulation of a hybrid renewable energy system in rural regions," in *IECON 2012-38th Annual Conference on IEEE Industrial Electronics Society*, 2012, pp. 1150-1155.

[82] T. Ma, H. Yang, and L. Lu, "Feasibility study and economic analysis of pumped hydro storage and battery storage for a renewable energy powered island," *Energy Conversion and Management*, vol. 79, pp. 387-397, 2014.

[83] K. Kusakana, "Optimal operation scheduling of grid-connected PV with ground pumped hydro storage system for cost reduction in small farming activities," *Journal of Energy Storage*, vol. 16, pp. 133-138, 2018.

[84] S. P. Koko, K. Kusakana, and H. J. Vermaak, "Optimal power dispatch of a grid-interactive micro-hydrokinetic-pumped hydro storage system," *Journal of Energy Storage*, vol. 17, pp. 63-72, 2018.

[85] P. Chaudhary and M. Rizwan, "Energy management supporting high penetration of solar photovoltaic generation for smart grid using solar forecasts and pumped hydro storage system," *Renewable Energy*, vol. 118, pp. 928-946, 2018.

[86] S. Koko, K. Kusakana, and H. Vermaak, "Optimal Sizing of a Micro-Hydrokinetic Pumped-Hydro-Storage Hybrid System for Different Demand Sectors," in *Sustainable Cloud and Energy Services*: Springer, 2018, pp. 219-242.

[87] K. Kusakana, "Hybrid PV-Wind with groundwater pumped hydro storage system for electricity cost minimization," *Advanced Science Letters*, vol. 24, no. 11, pp. 8176-8181, 2018.

[88] B. S. Pali and S. Vadhera, "A novel pumped hydro-energy storage scheme with wind energy for power generation at constant voltage in rural areas," *Renewable Energy*, vol. 127, pp. 802-810, 2018.

[89] K. Kusakana, "Hybrid DG-PV with groundwater pumped hydro storage for sustainable energy supply in arid areas," *Journal of Energy Storage*, vol. 18, pp. 84-89, 2018.

[90] S. Phommixay, M. L. Doumbia, and D. L. St-Pierre, "Optimal economic operation strategy of wind turbine-diesel unit with pumped hydro energy storage," in *Ecological Vehicles and Renewable Energies (EVER), 2018 Thirteenth International Conference on*, 2018: IEEE, pp. 1-6.

[91] H. Li, G. Parker, B. K. Johnson, J. D. Law, K. Morse, and D. F. Elger, "Modeling and simulation of a high-head pumped hydro system," in *T&D Conference and Exposition, 2014 IEEE PES*, 2014: IEEE, pp. 1-5.

[92] M. R. H. Asif and M. T. Iqbal, "Dynamic Modeling and Analysis of a Remote Hybrid Power System with Pumped Hydro Storage," *International Journal of Energy Science*, vol. 3, no. 5, 2013.

[93] W. Hu, P. Zhang, Z. Chen, J. Li, S. Chen, and W. Ruan, "Model-based control for doubly fed adjustable-speed pumped storage units with fast power support," in *2018 13th IEEE Conference on Industrial Electronics and Applications (ICIEA)*, 2018: IEEE, pp. 2227-2232.

[94] G. Pienta and S. Elmaddah, *Pumps & Pump Systems II*. American Society of Plumbing Engineers, 2015.

[95] N. K. Shammas and L. K. Wang, *Water engineering: Hydraulics, distribution and treatment*. John Wiley & Sons, 2015.

[96] R. G. Allen, L. S. Pereira, D. Raes, and M. Smith, "Crop evapotranspiration-Guidelines for computing crop water requirements-FAO Irrigation and drainage paper 56," *FAO, Rome,* vol. 300, no. 9, p. D05109, 1998.

[97] J. F. Petersen, D. Sack, and R. E. Gabler, *Physical Geography*. Cengage Learning, 2016.

[98] S. L. Dixon and C. Hall, *Fluid mechanics and thermodynamics of turbomachinery*. Butterworth-Heinemann, 2010.

[99] F. A. Morrison, *An introduction to fluid mechanics*. Cambridge University Press, 2013.

[100] M. Hasnaoui, A. B.-B. Abdelghani, and I. Slama-Belkhodja, "Control design and experimental set-up for a high-power PV generator emulator," in *Renewable Energy Congress (IREC), 2018 9th International*, 2018: IEEE, pp. 1-6.

[101] M. Grbić, D. Salamon, and J. Mikulović, "Analysis of influence of measuring voltage transformer ratio error on single-circuit overhead power line electric field calculation results," *Electric Power Systems Research,* vol. 166, pp. 232-240, 2019.

[102] C. Lupangu and R. Bansal, "A review of technical issues on the development of solar photovoltaic systems," *Renewable and Sustainable Energy Reviews,* vol. 73, pp. 950-965, 2017.

[103] T. Sarkar, A. Bhattacharjee, H. Samanta, K. Bhattacharya, and H. Saha, "Optimal design and implementation of solar PV-wind-biogas-VRFB storage integrated smart hybrid microgrid for ensuring zero loss of power supply probability," *Energy conversion and management,* vol. 191, pp. 102-118, 2019.

[104] S. Kosai, "Dynamic vulnerability in standalone hybrid renewable energy system," *Energy conversion and management,* vol. 180, pp. 258-268, 2019.

[105] C. K. Das, O. Bass, T. S. Mahmoud, G. Kothapalli, M. A. Masoum, and N. Mousavi, "An optimal allocation and sizing strategy of distributed energy storage systems to improve performance of distribution networks," *Journal of Energy Storage,* vol. 26, p. 100847, 2019.

[106] S. Dhundhara, Y. P. Verma, and A. Williams, "Techno-economic analysis of the lithium-ion and lead-acid battery in microgrid systems," *Energy conversion and management,* vol. 177, pp. 122-142, 2018.

[107] J. Liu, X. Chen, S. Cao, and H. Yang, "Overview on hybrid solar photovoltaic-electrical energy storage technologies for power supply to buildings," *Energy conversion and management,* vol. 187, pp. 103-121, 2019.

[108] K. Liu, X. Hu, Z. Yang, Y. Xie, and S. Feng, "Lithium-ion battery charging management considering economic costs of electrical energy loss and battery degradation," *Energy Conversion and Management,* vol. 195, pp. 167-179, 2019.

[109] C. K. Das, O. Bass, G. Kothapalli, T. S. Mahmoud, and D. Habibi, "Optimal placement of distributed energy storage systems in distribution networks using artificial bee colony algorithm," *Applied energy,* vol. 232, pp. 212-228, 2018.

[110] M. Das, M. A. K. Singh, and A. Biswas, "Techno-economic optimization of an off-grid hybrid renewable energy system using metaheuristic optimization approaches–Case of a radio transmitter station in India," *Energy conversion and management*, vol. 185, pp. 339-352, 2019.

[111] Q. Hou, N. Zhang, E. Du, M. Miao, F. Peng, and C. Kang, "Probabilistic duck curve in high PV penetration power system: Concept, modeling, and empirical analysis in China," *Applied Energy*, vol. 242, pp. 205-215, 2019.

[112] C. K. Das *et al.*, "Optimal allocation of distributed energy storage systems to improve performance and power quality of distribution networks," *Applied Energy*, vol. 252, p. 113468, 2019.

[113] A. Baniasadi, D. Habibi, O. Bass, and M. A. Masoum, "Optimal real-time residential thermal energy management for peak-load shifting with experimental verification," *IEEE Transactions on Smart Grid*, 2018.

[114] M. Guezgouz, J. Jurasz, B. Bekkouche, T. Ma, M. S. Javed, and A. Kies, "Optimal hybrid pumped hydro-battery storage scheme for off-grid renewable energy systems," *Energy Conversion and Management*, vol. 199, p. 112046, 2019.

[115] Y. Li, Z. Yang, G. Li, D. Zhao, and W. Tian, "Optimal scheduling of an isolated microgrid with battery storage considering load and renewable generation uncertainties," *IEEE Transactions on Industrial Electronics*, vol. 66, no. 2, pp. 1565-1575, 2018.

[116] P. Beires, M. Vasconcelos, C. Moreira, and J. P. Lopes, "Stability of autonomous power systems with reversible hydro power plants: A study case for large scale renewables integration," *Electric Power Systems Research*, vol. 158, pp. 1-14, 2018.

[117] N. Mousavi, G. Kothapalli, D. Habibi, M. Khiadani, and C. K. Das, "An improved mathematical model for a pumped hydro storage system considering electrical, mechanical, and hydraulic losses," *Applied energy*, vol. 247, pp. 228-236, 2019.

[118] V. Te Chow, *Advances in hydroscience*. Elsevier, 2013.

[119] M. Preene and M. Rosser, *Groundwater lowering in construction: a practical guide to dewatering*. CRC Press, 2012.

[120] N. Mousavi, "The Design and Construction of a High Efficiency Satellite Electrical Power Supply System," *Journal of Power Electronics*, vol. 16, no. 2, pp. 666-674, 2016.

[121] A. Orioli and A. Di Gangi, "A procedure to evaluate the seven parameters of the two-diode model for photovoltaic modules," *Renewable energy*, vol. 139, pp. 582-599, 2019.

[122] F. Rodríguez, A. Fleetwood, A. Galarza, and L. Fontán, "Predicting solar energy generation through artificial neural networks using weather forecasts for microgrid control," *Renewable Energy*, vol. 126, pp. 855-864, 2018.

[123] "Australian PV Institute (APVI) Solar Map, funded by the Australian Renewable Energy Agency." pv-map.apvi.org.au (accessed 7 January 2019.

[124] YR. "Weather forecast, Joondalup, Western Australia (Australia)." Norwegian Meteorological Institute. https://www.yr.no/place/Australia/Western_Australia/Joondalup/hour_by_hour_detailed.html (accessed 2018).

[125] M. Collotta and G. Pau, "An innovative approach for forecasting of energy requirements to improve a smart home management system based on BLE," *IEEE Transactions on Green Communications and Networking*, vol. 1, no. 1, pp. 112-120, 2017.

[126] "Irrigation calculator, Department of Primary Industries and Regional Development, Government of Western Australia." https://www.agric.wa.gov.au/irrigation-calculator (accessed 2019).

[127] C. Gamarra and J. M. Guerrero, "Computational optimization techniques applied to microgrids planning: A review," *Renewable and Sustainable Energy Reviews,* vol. 48, pp. 413-424, 2015.

[128] P. Nagapurkar and J. D. Smith, "Techno-economic optimization and social costs assessment of microgrid-conventional grid integration using genetic algorithm and Artificial Neural Networks: A case study for two US cities," *Journal of Cleaner Production,* vol. 229, pp. 552-569, 2019.

[129] S. Leonori, M. Paschero, F. M. F. Mascioli, and A. Rizzi, "Optimization strategies for Microgrid energy management systems by Genetic Algorithms," *Applied Soft Computing,* p. 105903, 2019.

[130] Q. A. Phan, T. Scully, M. Breen, and M. D. Murphy, "Determination of optimal battery utilization to minimize operating costs for a grid-connected building with renewable energy sources," *Energy conversion and management,* vol. 174, pp. 157-174, 2018.

[131] L. Liu, Q. Sun, H. Li, H. Yin, X. Ren, and R. Wennersten, "Evaluating the benefits of Integrating Floating Photovoltaic and Pumped Storage Power System," *Energy Conversion and Management,* vol. 194, pp. 173-185, 2019.

[132] A. Marszal-Pomianowska, P. Heiselberg, and O. K. Larsen, "Household electricity demand profiles–A high-resolution load model to facilitate modelling of energy flexible buildings," *Energy,* vol. 103, pp. 487-501, 2016.

[133] "Synergy Smart Home Plan, time-of-use tariff." https://www.synergy.net.au/Your-home/Energy-plans/Smart-Home-Plan?tid=Energy-plans:side_nav:Smart%20Home%20Plan (accessed 2019.

[134] R. A. Freeze and J. A. Cherry, "Groundwater Prentice-Hall Inc," *Eaglewood Cliffs, NJ,* 1979.

[135] K. Kusakana, "Optimal electricity cost minimization of a grid-interactive Pumped Hydro Storage using ground water in a dynamic electricity pricing environment," *Energy Reports,* vol. 5, pp. 159-169, 2019.

[136] M. Baumann, M. Weil, J. F. Peters, N. Chibeles-Martins, and A. B. Moniz, "A review of multi-criteria decision making approaches for evaluating energy storage systems for grid applications," *Renewable and Sustainable Energy Reviews,* vol. 107, pp. 516-534, 2019.

[137] A. Stoppato, G. Cavazzini, A. Benato, N. Destro, and G. Ardizzon, "Optimal Design and Management of a Hybrid Photovoltaic-Pump Hydro Energy Storage System," in *ASME 2014 12th Biennial Conference on Engineering Systems Design and Analysis*, 2014: American Society of Mechanical Engineers Digital Collection.

[138] N. Mousavi, G. Kothapalli, D. Habibi, and C. K. Das, "Operational Cost reduction of PV-PHS systems in farmhouses: Modelling, Design, and Experimental validation," in *IOP Conference Series: Earth and Environmental Science*, Deakin University, Australia, 2019, vol. 322, no. 1: IOP Publishing, p. 012011.

[139] T. Adefarati and R. Bansal, "Reliability and economic assessment of a microgrid power system with the integration of renewable energy resources," *Applied energy,* vol. 206, pp. 911-933, 2017.

[140] N. T. Mbungu, R. C. Bansal, and R. Naidoo, "Smart energy coordination of a hybrid wind/PV with battery storage connected to grid," *The Journal of Engineering,* vol. 2019, no. 18, pp. 5109-5113, 2019.

[141] N. T. Mbungu, R. C. Bansal, and R. M. Naidoo, "Smart energy coordination of autonomous residential home," *IET Smart Grid,* vol. 2, no. 3, pp. 336-346, 2019.

[142] N. T. Mbungu, R. C. Bansal, R. Naidoo, V. Miranda, and M. Bipath, "An optimal energy management system for a commercial building with renewable energy generation under real-time electricity prices," *Sustainable cities and society,* vol. 41, pp. 392-404, 2018.

[143] N. T. Mbungu, R. Naidoo, R. C. Bansal, and M. Bipath, "Optimisation of grid connected hybrid photovoltaic–wind–battery system using model predictive control design," *IET Renewable Power Generation,* vol. 11, no. 14, pp. 1760-1768, 2017.

[144] A. R. Jordehi, "Optimisation of demand response in electric power systems, a review," *Renewable and Sustainable Energy Reviews*, vol. 103, pp. 308-319, 2019.

[145] A. Baniasadi, D. Habibi, W. Al-Saedi, and M. A. Masoum, "Demonstration of Peak-Load Shifting with Optimal Residential Thermal Energy Management," EasyChair, 2516-2314, 2019.

[146] E. Mortaz, A. Vinel, and Y. Dvorkin, "An optimization model for siting and sizing of vehicle-to-grid facilities in a microgrid," *Applied energy*, vol. 242, pp. 1649-1660, 2019.

[147] S. Masebinu, E. Akinlabi, E. Muzenda, and A. Aboyade, "Techno-economics and environmental analysis of energy storage for a student residence under a South African time-of-use tariff rate," *Energy*, vol. 135, pp. 413-429, 2017.

[148] T. T. Tran and A. D. Smith, "Thermoeconomic analysis of residential rooftop photovoltaic systems with integrated energy storage and resulting impacts on electrical distribution networks," *Sustainable Energy Technologies and Assessments*, vol. 29, pp. 92-105, 2018.

[149] Y. Yang, M. Wang, Y. Liu, and L. Zhang, "Peak-off-peak load shifting: Are public willing to accept the peak and off-peak time of use electricity price?," *Journal of cleaner production*, vol. 199, pp. 1066-1071, 2018.

[150] S. A. Kalogirou, E. Mathioulakis, and V. Belessiotis, "Artificial neural networks for the performance prediction of large solar systems," *Renewable Energy*, vol. 63, pp. 90-97, 2014.

[151] C. Voyant *et al.*, "Machine learning methods for solar radiation forecasting: A review," *Renewable Energy*, vol. 105, pp. 569-582, 2017.

[152] H. Bazine and M. Mabrouki, "Chaotic dynamics applied in time prediction of photovoltaic production," *Renewable Energy*, vol. 136, pp. 1255-1265, 2019.

[153] K. B. Debnath and M. Mourshed, "Forecasting methods in energy planning models," *Renewable and Sustainable Energy Reviews*, vol. 88, pp. 297-325, 2018.

[154] J. Yan, M. Menghwar, E. Asghar, M. K. Panjwani, and Y. Liu, "Real-time energy management for a smart-community microgrid with battery swapping and renewables," *Applied Energy*, vol. 238, pp. 180-194, 2019.

[155] Y. Huang, K. Wang, K. Gao, T. Qu, and H. Liu, "Jointly optimizing microgrid configuration and energy consumption scheduling of smart homes," *Swarm and Evolutionary Computation*, vol. 48, pp. 251-261, 2019.

[156] C. K. Das, O. Bass, T. S. Mahmoud, G. Kothapalli, M. A. Masoum, and N. Mousavi, "An optimal allocation and sizing strategy of distributed energy storage systems to improve performance of distribution networks," *Journal of Energy Storage*, vol. 26, p. 100847, 2019

[157] "Retail Electricity Pricing Inquiry Final Report," June 2018. [Online]. Available: www.accc.gov.au

[158] C. K. Das, O. Bass, G. Kothapalli, T. S. Mahmoud, and D. Habibi, "Overview of energy storage systems in distribution networks: Placement, sizing, operation, and power quality," *Renewable and Sustainable Energy Reviews*, vol. 91, pp. 1205-1230, 2018.

[159] D. Burtt, "Cost-effectiveness of renewable energy subsidies in reducing greenhouse gas emissions in Australia," PhD Thesis, School of Geography, Planning and Environmental Management, The University of Queensland, 2016.

[160] S. Agnew, "A study of residential solar power and battery energy storage adoption dynamics," PhD Thesis, School of Earth and Environmental Sciences, The University of Queensland, 2018.

[161] B. S. Pali and S. Vadhera, "A novel solar photovoltaic system with pumped-water storage for continuous power at constant voltage," *Energy conversion and management,* vol. 181, pp. 133-142, 2019.

[162] N. Mousavi, G. Kothapalli, D. Habibi, C. K. Das, and A. Baniasadi, "Modelling, design, and experimental validation of a grid-connected farmhouse comprising a photovoltaic and a pumped hydro storage system," *Energy Conversion and Management,* vol. 210, p. 112675, 2020.

[163] N. Mousavi, G. Kothapalli, D. Habibi, C. K. Das, and A. Baniasadi, "A novel photovoltaic-pumped hydro storage microgrid applicable to rural areas," *Applied Energy,* vol. 262, p. 114284, 2020.

[164] M. S. Mahmoud, N. M. Alyazidi, and M. I. Abouheaf, "Adaptive intelligent techniques for microgrid control systems: A survey," *International Journal of Electrical Power & Energy Systems,* vol. 90, pp. 292-305, 2017.

[165] N. M. Alyazidi and M. S. Mahmoud, "On LQG control design for network systems with/without acknowledgments using a particle filtering technology," *Applied Mathematics and Computation,* vol. 359, pp. 52-70, 2019.

[166] A. B. Siddique, M. S. Munsi, S. K. Sarker, S. K. Das, and M. R. Islam, "Voltage and current control augmentation of islanded microgrid using multifunction model reference modified adaptive PID controller," *International Journal of Electrical Power & Energy Systems,* vol. 113, pp. 492-501, 2019.